Russian Research Centre "Kurchatov Institute"

Final Technical Report:

The effects of high-energy proton beams on LHC collimator materials.

Coordinator of Project,
Head of Laboratory,
Russian Research Centre "Kurchatov Institute",
Professor **A.I.Ryazanov**

Moscow 2008

Abstract

The investigations of physical-mechanical property changes of graphite collimator materials for LHC (CERN) produced in Japan and irradiated on cyclotron of RRC-KI by protons with the energies up to 30 MeV have been performed. Accomplished analysis includes comparative investigations of physical-mechanical properties of irradiated and non irradiated graphite collimator materials for LHC, including analysis of degradation of such main physical properties of these materials: coefficient of thermal conductivity, changes of electrical resistivity, thermal expansion coefficient, changes of density, changes of mechanical properties of these materials: strength analysis, elastic modulus changes, stress to rupture, yield stress, ultimate tensile stress, deformation to rupture, which were performed at room irradiated temperatures (that is below 100 degree Centigrade) up to maximum irradiation dose 3.10^{19}proton/cm^2. All investigations have been made for three orientations of anisotropic composite graphite. The dose dependencies for the main physical-mechanical properties of irradiated collimator materials of LHC have been obtained. The numerical calculations of radiation damage accumulation in the collimator materials for LHC under proton beam irradiation in the energy interval from 20 MeV up to 35 MeV and up to irradiation doses 3.10^{19} proton/cm^2 have been made for the chose of best irradiation conditions on RRC KI cyclotron. The more strong degradation of physical-mechanical properties of graphite collimator materials in the dependence on irradiation dose has been observed along the **graphite fiber** in graphite collimator composite materials for LHC.

List of Participations:

A.I.Ryazanov, A.N.Bruchanov, O.K, Chugunov, S.M.Ivanov, S.T.Latushkin, E.V.Semenov, V.N, Unezhev

Contents

1. Introduction.

Present report is devoted to the study of radiation resistance of graphite composite materials AC-150 produced in Japan, which supposed to be used as materials for collimators of LHC machine in CERN. The work was carried out under irradiation at room temperature of graphite samples cooled with water coolant at the cyclotron facility of Russian Research Center “Kurchatov Institute” (RRC KI) using proton beam with energy up to 30 MeV.

Investigations of radiation resistance of collimator materials with such complex structure has been performed in a first time in a very short period of time (about 3 months) through the use of the cyclotron and developed techniques for irradiation. It would take years of radiation for reactor to get a maximum dose of about 2 dpa.

Experimental investigations in this scope include the development and determination of a general procedure for performing investigations of radiation resistance of LHC collimator graphite materials at the cyclotron facility of RRC-KI using protons with energy up to 30 MeV, as well as studies of changes physical-mechanical properties of the initial (non irradiated) and irradiated LHC collimator graphite materials (AC-150) using protons with energies up to 30 MeV. Analysis of changes in the physical properties of both initial and irradiated materials includes the measurements of following physical quantities:

- thermal conductivity coefficient,
- electrical resistivity,
- coefficient of thermal expansion,
- changes in density and parameters of a crystal lattice
- analysis of changes in mechanical properties: analysis of changes in modules of elasticity, rupture stress (ultimate tensile stress), deformation up to rupture.

Investigations of changes in these properties of irradiated graphite collimator materials will be carried out for the various directions of thread (graphite fiber) orientation in graphite composite material AC-150 with different radiation doses of proton beam.

2 Development of needed target unit for carrying out the irradiation of AC-150 graphite samples using proton beam on RRC-KI cyclotron

To perform the needed investigations of radiation resistance and changes in physical-mechanical properties of irradiated by protons LHC graphite composite collimator materials (AC-150) manufactured in Japan and irradiated at different proton doses at RRC-KI cyclotron a special cooling system and water-cooled target unit were developed for irradiation of prepared graphite samples of these materials. This target allows for irradiation of these materials using proton beam with energies up to 30 MeV with a maximum fluence of 10^{19} protons/cm^2.

Key technical requirements for developed and created target unit for the cyclotron facility of RRC-KI for these experiments include the following basic parameters:

- **particle type** — **protons**
- **energy** — **at least (minimum) 28,6 MeV**
- **beam current** — **up to 25 μA**
- **dimensions of samples** — **4 X 4 X 25 mm**
- **number of simultaneously irradiated samples** — **3**
- **irradiation area** — **15 mm X 15 mm**
- **irradiation depth** — **> 4 mm**
- **fluence** — **10^{19} particles/cm^2**
- **irradiation field nonuniformity** — **± 15%**
- **sample temperature under irradiation** — **at most 80 ^{o}C**
- **cooling of samples** — **distilled water**
- **pressure of water** — **up to 4 atm.**

To fulfil the listed requirements on the irradiation of graphite samples a target unit which represented in Fig.1 and Fig. 2 has been developed and built.

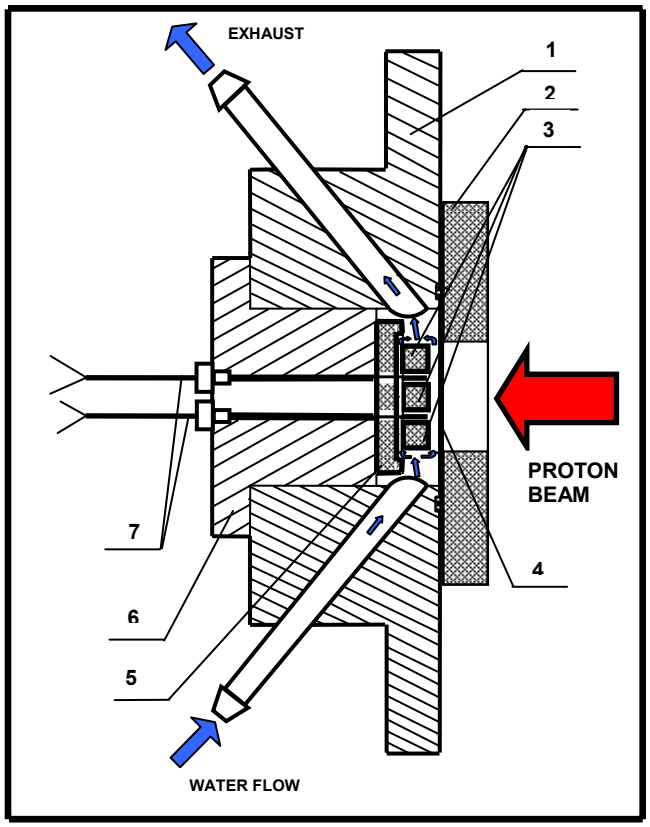

Fig. 1. Diagram of target structure for irradiation of the composite graphite samples of LHC collimator materials.

1. A frame of the target unit. **2.** Graphite diaphragm. **3.** Samples. **4.** Foil window. **5.** Sample holder. **6.** A base of the sample holder. **7.** Measuring thermocouples.

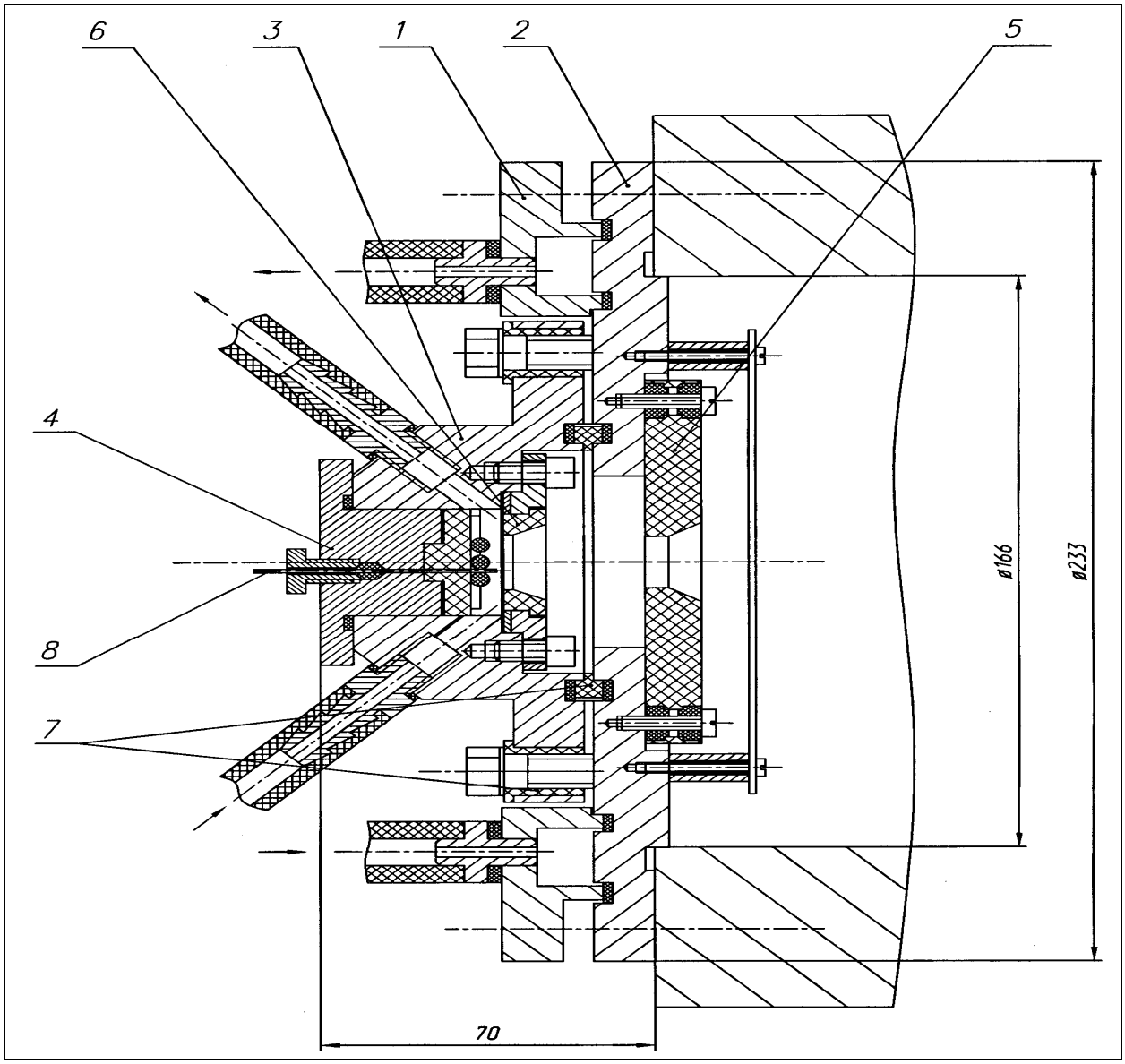

Fig. 2. Diagram of the target unit for irradiation of composite graphite samples using a proton beam with energies up to 30 MeV at RRC-KI cyclotron facility.

1. Water cooling jacket. **2.** Flange of ion guide. **3.** Target frame. **4.** Sample holder. **5.** Four-sector diaphragm. **6.** Foil window unit. **7.** Isolator. **8.** Measuring thermocouples. Arrow signs correspond to directions of water flow.

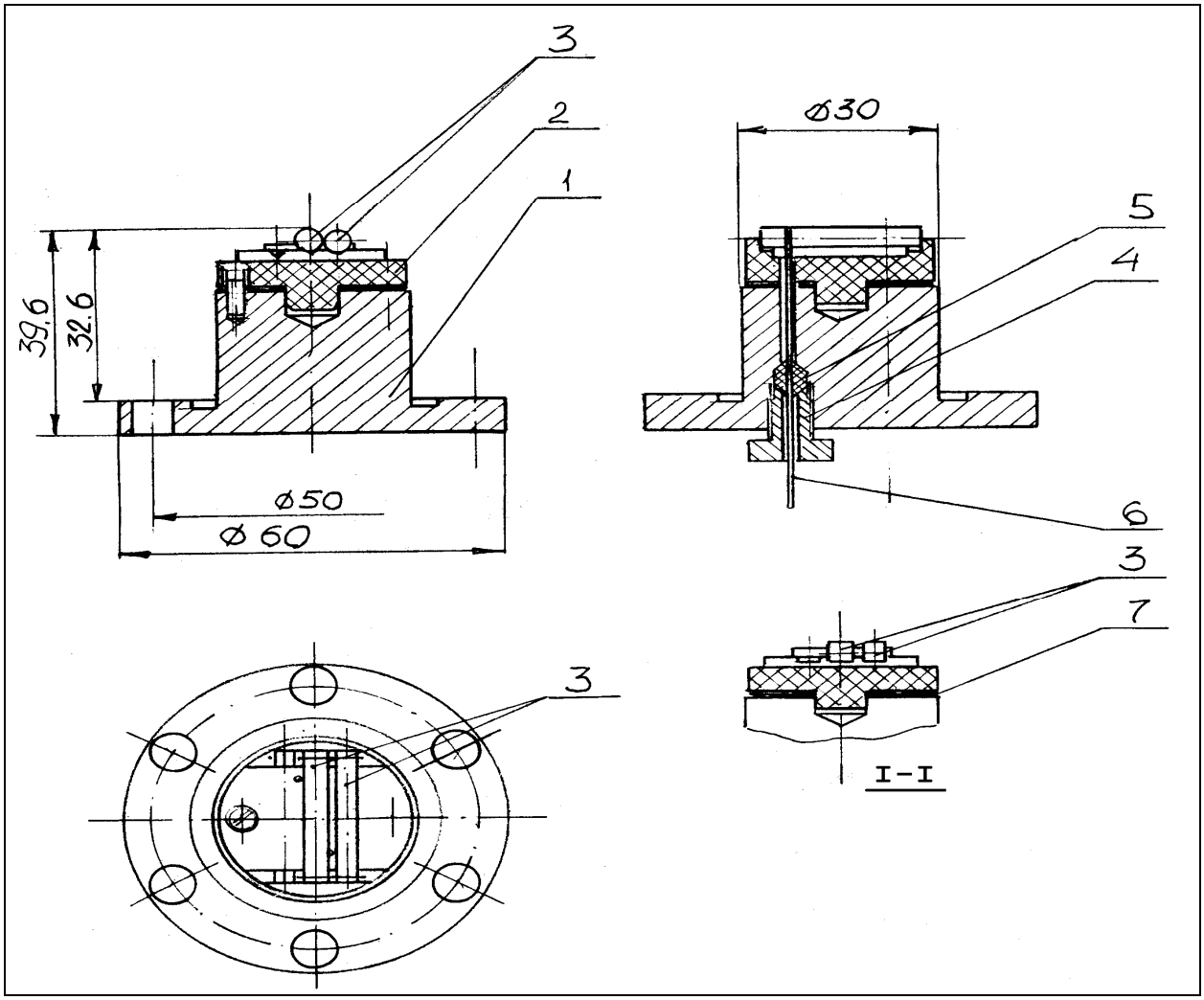

Fig.3. Sample holder.

1. Base. 2. Substrate. 3. Samples. 4. Thermocouple seal. 5. Mount screw. 6. Thermocouples. 7. Adjusting spacers. I-I – the mounting method of square graphite samples.

A proton beam with the energy 32 MeV taken out from RRC-KI isochronous cyclotron passes through the beam transport ion-optical system to the experimental hall, where the target unit is installed on the diagnostic device. Beam passes through restrictive thick graphite diaphragm with a window 15 X 15 mm (2) from diagnostic device to samples (3) through the foil window (4) that made of 0.45 mm thick aluminum foil and a thin gap that is less than 0.8 mm with flow of distilled water inside cooling area. As a result, proton beam faces with the energy not less than 28.6 MeV. Maximum range of a proton with energy 28.6 MeV in graphite with a density of 1.7 g/cm^3 is more than 4 mm, which meets the necessary technical requirements for irradiation. Gap

between foil (4) and samples (3) is adjusted by installing spacers between frame of the target unit (1) and base of the sample holder (6). To control the temperature of samples chromel-alumel thermocouples that is 1 mm in diameter (7) have been placed in a gap between upper and lower samples. Thermocouples have been hermetically compacted at the base of the sample holder (6). Thermocouples are shifted by 10 mm relative to each other in a horizontal plane. Graphite sample holder (5) is made with the cradles for samples in a way that samples rigidly fixed to each other and to the holder which has a gap in the middle part to ensure the free water flow. About 20 liters of water per each minute pass through the target area at pressure in the cooling system cyclotron of distilled water of 4 atm. This amount of water is guaranteed enough to manage a beam with output power up to 750 W.

The target unit is isolated from ion guide for the current measurement of proton beam irradiated target.

In Fig.4 a structural and functional scheme of experiment for irradiation of graphite samples with flowing water cooling are represented.

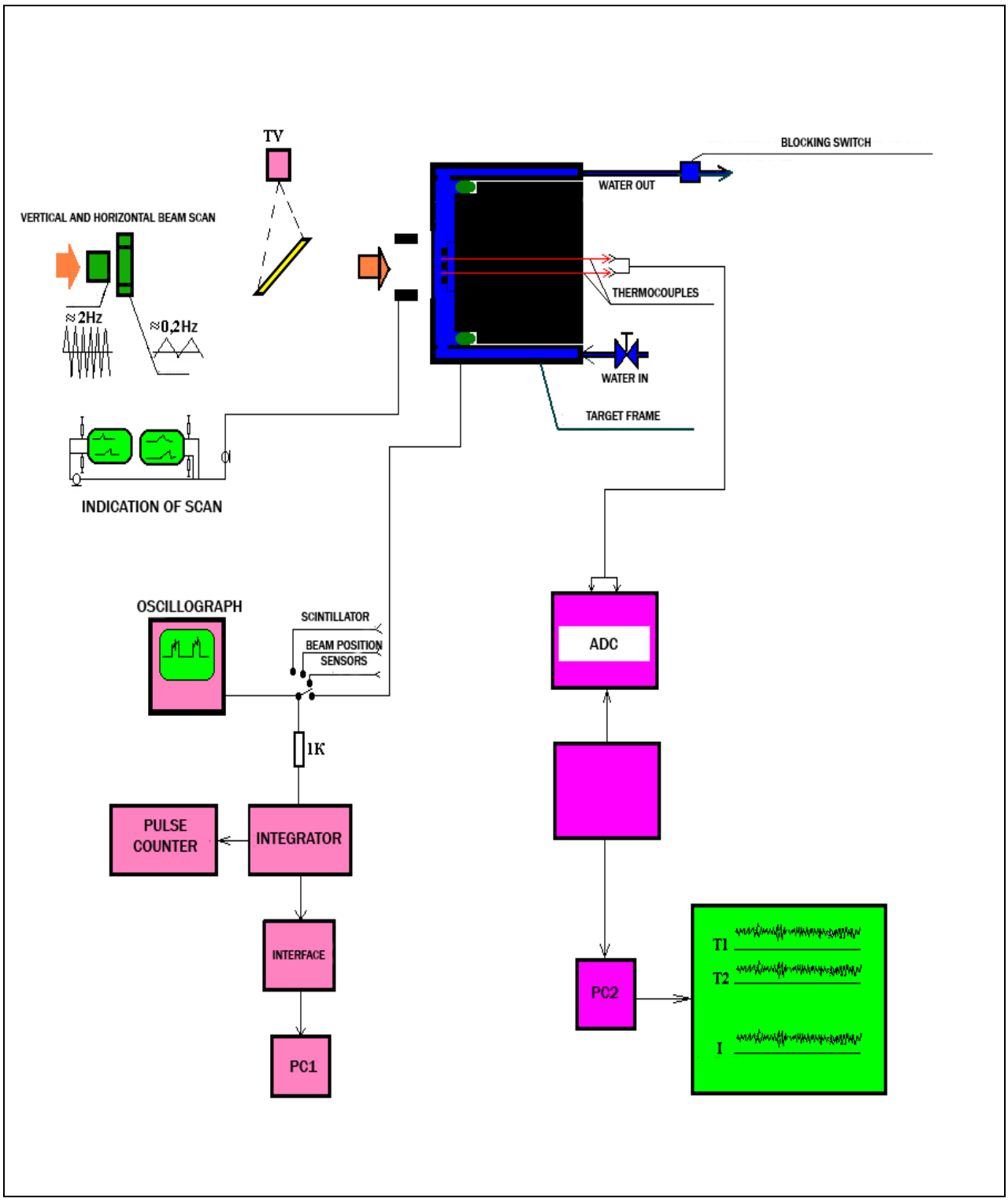

Fig. 4. Functional scheme of experiment for irradiation of graphite samples at RRC-KI cyclotron facility.

The following units are presented in Fig.4.:

- A part of ion guide with electromagnets of two-coordinate system of beam scanning and diagnostic device with a television control of the beam location;
- oscillographic control device of beam location during scan;
- computer control system of 2 thermocouple signals;
- computer system and oscillographic control of value beam current on target and probes, as well as accumulated charge of ion current on target and diaphragm;
- water cooling system of the target node with trigger device for shutting down high frequency accelerating voltage in case of missing water flow.

Necessary uniformity of the area of irradiated samples of 15 mm X 15 mm is achieved by inclusion in the system two-coordinate scanning of beam on the target. Uniformity of irradiation is achieved by optimal choice of parameters for scanning proton beam and parameters of manipulation for accelerating voltage of the cyclotron. With the frequency manipulation of 100 Hz and duty factor of 20 the choice of the scanning frequency is about 3 Hz vertically, and about 0.2 Hz horizontally, thus the beat frequency does not significantly modulate the temperature of the target. Control of scanning beam is carried out using 4 lamellas of graphite diaphragm. Due to the presence of current signals from scanning frequencies on lamellas which equal in length to pulse duration cyclotron, they conveniently can be seen in multichannel oscilloscope or through a digital system of control on the computer.

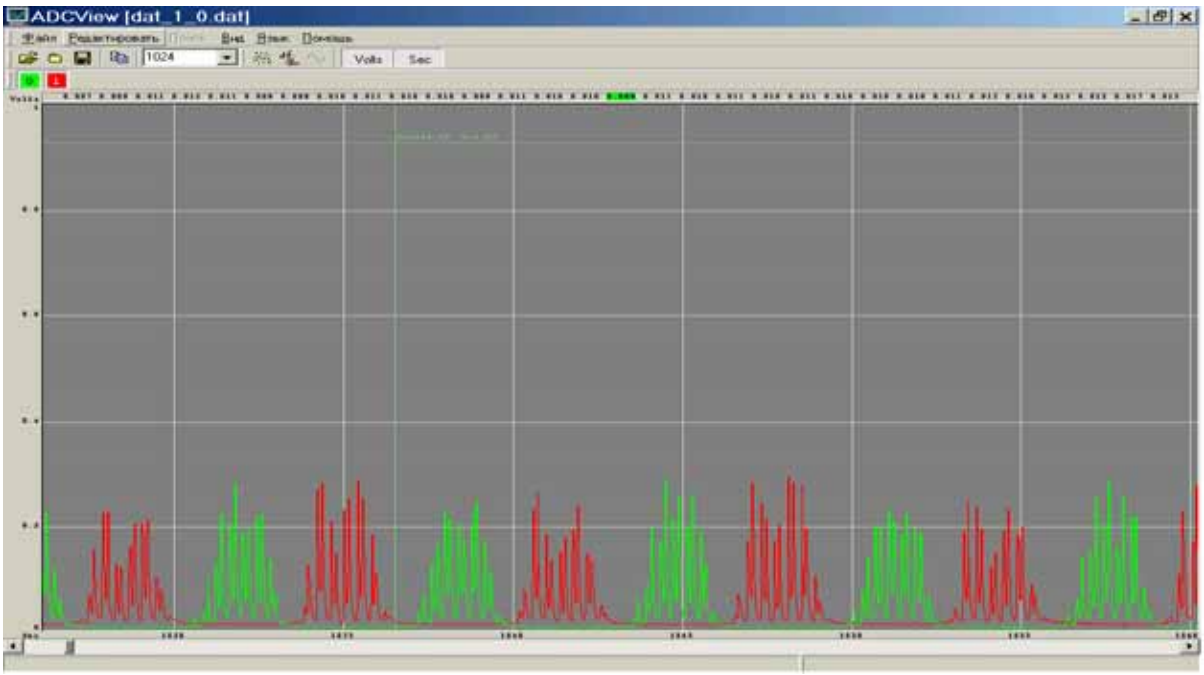

Fig. 5. Thermal changes of graphite samples under irradiation of the proton beam.

The oscillogram of digital signals from 2 thermocouples in the standard regime of sample irradiation is represented in Fig.5. The diagram shows the change in temperature of thermocouples when a beam of protons with two-coordinate scanning hit them. The temperature of thermocouples at the peak of beam distribution profile reaches 200 ^{o}C with an average beam current of 20 μA. Given the difference thermo physical properties of material of thermocouples (stainless steel and magnesium oxide) and material of the samples, as well as their distinct difference in mass, one can assume that the temperature inside the target volume and, a fortiori, on its surface does not exceed the value 100 ^{o}C.

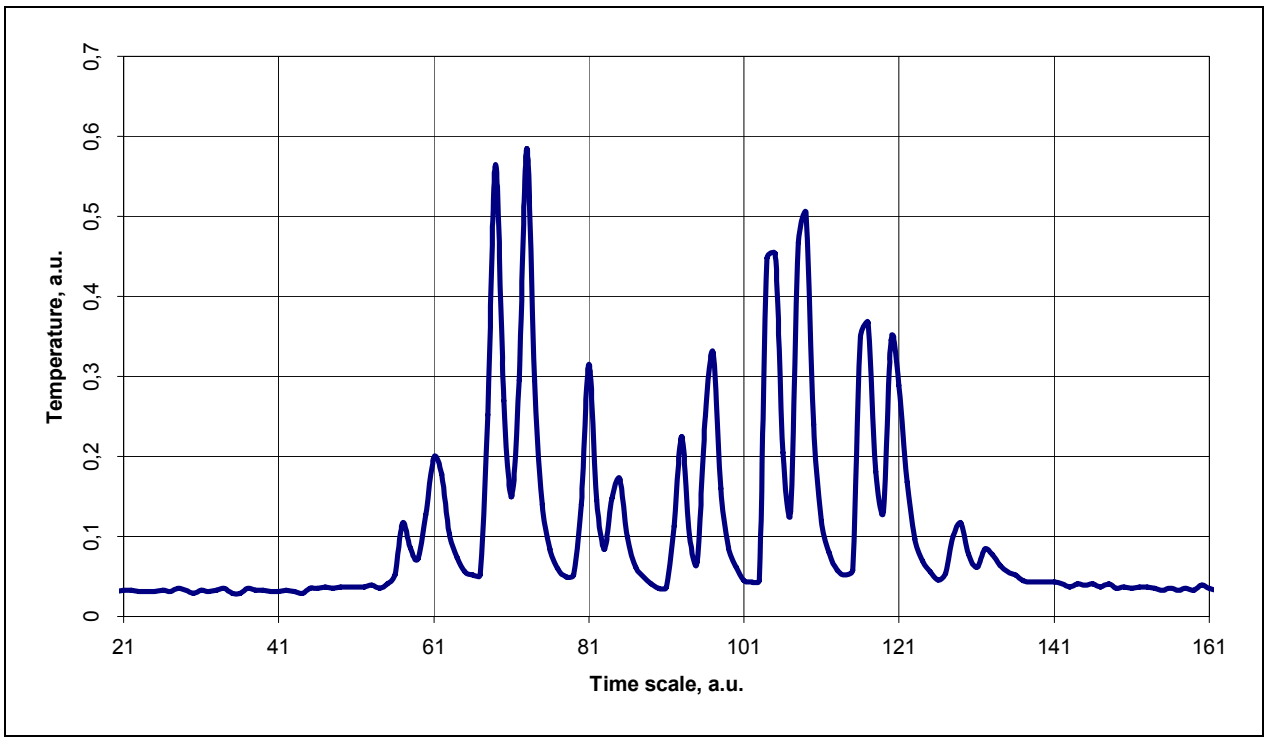

Fig. 6. Oscillogram of thermocouple readings.

A digital oscillogram of one of the cycles of irradiation with fast scan (0.6 sec/square) is represented in Fig. 6. It can be seen that the response time of thermocouple cooled with water is about 50 ms, that is about 10 times faster than the speed thermocouple in the air environment.

Due to the activation of the target materials due to direct current and the secondary particles during gain of the target fluence to 10^{19} protons/cm^2 it is possible to work with samples in a 2nd class laboratory only after 5 days. As demonstrated by spectral analysis of irradiated samples, the main contribution to the activity of samples makes ^{7}Be which formed in the bombardment of graphite with protons with the energy more than 23 MeV. Half-life of this nuclide is 53.44 days.

Calculation of sample irradiation regime

Required fluence $\Phi = 10^{19}$ protons/cm^2 was accumulated on the basis of the following parameters:

- irradiation area: $S = 1.5 * 1.5 = 2.25$ cm^2
- number of protons N passing through area S $N = S * \Phi = 2.25 * 10^{19}$ part.

- necessary charge of protons to hit the target to obtain necessary fluence q = N * e = 2.25 * 10^{19} * 1.6 * 10^{-19} = 3.6 C
- this charge q corresponds to the total number of impulses for current integrator Ni

  Ni = q / n = 3.6 / 10^{-8} = 360 *10^{6},

  n = 10^{-8} - charge of the single pulse of current integrator

- irradiation time T, provided that the mean value of beam current i = 18 μA that is 18 *10^{-6} C/sec, will be:

  T = q / i = 3.6 / 18 x 10^{-6} =200 000 sec = 56 hours

3. Preparation of graphite samples of the LHC collimator materials for experimental investigations.

Graphite composite material AC-150 is produced by impregnating filamentous carcass (carbon threads (fibers) of micron thickness) with pitch, which after graphitization turns into a matrix graphite. In fact, the way of threads winding (3D modification) determines anisotropy of its properties. In relation to the winding axis 3 directions can be identified: axial (A) tangential (T) and radial (R). The structure of the material is shown in Figures 7 and 8.

For the research 3 billets (bars) of graphite AC-150 with 40x50x100 mm^3 dimensions were given. They were assigned numbers № 4, № 10 and № 11 for the convenience of sample labelling.

From those billets cylindrical samples (5 mm diameter) were made as well as samples of parallelepiped section (4 mm x 4 mm and a length of 25 mm). The list of samples presented in Table 1. 6 series of samples were produced (three samples of various cuttings from billets № 4 and 10 and 3 samples from billet № 11)

Samples we polished in special jigs for the plane-parallel surfaces, a surface which has been subjected to radiation, polished to a high finish. The size of the samples is given in Table 1.

The scheme of billet cutting for research is shown in Fig. 7.

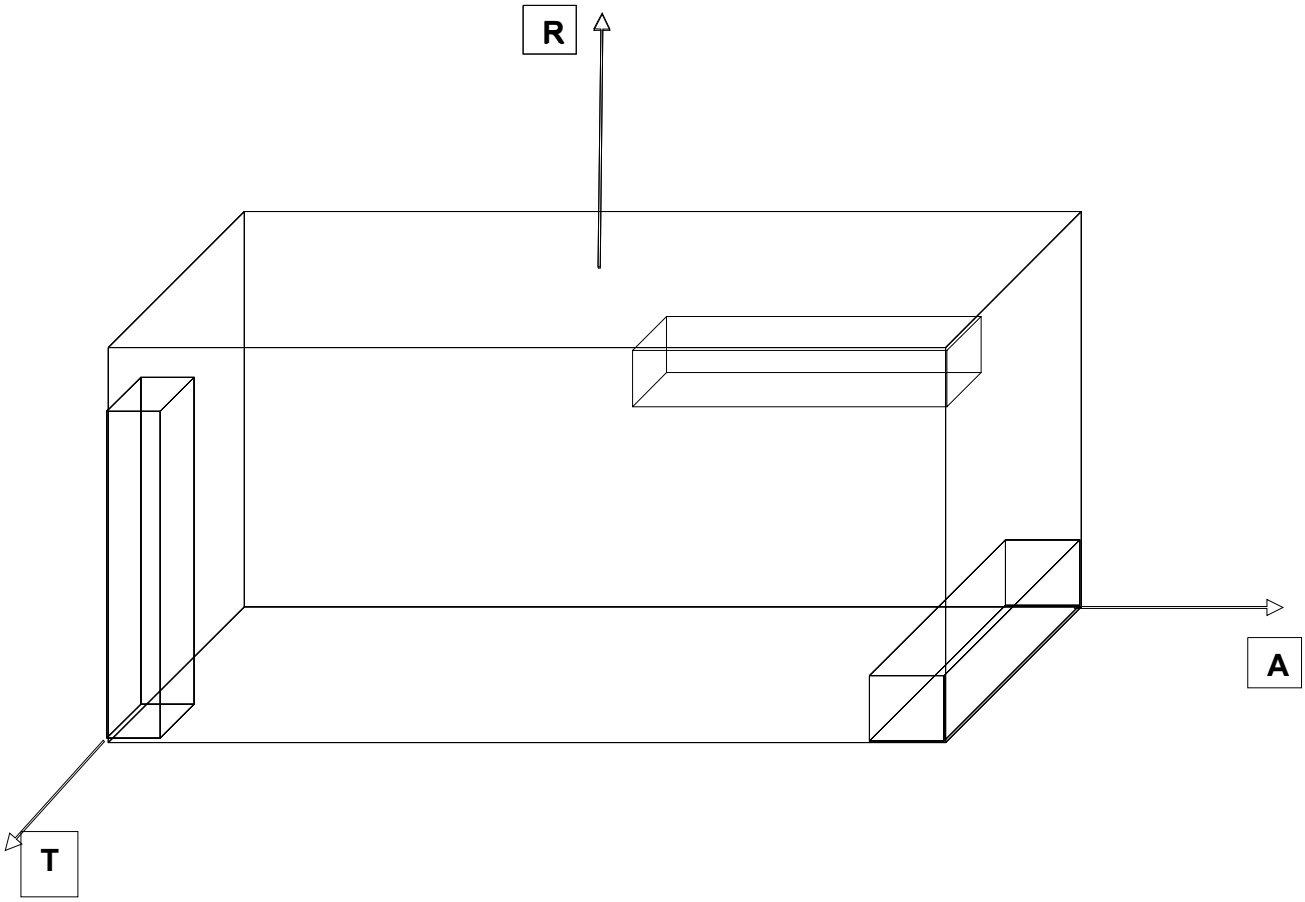

Fig.7. The scheme of billet cutting for investigations of composite graphite material in different directions of threads (fibers) winding in this material.

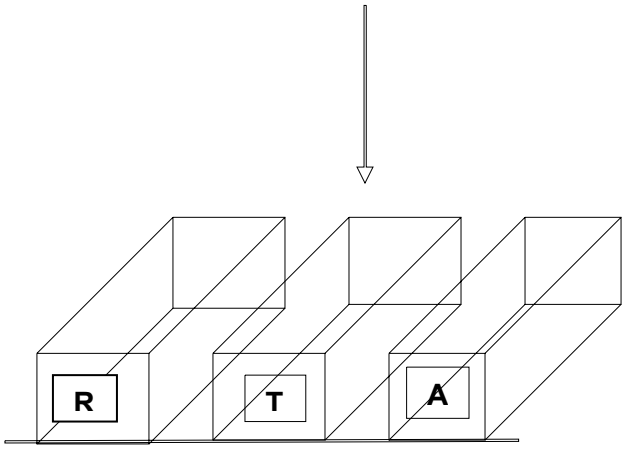

Fig. 8. Location of graphite samples in the target unit in relation to the incident proton beam. The scheme of billet cutting for research is shown in Fig. 7.

Studies of physical-mechanical properties of AC-150 graphite showed that this is a composite material (composite) with a three-dimensional structure. Its carcass (a winding of graphite threads (fibers)) is three-dimensional modification. According to this, it should have the texture in three mutually perpendicular directions. Conditionally these directions were identified as **R** (radial direction - perpendicular to the winding plane), **T** (tangential direction) and **A** (axial direction).

Table 1. Samples for determining the changes of physical-mechanical properties. Billet №4

Sample №	L, mm	B, mm	H, mm
4R(TA-1)	**24.35**	**4.06**	**3.96**
4R(TA-2)	**24.26**	**3.97**	**4.14**
4R(TA-3)	**24.19**	**4.01**	**3.9**
4T(AR-1)	**24.31**	**4.04**	**4.02**
4T(AR-2)	**24.64**	**3.89**	**4.02**
4T(AR-3)	**24.18**	**4.02**	**4.12**
4A(RT-1)	**24.17**	**4.07**	**4.12**
4A(RT-2)	**24.66**	**4.07**	**3.98**
4A(RT-3)	**24.23**	**4.09**	**4.09**

Note: Sample designation.

1. First digit is a sample number (4, 10 and 11).

2. First letter is a cutting direction (basic texture direction along the sample axis: **R, T, A**).

3. First letter in the brackets is a texture direction of plane (direction by proton beam under subsequent irradiation: **R, T, A**).

4. Second letter in the brackets is perpendicular plane.

5. Last digit is an ordinal number of the sample in a series.

Example: **4R(T, A-1)** – a sample from 4th billet, cute in the texture direction of **R**, irradiated from side **T**, perpendicular plane is **A,** ordinal number is 1.

Table 2. Samples for determining the changes of physical-mechanical properties. Billet №10

Sample №	L, mm	B, mm	H, mm
10R(TA-1)	24.72	2.02	4.17
10R(TA-2)	24.95	2.08	3.99
10R(TA-3)	24.78	3.96	4.13
10T(AR-1)	24.95	4.05	4.21
10T(AR-2)	23.95	4.11	4.15
10T(AR-3)	24.92	3.89	4.05
10A(RT-1)	24.6	4.05	4.12
10A(RT-2)	24.6	4.08	3.92
10A(RT-3)	24.81	4.18	4.17

Table 3. Samples for determining the physical-mechanical properties. Billet №11

Sample №	L, mm	B, mm	H, mm
11R(AT)	25.5	4.4	5.87
11T(RA)	40.25	4.7	6
11A(RT)	39.85	6.35	5.57

4. Investigations of primary physical-mechanical properties of AC-150 graphite samples of the LHC collimator materials.

4.1. Investigations of basic properties.

Studies physical-mechanical properties of graphite samples include:

- Research of material structure, density (d)
- Investigation of electrical resistivity ρ (at room temperature and the temperature dependence of this parameter to the temperature of 700 ^{o}C)
- Thermophysical properties – coefficient of thermal expansion (α) and thermal conductivity (λ) up to 700 ^{o}C.
- Strength properties – modulus of elasticity (E) both static and dynamic, compression strength (σ_{comp}).

All these properties were determined by standard methods specified in the "Norms of calculating the strength of typical units and graphite parts of uranium-graphite reactors" NGR-01-90.

The values of electrical resistivity and thermal conductivity (λ) were measured using Kohlrausch method under heating of samples by transmiting alternating current through it and measurement of emerging temperature fields along the sample length using thermocouple (at 3 points).

Elasticity module (dynamic) for graphite samples is determined by estimation of resonant frequencies of the sample, while exciting ultrasonic waves of longitudinal polarization.

The strength of graphite was determined by compression test of cylindrical samples at tensile machine "INSTRON" with maximum output stress of 5 tons.

Measurements are presented in tables 4 and 5 and in figures 5-6.

Table 4. Results of investigations of physical-mechanical properties of graphite samples. Billet 4.

Sample №.	d, g/cm^3	E, GPa	ρ, 10^{-6} Ohm*m	α, 10^{-6}, 1/K
4R(TA-1)	1.59	4.6	30	10.17
4R(TA-2)	1.68	4.8	28.9	10.17
4R(TA-3)	1.68	3.7	27.6	
Average value	1.65	4.36666667	28.8333333	
Standart deviation	0.05196152	0.58594653	1.20138809	
4T(AR-1)	1.7	8.1	5.6	0.25
4T(AR-2)	1.73	9.3	5.7	
4T(AR-3)	1.66	8.3	5.56	
Average value	1.69666667	8.56666667	5.62	
Standart deviation	0.03511885	0.64291005	0.07211103	
4A(RT-1)	1.66	9.2	6.2	0.20
4A(RT-2)	1.7	8.8	5.8	
4A(RT-3)	1.73	9.4	5.5	
Average value	1.696666667	9.133333333	5.833333333	
Standart deviation	0.035118846	0.305505046	0.351188458	

Table 5. Results of investigations of physical-mechanical properties of graphite samples. Billet 10.

Sample №.	d, g/cm^3	E, GPa	ρ, 10^{-6} Ohm*m	α, 10^{-6}, 1/K
10R(TA-1)	1.66	3.2	27.8	10.31
10R(TA-2)	1.66	2.96	30	
10R(TA-3)	1.66	3.2	29.1	
Average value	1.66	3.12	28.9666667	
Standart deviation	0	0.13856406	1.106044	
10T(AR-1)	1.65	9.3	5.6	0.25
10T(AR-2)	1.64	9.1	5.1	
10T(AR-3)	1.56	9.3	5.7	
Average value	1.61666667	9.23333333	5.46666667	
Standart deviation	0.04932883	0.11547005	0.32145503	
10A(RT-1)	1.54	8.4	5.5	0.167
10A(RT-2)	1.64	8.4	5.7	
10A(RT-3)	1.63	9.16	5.6	
Average value	1.603333333	8.653333333	5.6	
Standart deviation	0.055075705	0.438786205	0.1	

Table 6. Results of investigations of physical-mechanical properties of graphite samples. Billet 11.

Sample №.	d, g/cm^3	E, GPa	ρ, 10^{-6} Ohm*m
11R(AT)	1.73	4	26
11T(RA)	1.67	6.7	5.4
11A(RT)	1.75	5.5	5.7

4.2. Density measurements of graphite samples.

Measurements of sample density (the so-called seeming density d) were carried out by dividing its weight by the volume of the sample. The results showed that the density of AC-150 composite lies within interval: 1.55-1.7 g/cm^3 with an average value of density 1.65 g/cm^3 for all samples from different billets and for different directions of cutting. See Tables 5 and 6.

By comparing these values with the density of domestic nuclear graphite blocks GR-280 (1.71 g/cm^3), we can say that the density of graphite AC-150 composite slightly lower than this value by approximately 10%.

4.3. Modulus of elasticity (Young modulus, E_{dyn}) measurements of graphite samples.

Research of elasticity modulus of graphite using dynamic method (Tables 1-3) showed the following results:

Radial direction of sample cutting (R)

For samples from billet 4 elasticity modulus values for 3 samples were within the limits of (3.7-4.8) GPa, with an average value of 4.4 GPa. Standard deviation is 0.58 GPa (13%).

For samples from billet 10 elasticity modulus values for 3 samples were within the limits of (3-3.2) GPa with an average value of 3.12 GPa. Standard deviation is 0.14 GPa (5%).

For sample from billet 11 elasticity modulus value was equal to 4 MPa.

Tangential direction of sample cutting (T)

For samples from billet 4 elasticity modulus values for 3 samples were within the limits of (8.1-9.3) GPa with an average value of 8.6 GPa. Standard deviation is 0.64 GPa (7%).

For samples from billet 10 elasticity modulus values for 3 samples were within the limits of (9.1-9.3) GPa with an average value of 9.23 GPa. Standard deviation is 0.11 GPa (1%).

For sample from billet 11 (1 sample) elasticity modulus value was equal to 6.7 MPa.

Axial direction of sample cutting (A)

For samples from billet 4 elasticity modulus values for 3 samples were within the limits of (8.8-9.4) GPa, with an average value of 9.13 GPa. Standard deviation is 0.30 GPa (3%).

For samples from billet 10 elasticity modulus values for 3 samples were within the limits of (8.4-9.2) GPa, with an average value of 8.65 GPa. Standard deviation is 0.44 GPa (5%).

For sample from billet 11 elasticity modulus value was equal to 5,5 MPa.

Analyzing given results the following conclusions can be made:

Samples with the largest value of elasticity module represent tangential and axial directions of cutting (8.6 and 9.2 MPa respectively). The difference in values of E for samples from billets 4 and 10 lies practically within the standard deviation reflecting a sufficiently uniform structure of composite material.

The lowest value for E observed for radially cut samples from all 3 billets and its value is within 3.1-4.4 GPa, which is also an indication of the homogeneity of the material. The difference in the value of elasticity module for radial and tangential and axial directions of cutting (almost 3 times) can be explained by composite texture, which seems to be a 3D modification. This clearly visible on microphotography of the samples of all three directions of cutting

Comparing obtained elasticity module values with similar values for standard graphite reactor GR-280 - 6.5/5.0 GPa for the parallel and perpendicular directions of cutting in relation with the axis of graphite block forming one can conclude that the elasticity module of AC-150 composite slightly more for tangential and axial directions (about 1.5 times) and approximately one and a half times less for the radial direction.

4.4. Compression strength (σ_{comp}) measurements of graphite samples.

The strength experiments were performed using tensile machine "INSTRON"

Samples of cylindrical form (6 mm in diameter and a height of 11-13 mm) were made according to the standard for testing. The speed of movement of the upper stand racker is 1 mm/min. The test results are given in Table 7.

Table 7. Strength characteristics of the measured samples.

	l, mm	d, mm	S, mm^2	P_{max}, kgf	σ_{comp}, kgf/mm^2	σ_{comp} MPa
10T-1	12.50	5.80	26.42	149.00	5.64	55.30
2	12.80	6.00	28.27	185.00	6.54	64.17
3	12.90	6.00	28.27	162.50	5.75	56.36
4	13.00	5.40	22.90	131.00	5.72	56.09
10R-1	12.50	5.80	26.42	145.00	5.49	53.82
2	13.10	5.90	27.34	176.00	6.44	63.13
3	12.90	5.80	26.42	170.00	6.43	63.10
4A-1	13.20	5.70	25.52	152.50	5.98	58.61
2	13.00	5.40	22.90	140.00	6.11	59.95
3	12.80	5.70	25.52	162.50	6.37	62.45
4	12.50	5.40	22.90	112.50	4.91	48.17
4R-1	11.90	5.80	26.42	174.00	6.59	64.58
2	12.00	5.80	26.42	166.00	6.28	61.61
3	13.40	5.90	27.34	146.00	5.34	52.37
4T-1	13.20	5.56	24.28	135.00	5.56	54.53
2	13.30	5.50	23.76	142.50	6.00	58.82
3	12.50	5.60	24.63	147.50	5.99	58.73

The test results showed that the ultimate compression strength of AC-150 graphite for samples from all the billets is within the 55-63 MPa, with an average value (St. Div. = 60 MPa) and practically does not depend on the direction of sample cutting . By comparing these values to the strength of domestic reactor graphite GR-280 (34/24 MPa) for axial and radial lines cuttings samples respectively, it may be noted that the strength of the AC-150 composite significantly exceeds its values approximately 1.5-2 times.

4.5. Analysis of electrical resistivity change of irradiated samples.

The value of electrical resistivity (ρ) was measured by two methods. First, at the device "Elektrosoprotivlenie" using potential method (only at room temperature (see Table 4 - 6), and then at the "Teploprovodnost" device using Kohlrausch method to measure a temperature dependence of the sample. The fact that the results of the measurements (at room temperature) almost completely coincide shows complete reliability of the performed measurements

Measurements showed the following data:

Measuring the value of electrical resistivity using potentiometric method at room temperature (Table 4 - 6)

Radial direction of sample cutting (R)

For samples from billet 4 the electrical resistivity values for 3 samples were within the limits of (28-30) 10^{-6} Ohm*m with an average value of 28.8 10^{-6} Ohm*m. Standard deviation is 1.2 10^{-6} Ohm*m (4%).

For samples from billet 10 the electrical resistivity values for 3 samples were within the same limits with an average value of 29 10^{-6} Ohm*m. Standard deviation is 1.2 10^{-6} Ohm*m (4%).

For sample from billet 11 the electrical resistivity value was equal to 26.10^{-6} Ohm*m.

Tangential direction of sample cutting (T)

For samples from billet 4 the electrical resistivity values for 3 samples were within the limits of (5.5-5.7) 10^{-6} Ohm*m with an average value of 5,6210^{-6} Ohm*m. Standard deviation is 0,0710^{-6} Ohm*m (1%).

For samples from billet 10 the electrical resistivity values for 3 samples were within the limits of (5.1-5.7) 10^{-6} Ohm*m with an average value of 5.4610^{-6} Ohm*m. Standard deviation is 0.32 10^{-6} Ohm*m (6%).

For sample from billet 11 (1 sample) the electrical resistivity value was equal to 5.4.10^{-6} Ohm*m.

Axial direction of sample cutting (A)

For samples from billet 4 the electrical resistivity values for 3 samples were within the limits of (5.5-6.2) 10^{-6} Ohm*m with an average value of 5.8310^{-6} Ohm*m. Standard deviation is 0.3510^{-6} Ohm*m (6%).

For samples from billet 10 the electrical resistivity values for 3 samples were within the limits of (5.5-5.7) 10^{-6} Ohm *m with an average value of 5.6. 10^{-6} Ом.м Ohm*m. Standard deviation is 0.110^{-6} Ohm *m (2%).

For sample from billet 11 the electrical resistivity value was equal to 5.7 10^{-6} Ohm *m.

Analyzing given results the following conclusions can be made:

Samples with the largest value of electrical resistivity represent radial directions of cutting (around 30.10^{-6} Ohm*m) and for tangential and axial directions of cutting its value is sufficiently smaller (approximately 5 times) and practically doesn't vary even for the samples from different billets.

Comparing obtained values of electrical resistivity with similar values for standard graphite reactor GR-280 - 10/13 10^{-6} Ohm*m for the parallel and perpendicular directions of cutting in relation with the axis of graphite block forming one can conclude that the electrical resistivity of AC-150 composite significantly more for the radial direction (about 2.5-3 times) and considerably less than that (about 2 times) for tangential and axial directions.

Using Kohlrausch method for measurements of electrical resistivity.

This method of measurement, as noted above, allows for measurement of the temperature dependence of this value. Temperature dependence of electrical resistivity for AC-150 graphite for all three billets and for different directions of sample cuttings presented in figures 5-6.

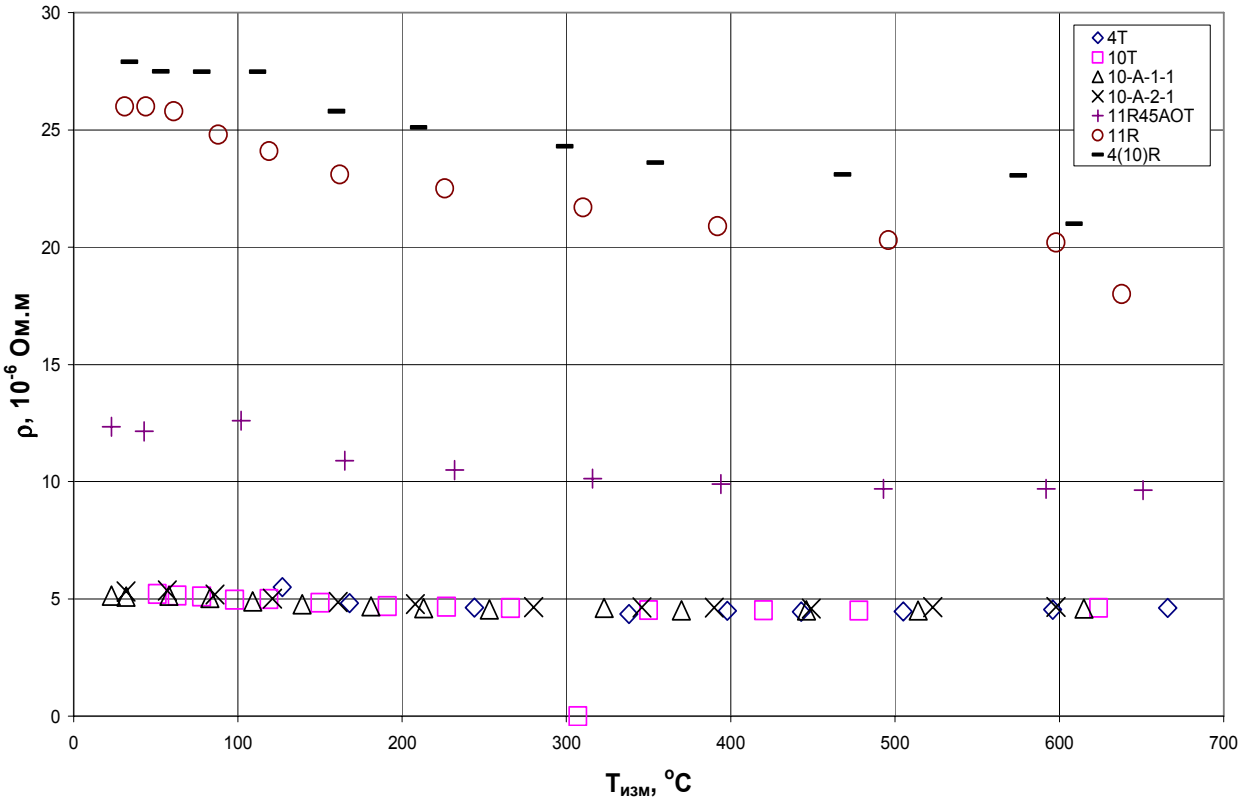

Fig.9. Results of electrical resistivity measurements for the various billets of graphite samples.

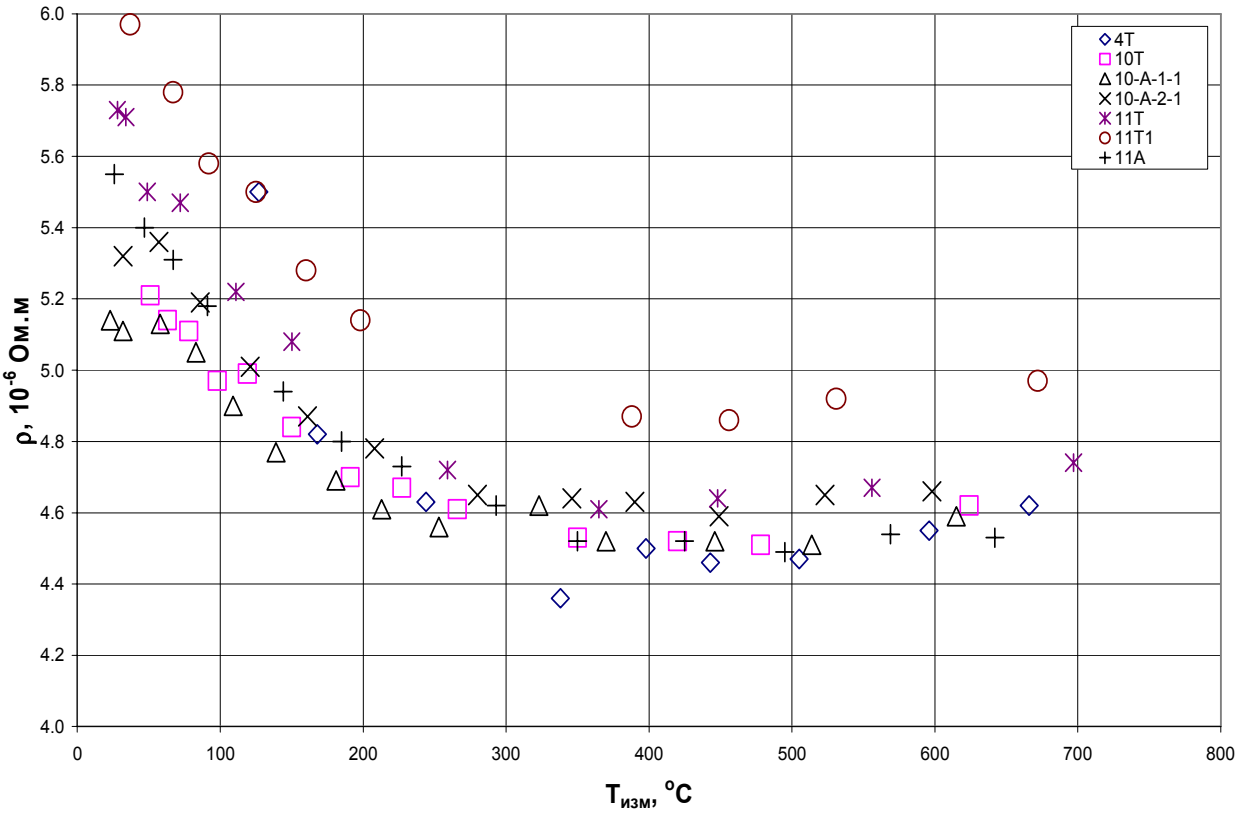

Fig.10. Results of electrical resistivity measurements for the various directions of graphite samples.

The figures show that the value of electrical resistivity for all samples initially almost linearly decreases with increasing temperature of measurement in the interval 250-300 º C, and then changes very little with further increase of temperature.

Comparing received absolute values of electrical resistivity of samples with measurements obtained by potentiometric method one can confidently state that at a temperature of 20-50 ºC those values are almost identical. This provides an opportunity to build a reliable correlation between value of electrical resistivity and the coefficient of thermal conductivity allowing in turn reliably evaluation for the changing values of of thermal conductivity under irradiation of sample by measuring the value of its electrical resistivity. See Section 5.

5. Measurements of thermo physical properties of graphite collimator materials.

5.1. The measurement of thermal conductivity of graphite samples.

The coefficient of thermal conductivity (λ) was measured using Kohlrausch method on specially made samples 6 mm in diameter and a length 25-40 mm. Curves of temperature dependence of this parameter in the range of 20-700 ºC for AC-150 graphite composite are represented in the figures 11 - 12.

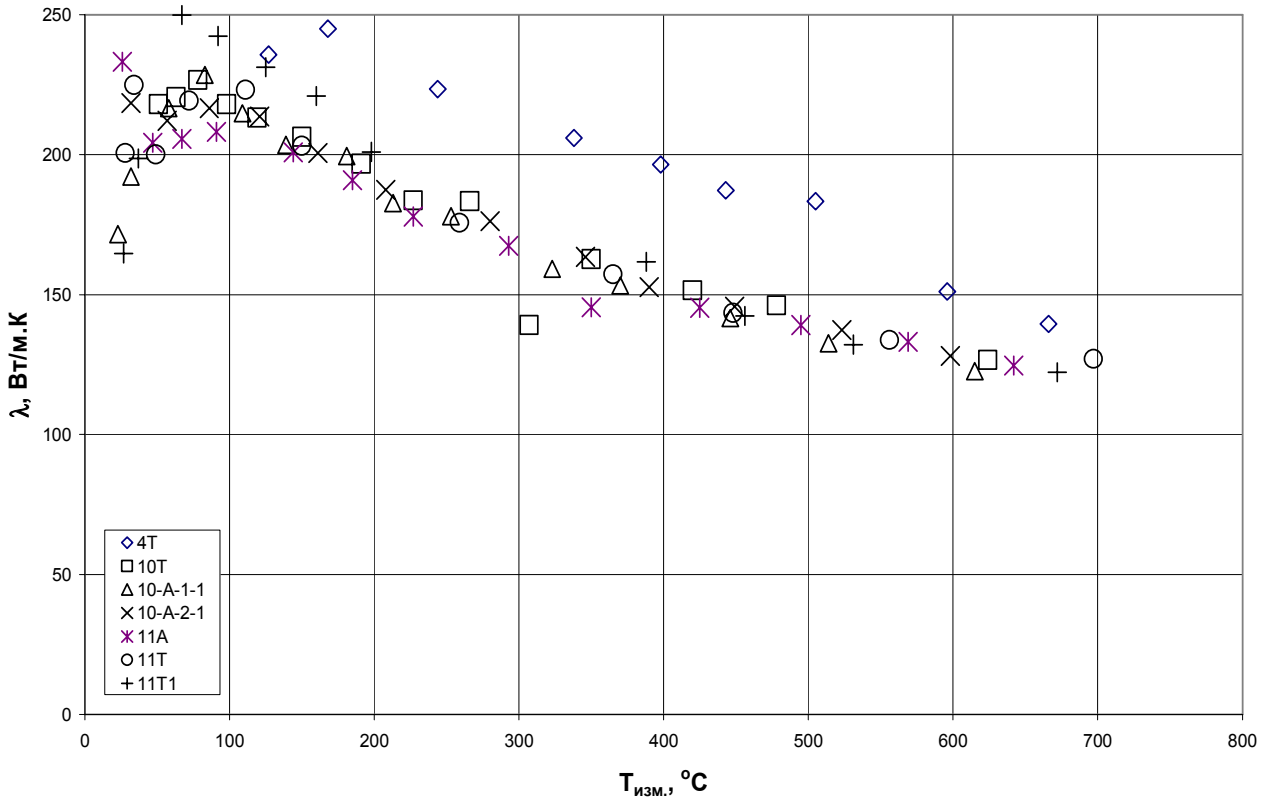

Fig. 11. Temperature dependence of the coefficient of thermal conductivity of investigated graphite materials.

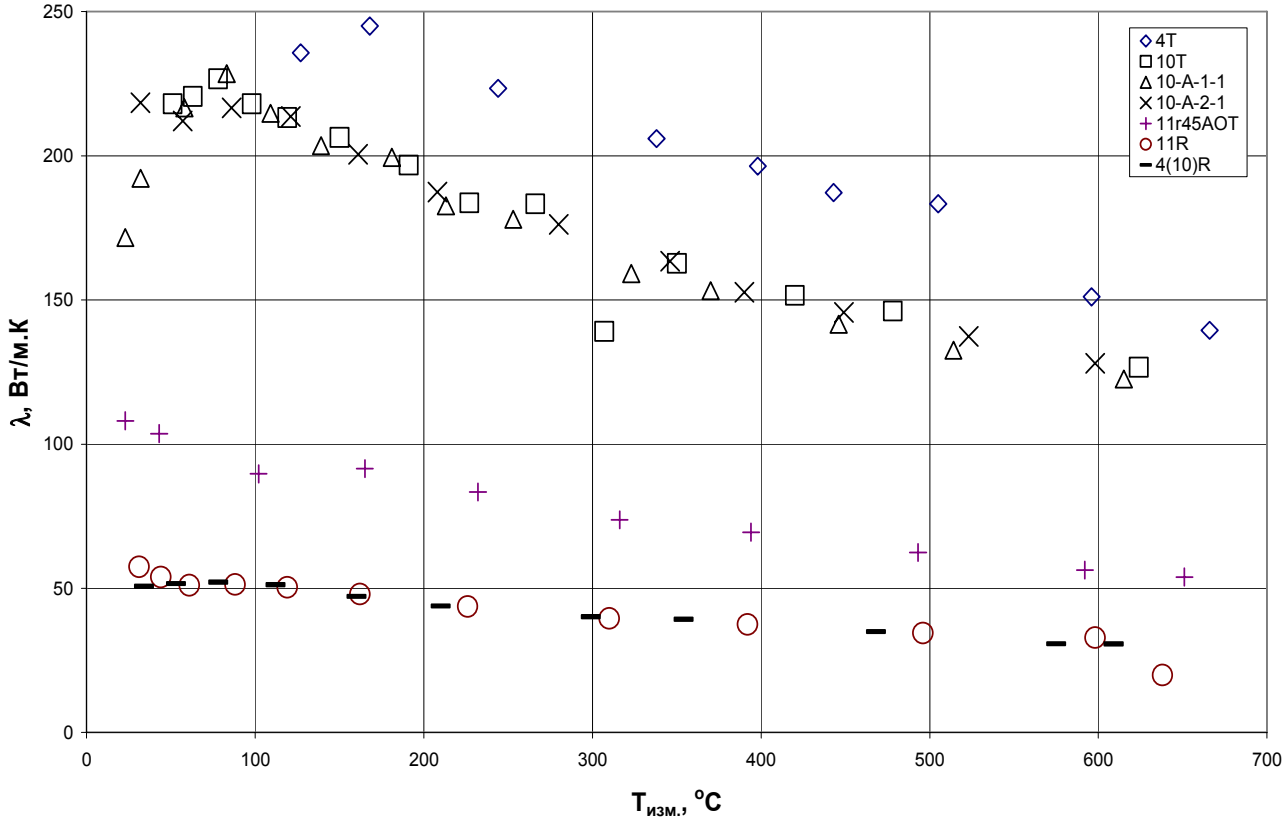

Fig. 12. Temperature dependence of the coefficient of thermal conductivity of investigated AC-150 graphite samples.

From the figures we can suggests that the coefficient of thermal conductivity of all samples logarithmically decreases with the increase in temperature measurement. As for its absolute values, it is intuitively seen a texture dependence (as well as for the value of electrical resistivity, but with opposite sign).

So, for samples with radial direction its minimum value is about 50 W/mK and for samples with tangential and axial cuttings it maxes out about 210-220 W/mK, with the value of the coefficient of thermal conductivity samples for these type of cuttings practically does not vary in terms of collected statistical data.

To adjust the texture dependence of this parameter a specific sample cut from billet № 11 at an angle of 45^{o} to the axis R was made. The value of its coefficient of thermal conductivity (100 W/mK) was about half lower than for samples of the axial and tangential directions of cuttings and about half more than the samples for the radial direction tenderloin (see Fig.12).

According to the results of these measurements a correlation between coefficient of thermal conductivity and electrical resistivity was built (see Fig.13).

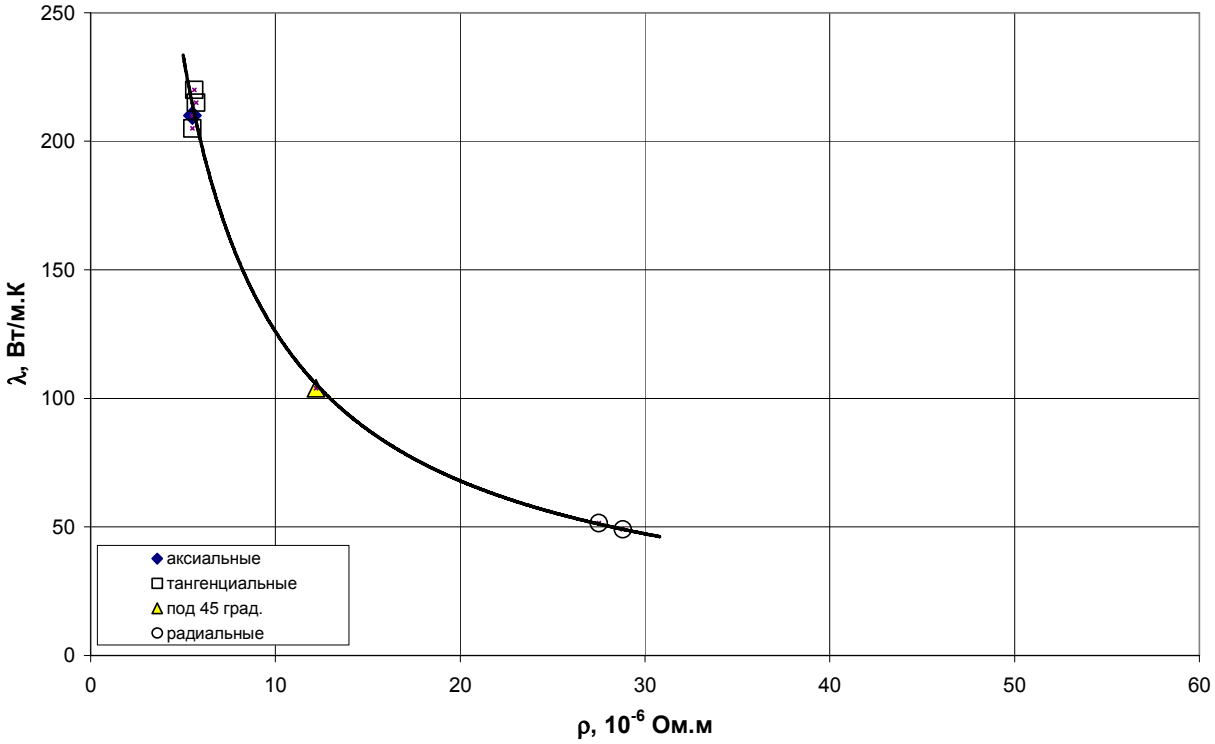

Fig.13. Correlation dependence between coefficient of thermal conductivity and electrical resistivity for AC-150 material.

5.2. Measurement of linear coefficient of thermal expansion (CTE).

Coefficient of thermal expansion (α) was measured using quartz dilatometer in the following temperature interval 20-700ºC. The research results of the value of coefficient of thermal expansion for AC-150 graphite samples are available in Fig.14 -15.

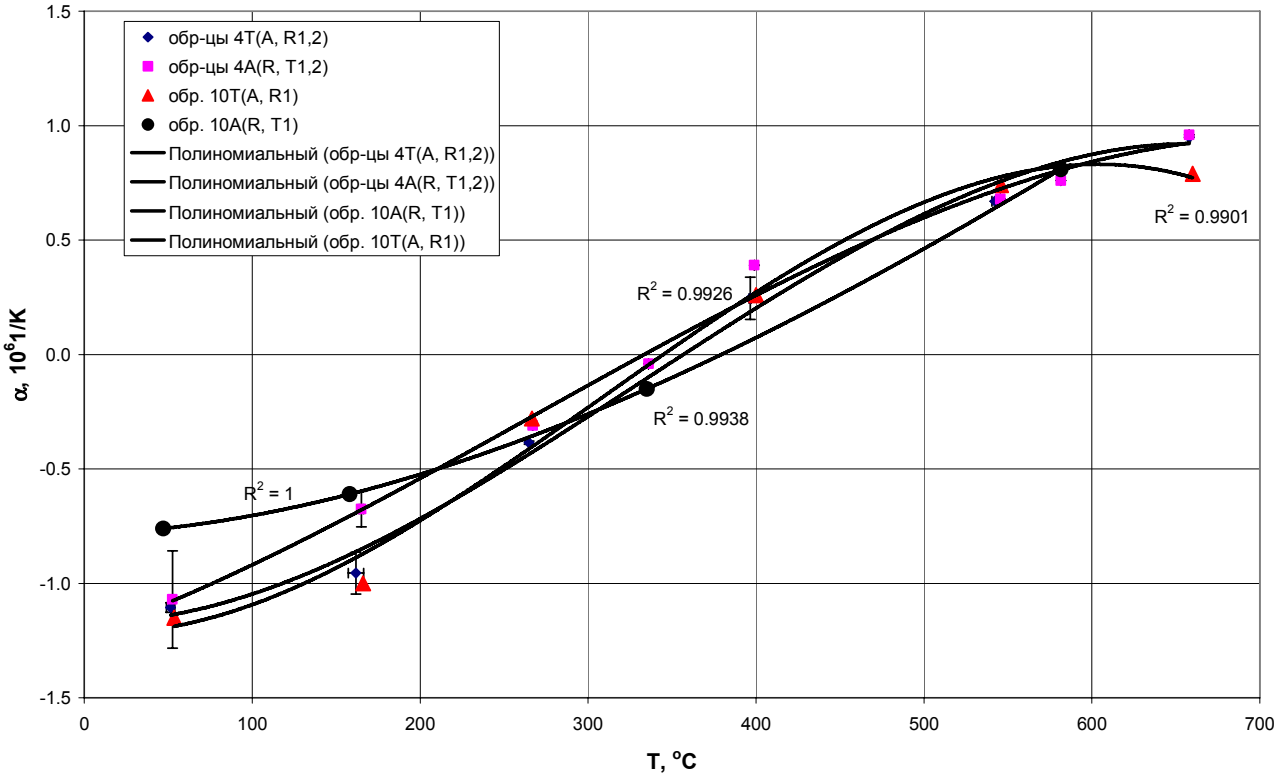

Fig.14. Investigated results of the value of coefficient of thermal expansion for AC-150 graphite samples.

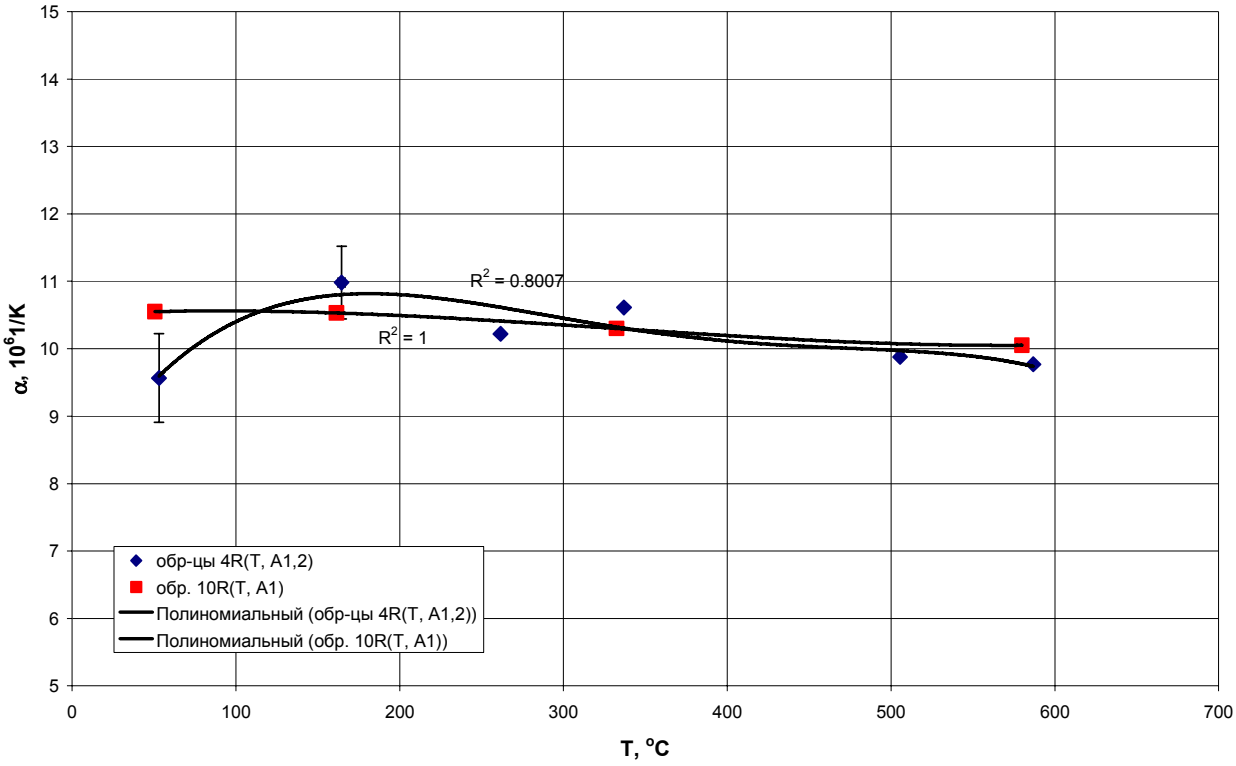

Fig.15. Investigated results of the value of thermal expansion coefficient for AC-150 graphite samples.

From figures 14 - 15 it follows that the value of CTE also greatly depends on the direction of cuttings of sample (texture dependence).

So, for samples of radial cuttings its value ($10.5*10^{-6}$ 1/K - at a measuring temperature 400 ºC) is about an order of magnitude higher than for samples with axial and tangential cuttings (0.15-0.3) 10^{-6} 1/K, though, in essence, these two directions differ little in terms of CTE value.

It worth mentioning that character of the temperature dependence of CTE varies significantly. Thus, for the samples with A and T directions CTE value grows smoothly with the increase in temperature of measurement, opposite to that the value of CTE for samples with R direction smoothly decreases. Moreover, for samples cut in A and T directions at a temperature of less than 350-400 ºC CTE is a negative value, and at 400 ºC it becomes zero. Such dependence of CTE values typical for monocrystals of graphite at its basis planes in the hexagonal crystal lattice (α_a). The value of CTE in the hexagonal direction (α_c) for monocrystal of graphite is equal to $27*10^{-6}$ 1/K.

6. Investigation of a texture of graphite samples.

Initial properties of AC-150 graphite from all 3 billets are very close (for corresponding cutting directions), indicating a fairly uniform material (the standard deviation does not exceed the value of 1-6%).

However, on various directions of cutting properties of graphite are dramatically different, that is a manifestation of its texture. The biggest differences are observed between the directions of R and T, A. The difference between tangential and axial directions cutting is significantly less or almost non-existent.

7. Performing a calculation of profile for radiation defects distribution and determination of optimal irradiation regime for the LHC graphite collimator materials under irradiation by proton beam from RRC-KI cyclotron with the energy up to the 35 MeV.

To study the impact of proton radiation on changes in physical-mechanical properties of LHC graphite collimator materials depending on the irradiation doses the optimal regimes should be selected to calculate the distribution profiles of the radiation defects and profiles of stopped protons for different energies of protons with a maximum energy of 35 MeV. The results of numerical calculations of profiles for distribution of primary radiation defects (vacancies) and profiles for stopped protons for different energies of protons and various doses of radiation graphite with protons at energies from 20 MeV to 35 MeV using displacement energy for atoms in graphite lattice (E_d = 28 eV) are presented at Fig.16 -18.

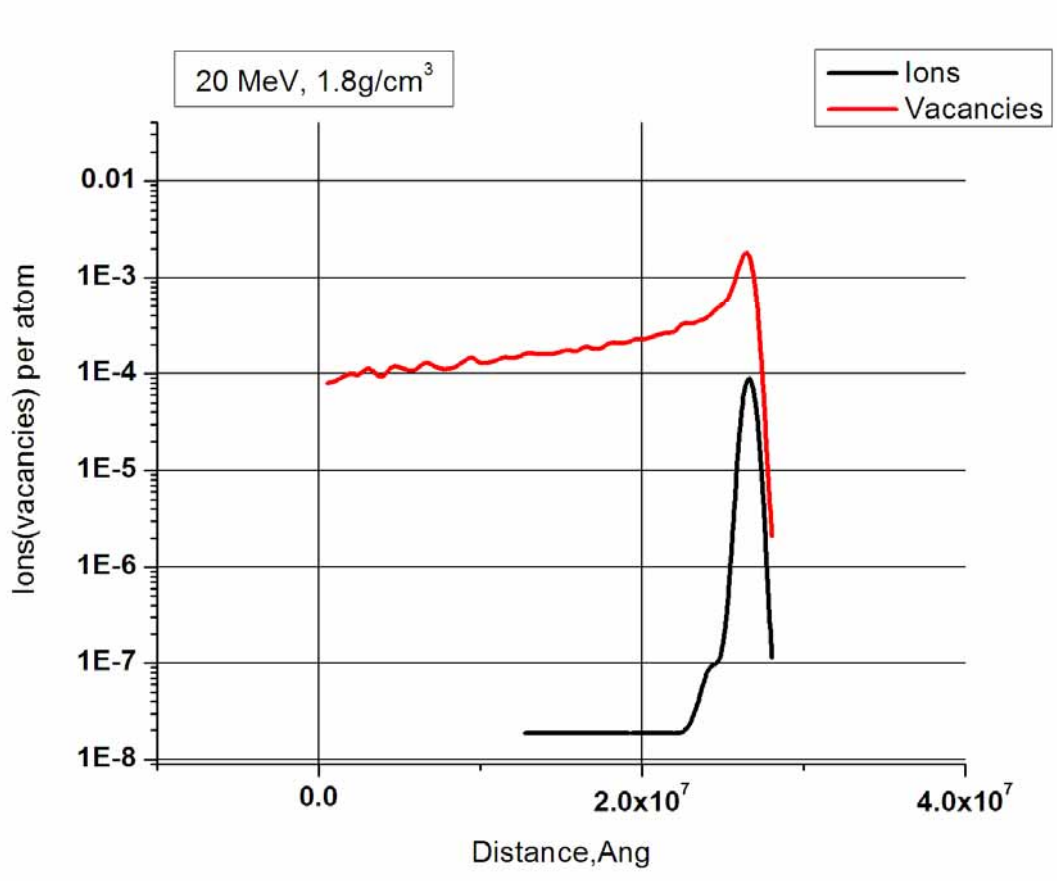

Fig. 16. Calculation results of profile distribution for primary radiation defects (vacancies, the red curve) and profile of stopped protons (black curve), depending on the penetration depth of protons in the graphite material with the density ρ_1 = 1.8 g/cm^3 under irradiation of protons with energy 20 MeV and the full dose of irradiation Φ = 10^{17} protons/cm^2. The levels of radiation damage presented here for D_{max} = 2.18 x10^{-3} dpa; D_{min} = 3.99 x10^{-7} dpa and <D> = 2.58 x10^{-4} dpa.

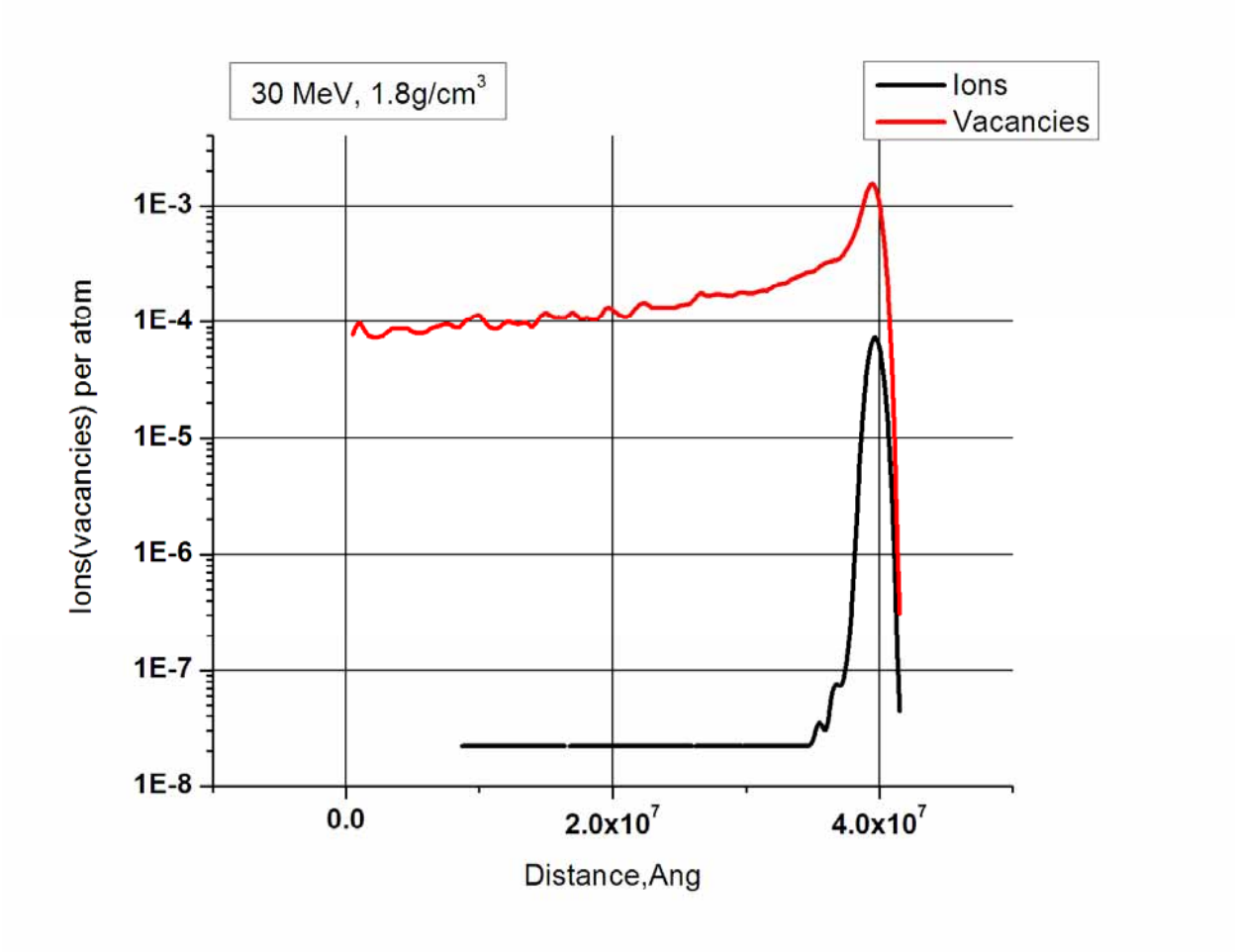

Fig. 17. Calculation results of profile distribution for primary radiation defects (vacancies, the red curve) and profile of stopped protons (black curve), depending on the penetration depth of protons in the graphite material with the density ρ_1 = 1.8 g/cm^3 under irradiation of protons with energy 25 MeV and the full dose of irradiation $\Phi = 10^{17}$ protons/cm^2. The levels of radiation damage presented here for $D_{max} = 1.72 \times 10^{-3}$ dpa; $D_{min} = 3.08 \times 10^{-7}$ dpa and $\langle D \rangle = 2.01 \times 10^{-4}$ dpa.

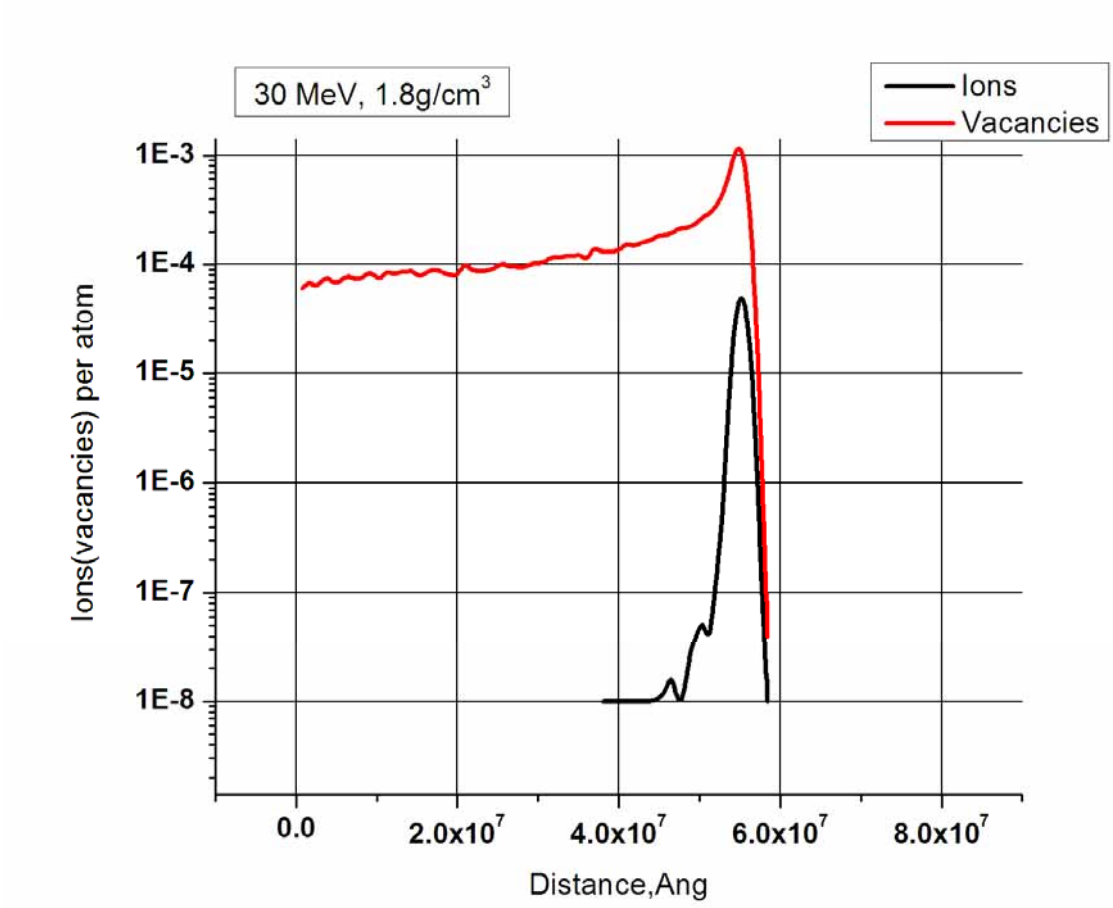

Fig. 18. Calculation results of profile distribution for primary radiation defects (vacancies, the red curve) and profile of stopped protons (black curve), depending on the penetration depth of protons in the graphite material with the density ρ_1 = 1.8 g/cm^3 under irradiation of protons with energy 30 MeV and the full dose of irradiation $\Phi = 10^{17}$ protons/cm^2. The levels of radiation damage presented here for $D_{max} = 1.23\times10^{-3}$ dpa; $D_{min} = 3.99\times10^{-8}$ dpa and $\langle D \rangle = 1.63\times10^{-4}$ dpa.

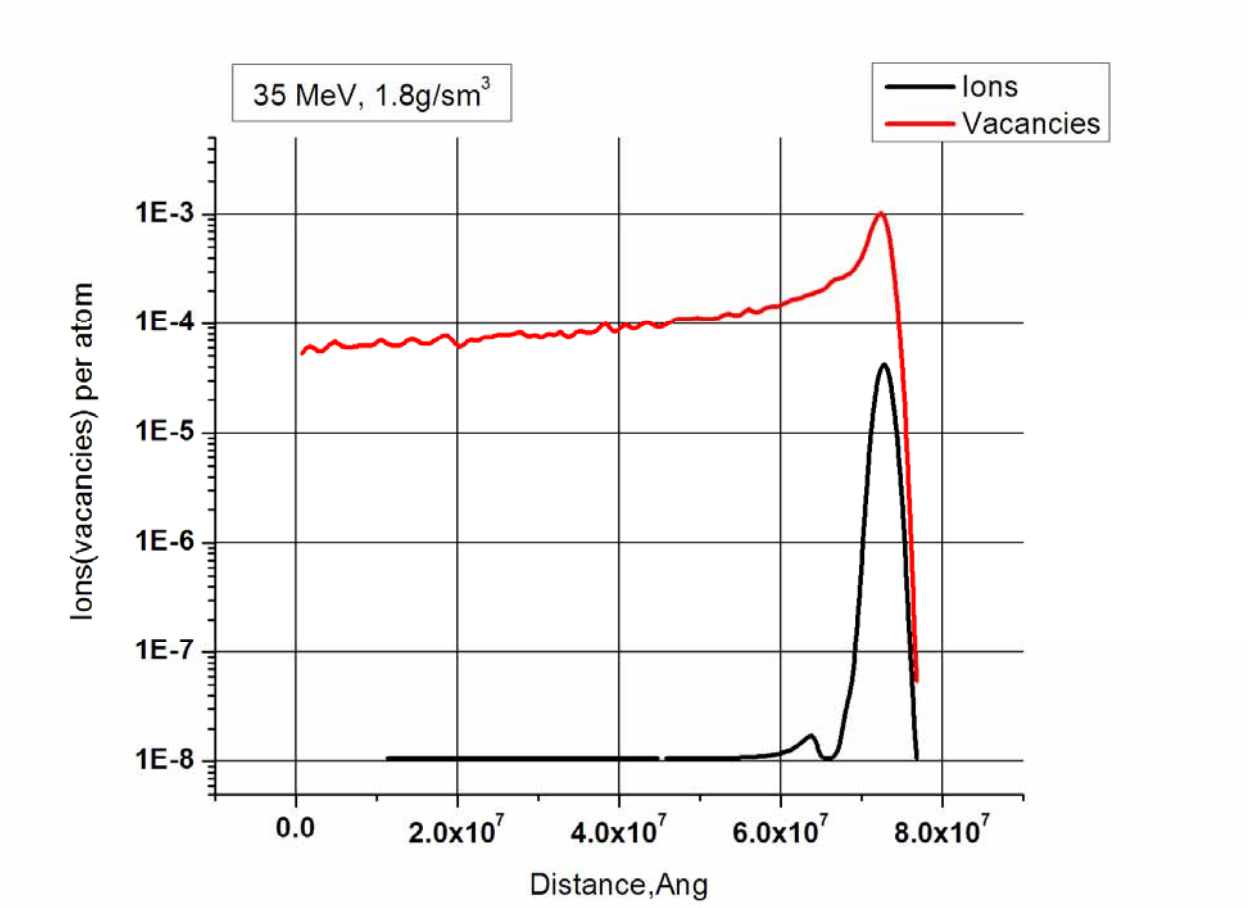

Fig. 19. Calculation results of profile distribution for primary radiation defects (vacancies, the red curve) and profile of stopped protons (black curve), depending on the penetration depth of protons in the graphite material with the density ρ_1 = 1.8 g/cm^3 under irradiation of protons with energy 35 MeV and the full dose of irradiation Φ = 10^{17} protons/cm^2. The levels of radiation damage presented here for D_{max} = 1.04x10^{-3} dpa; D_{min} = 5.37x10^{-8} dpa and <D> = 1.38x10^{-4} dpa.

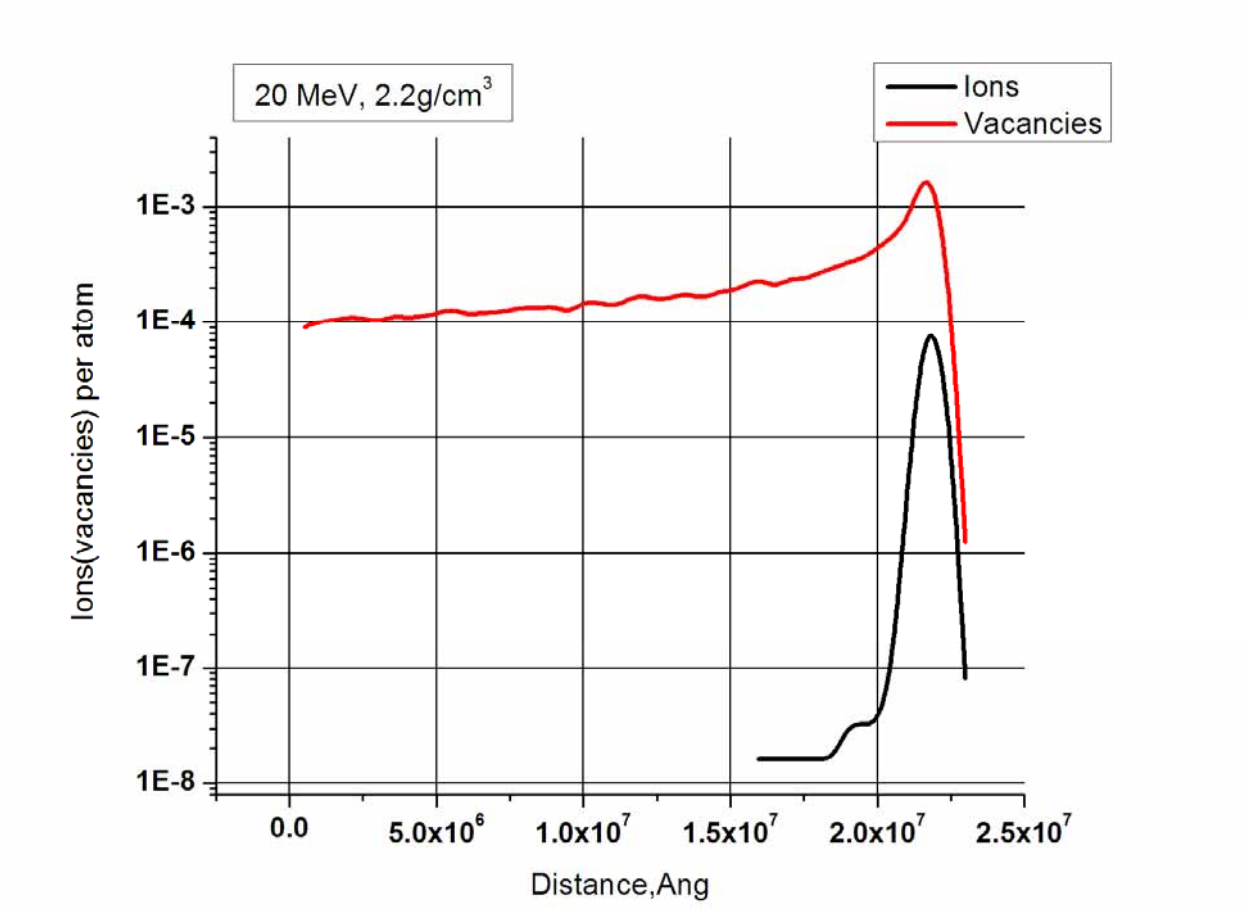

Fig. 20. Calculation results of profile distribution for primary radiation defects (vacancies, the red curve) and profile of stopped protons (black curve), depending on the penetration depth of protons in the graphite material with the density ρ_1 = 2.2 g/cm^3 under irradiation of protons with energy 20 MeV and the full dose of irradiation Φ = 10^{17} protons/cm^2. The levels of radiation damage presented here for D_{max} = 1.84x10^{-3} dpa; D_{min} = 1.25x10^{-6} dpa and <D> = 2.54x10^{-4} dpa.

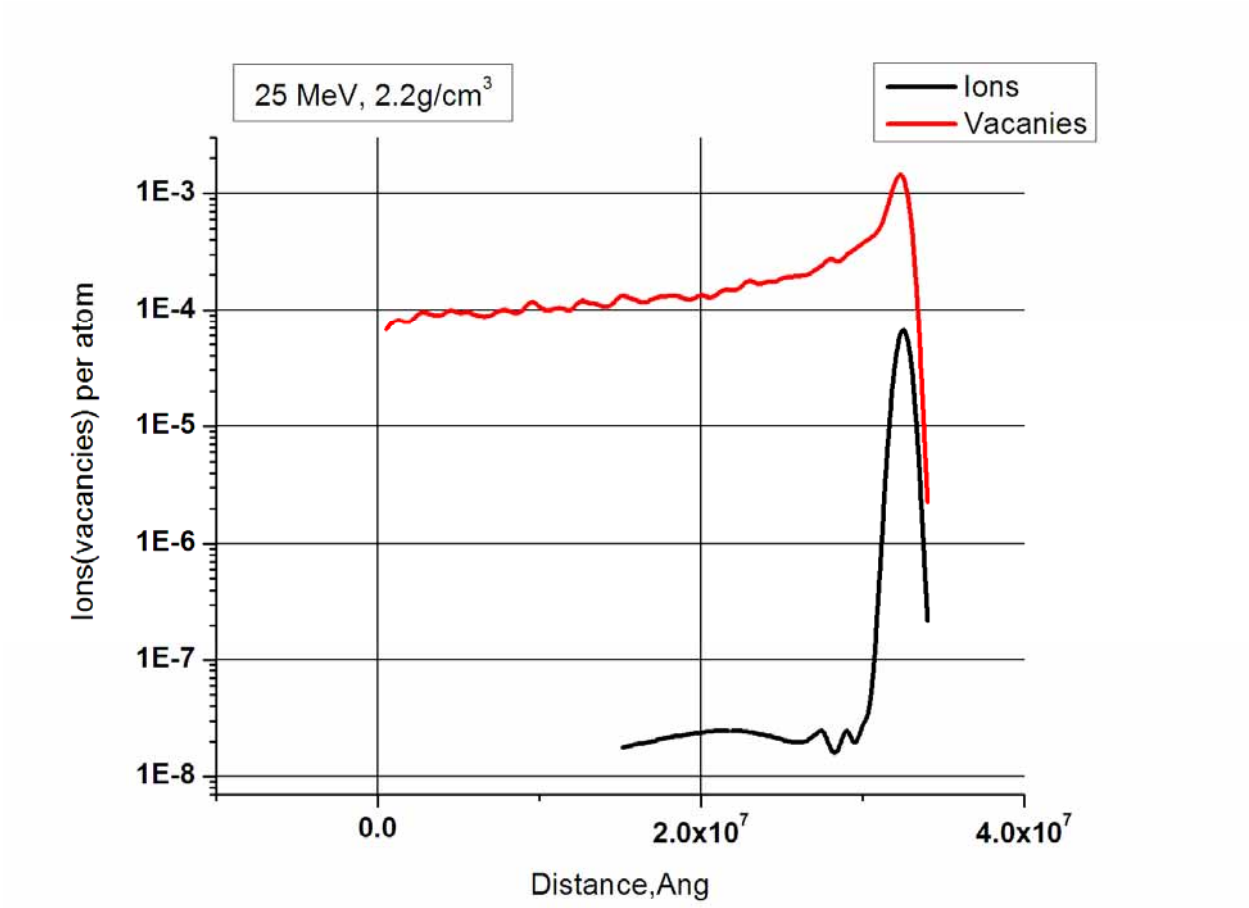

Fig. 21. Calculation results of profile distribution for primary radiation defects (vacancies, the red curve) and profile of stopped protons (black curve), depending on the penetration depth of protons in the graphite material with the density ρ_1 = 2.2 g/cm^3 under irradiation of protons with energy 25 MeV and the full dose of irradiation $\Phi = 10^{17}$ protons/cm^2. The levels of radiation damage presented here for $D_{max} = 1.61 \times 10^{-3}$ dpa; $D_{min} = 2.26 \times 10^{-6}$ dpa and $\langle D \rangle = 2.03 \times 10^{-4}$ dpa.

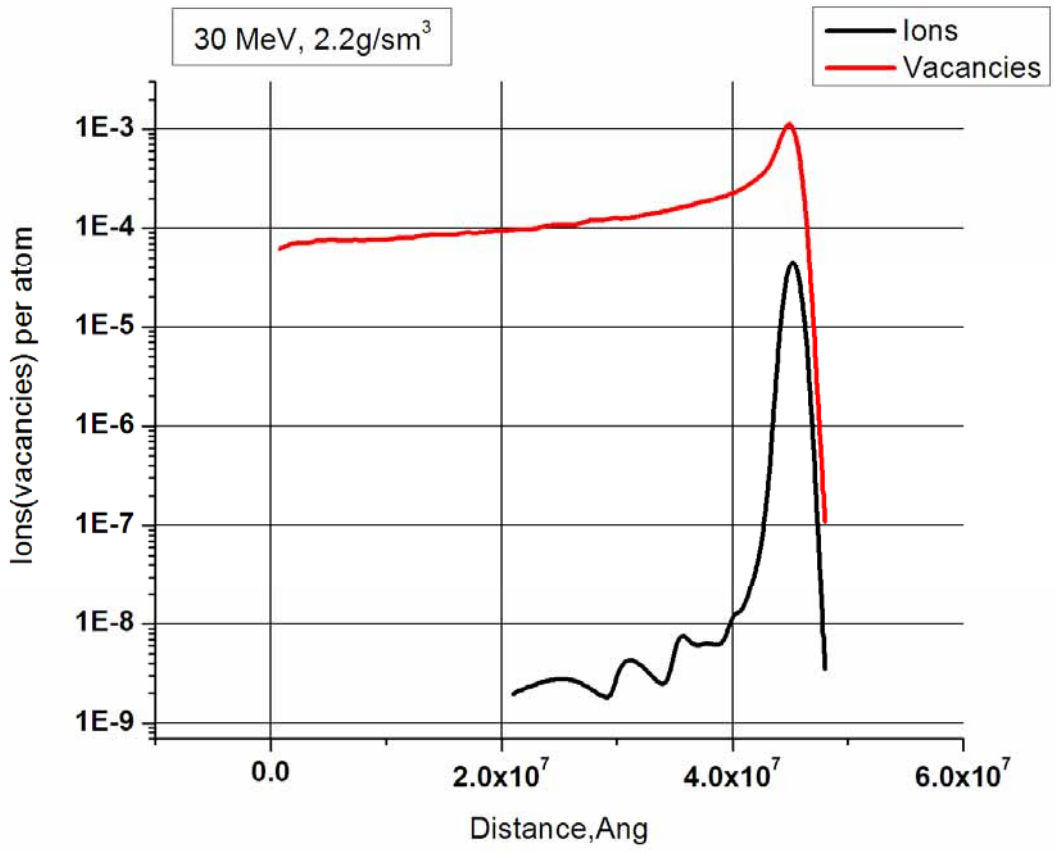

Fig. 22. Calculation results of profile distribution for primary radiation defects (vacancies, the red curve) and profile of stopped protons (black curve), depending on the penetration depth of protons in the graphite material with the density ρ_1 = 2.2 g/cm^3 under irradiation of protons with energy 30 MeV and the full dose of irradiation Φ = 10^{17} protons/cm^2. The levels of radiation damage presented here for D_{max} = 1.28x10^{-3} dpa; D_{min} = 1.08x10^{-7} dpa and <D> = 1.63x10^{-4} dpa.

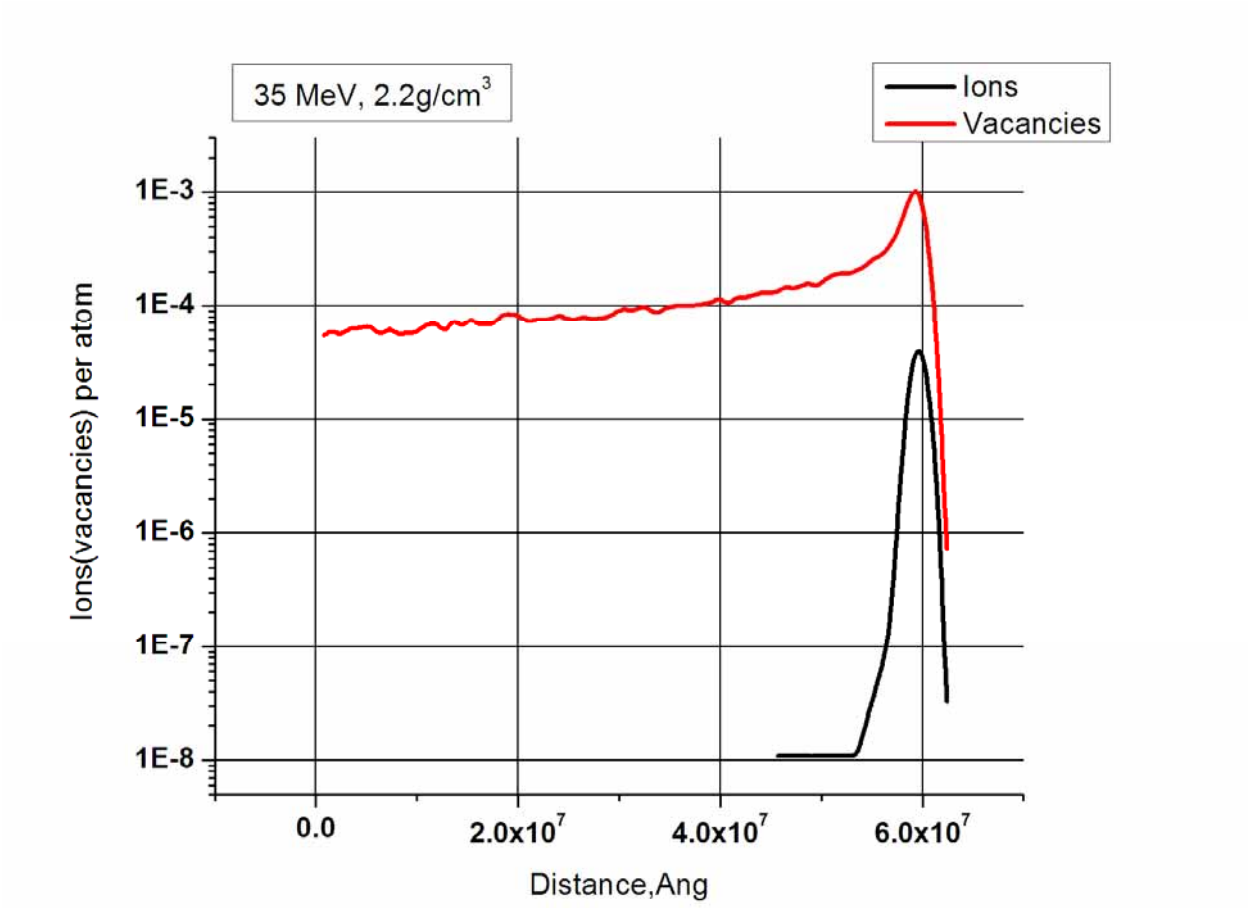

Fig. 23. Calculation results of profile distribution for primary radiation defects (vacancies, the red curve) and profile of stopped protons (black curve), depending on the penetration depth of protons in the graphite material with the density ρ_1 = 2.2 g/cm^3 under irradiation of protons with energy 35 MeV and the full dose of irradiation Φ = 10^{17} protons/cm^2. The levels of radiation damage presented here for D_{max} = 1.13x10^{-3} dpa; D_{min} = 7.3x10^{-8} dpa and <D> = 1.41x10^{-4} dpa.

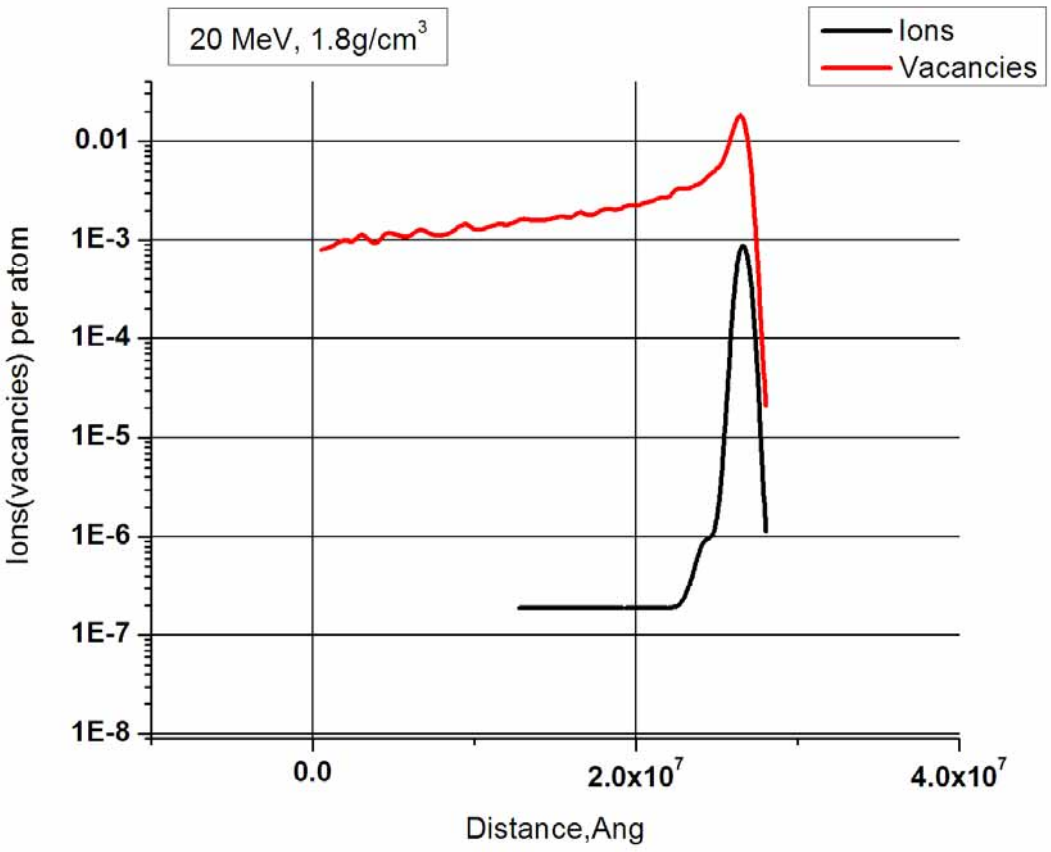

Fig. 24. Calculation results of profile distribution for primary radiation defects (vacancies, the red curve) and profile of stopped protons (black curve), depending on the penetration depth of protons in the graphite material with the density ρ_1 = 1.8 g/cm^3 under irradiation of protons with energy 20 MeV and the full dose of irradiation $\Phi = 10^{18}$ protons/cm^2. The levels of radiation damage presented here for $D_{max} = 2.18 \times 10^{-2}$ dpa; $D_{min} = 3.99 \times 10^{-7}$ dpa and $\langle D \rangle = 2.58 \times 10^{-3}$ dpa.

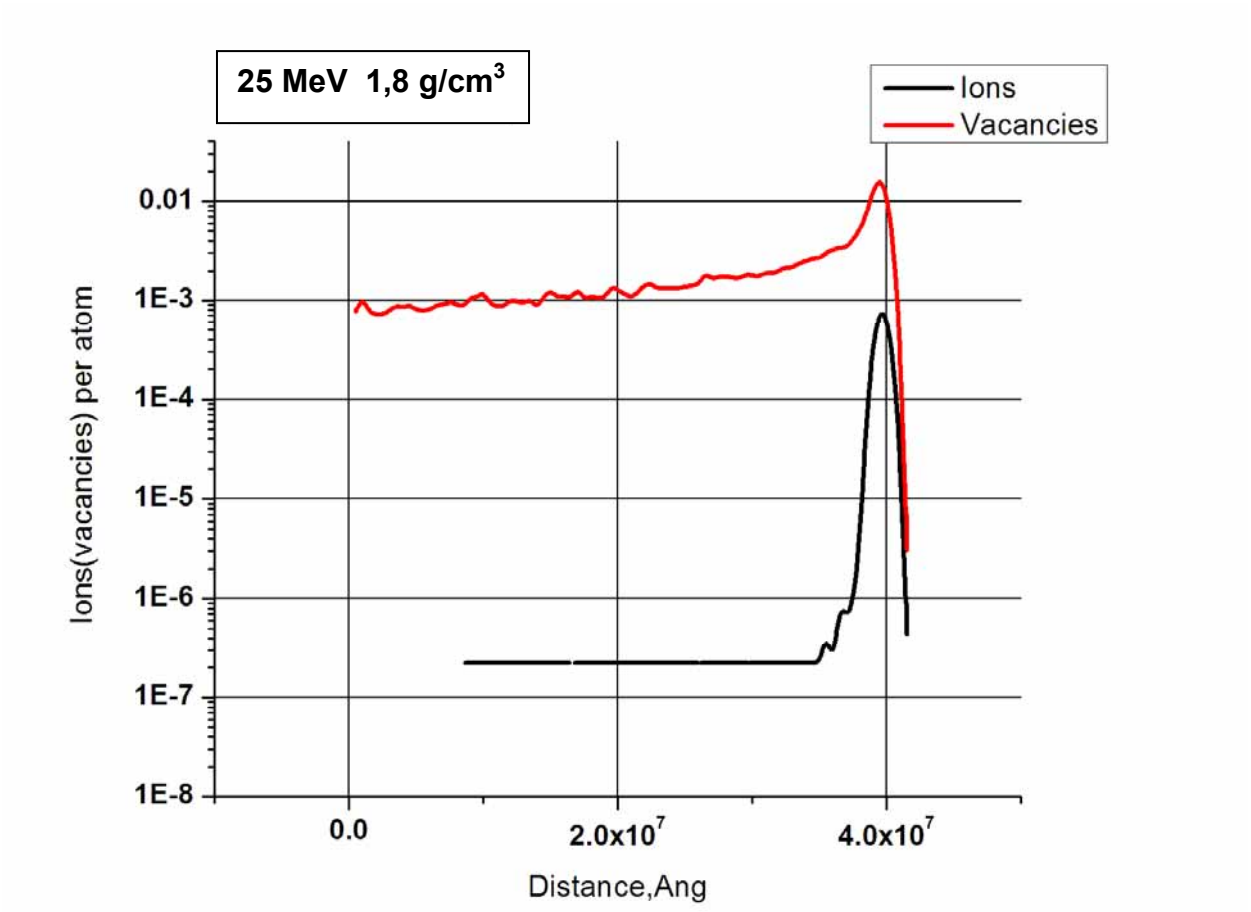

Fig. 25. Calculation results of profile distribution for primary radiation defects (vacancies, the red curve) and profile of stopped protons (black curve), depending on the penetration depth of protons in the graphite material with the density ρ_1 = 1.8 g/cm^3 under irradiation of protons with energy 25 MeV and the full dose of irradiation $\Phi = 10^{18}$ protons/cm^2. The levels of radiation damage presented here for $D_{max} = 1.72 \times 10^{-2}$ dpa; $D_{min} = 3.08 \times 10^{-6}$ dpa and $\langle D \rangle = 2.01 \times 10^{-3}$ dpa.

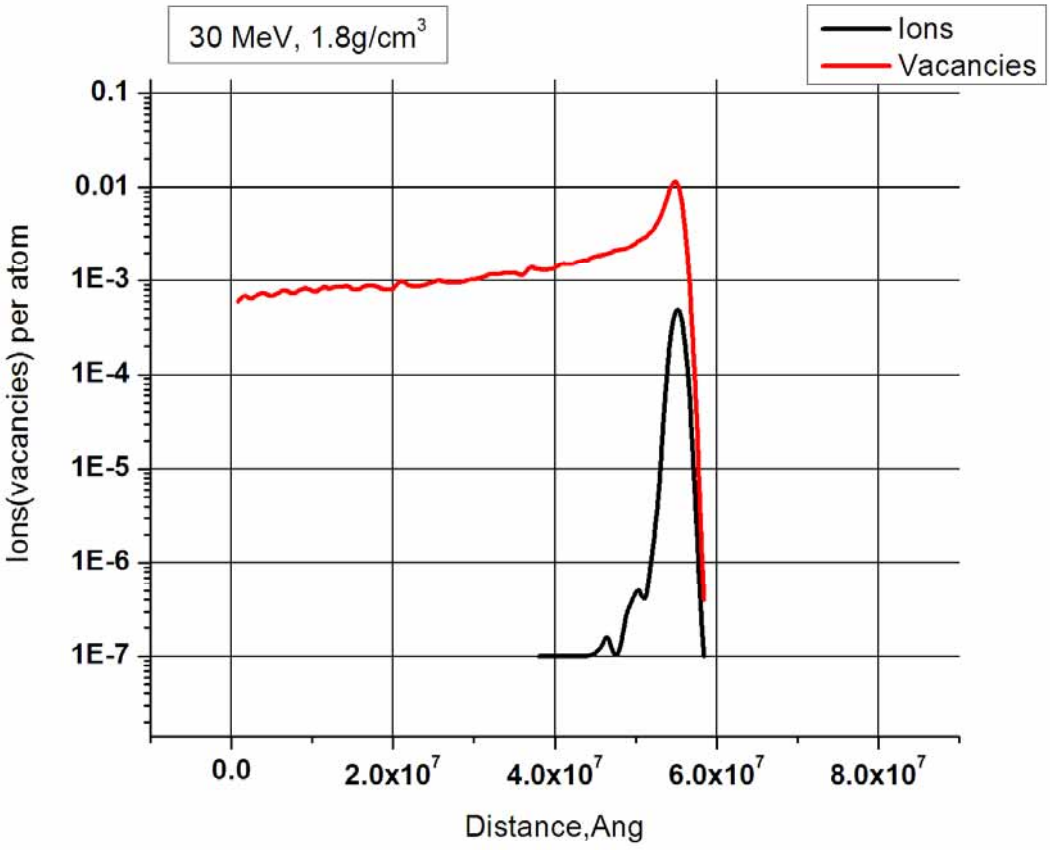

Fig. 26. Calculation results of profile distribution for primary radiation defects (vacancies, the red curve) and profile of stopped protons (black curve), depending on the penetration depth of protons in the graphite material with the density ρ_1 = 1.8 g/cm^3 under irradiation of protons with energy 30 MeV and the full dose of irradiation Φ = 10^{18} protons/cm^2. The levels of radiation damage presented here for D_{max} = 1.23x10^{-2} dpa; D_{min} = 3.99x10^{-7} dpa and <D> = 1.63x10^{-3} dpa.

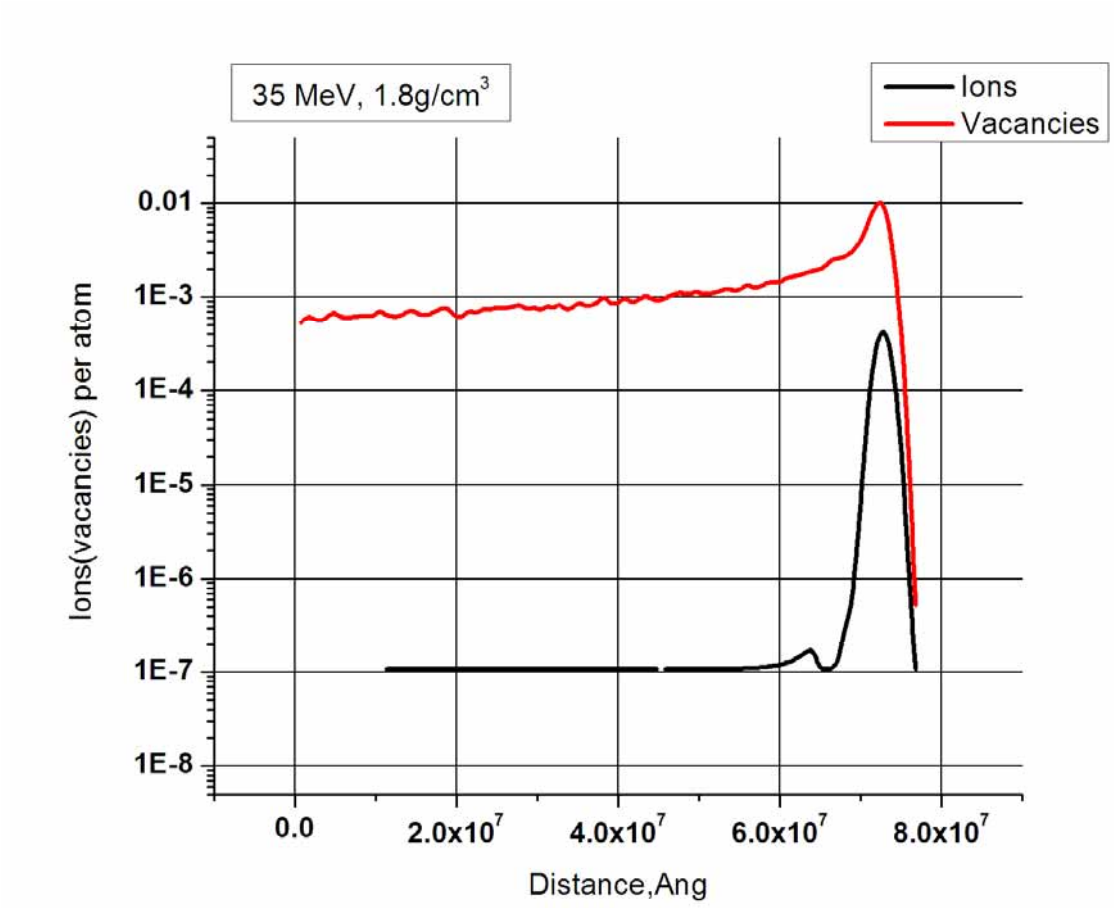

Fig. 27. Calculation results of profile distribution for primary radiation defects (vacancies, the red curve) and profile of stopped protons (black curve), depending on the penetration depth of protons in the graphite material with the density ρ_1 = 1.8 g/cm^3 under irradiation of protons with energy 35 MeV and the full dose of irradiation $\Phi = 10^{18}$ protons/cm^2. The levels of radiation damage presented here for $D_{max} = 1.04 \times 10^{-2}$ dpa; $D_{min} = 5.37 \times 10^{-7}$ dpa and $\langle D \rangle = 1.38 \times 10^{-3}$ dpa.

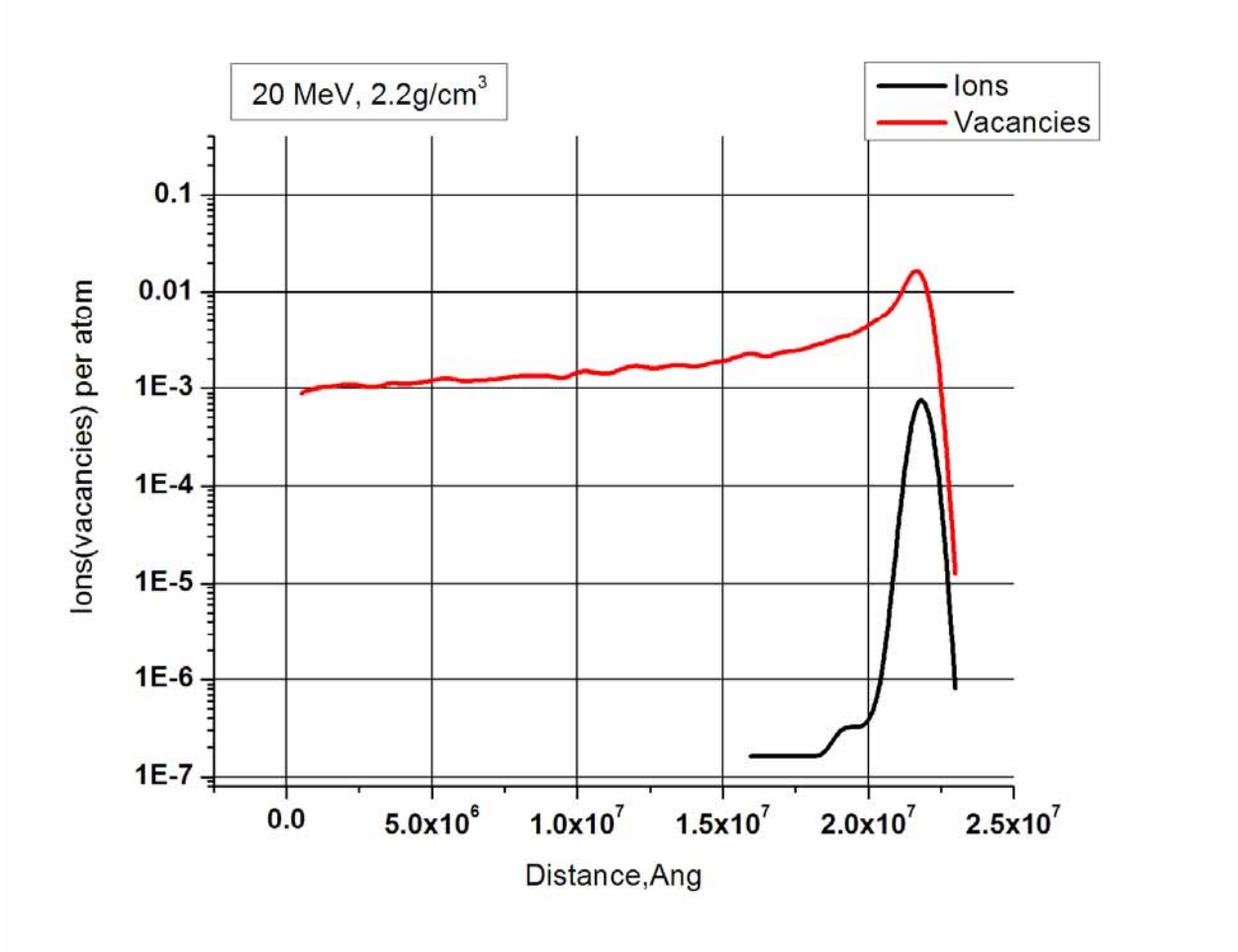

Fig. 28. Calculation results of profile distribution for primary radiation defects (vacancies, the red curve) and profile of stopped protons (black curve), depending on the penetration depth of protons in the graphite material with the density ρ_1 = 2.2 g/cm^3 under irradiation of protons with energy 20 MeV and the full dose of irradiation Φ = 10^{18} protons/cm^2. The levels of radiation damage presented here for D_{max} = 1.84x10^{-2} dpa; D_{min} = 1.25x10^{-5} dpa and <D> = 2.54x10^{-3} dpa.

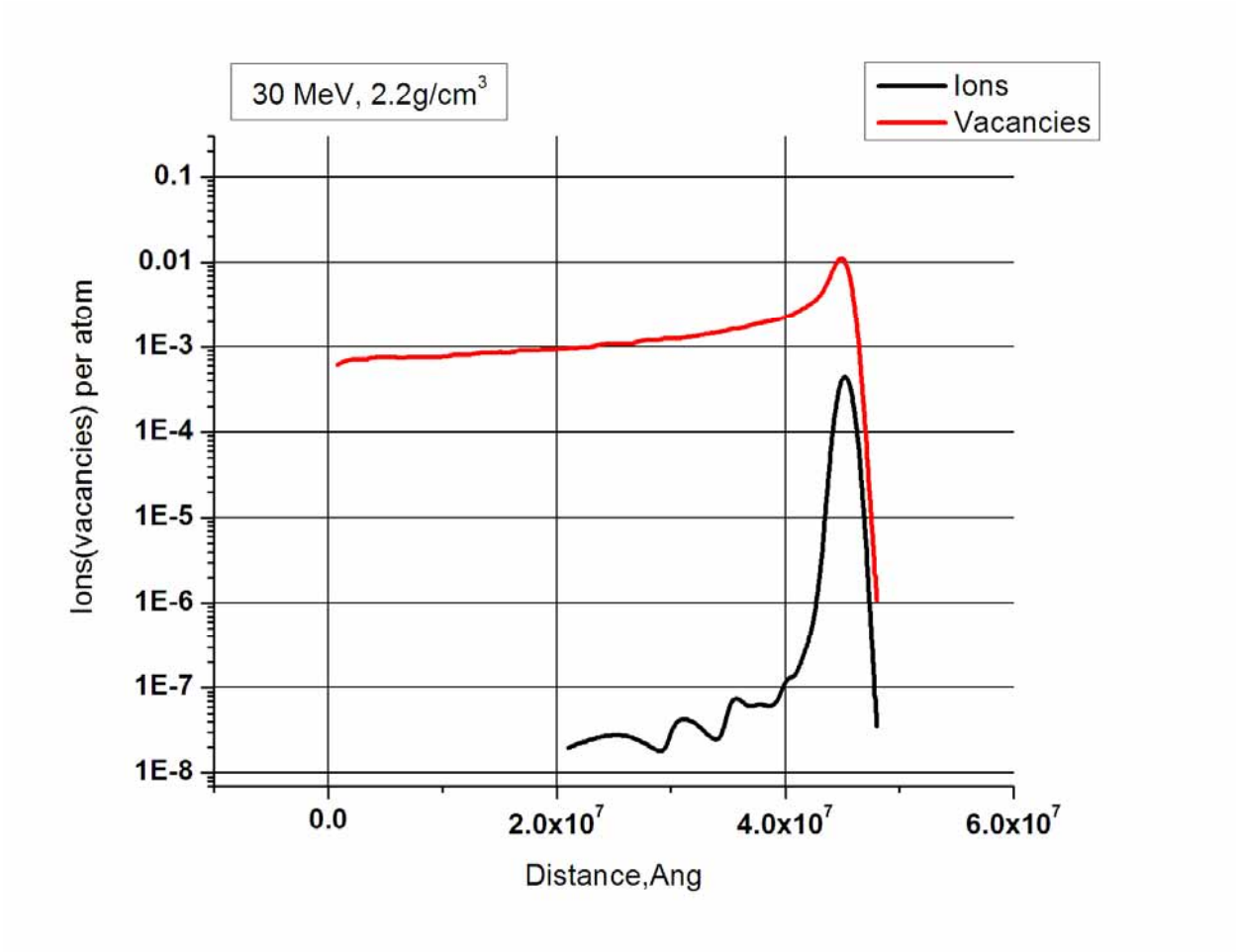

Fig. 29. Calculation results of profile distribution for primary radiation defects (vacancies, the red curve) and profile of stopped protons (black curve), depending on the penetration depth of protons in the graphite material with the density ρ_1 = 2.2 g/cm^3 under irradiation of protons with energy 25 MeV and the full dose of irradiation Φ = 10^{18} protons/cm^2. The levels of radiation damage presented here for D_{max} = 1.61x10^{-2} dpa; D_{min} = 2.26x10^{-5} dpa and <D> = 2.03x10^{-3} dpa.

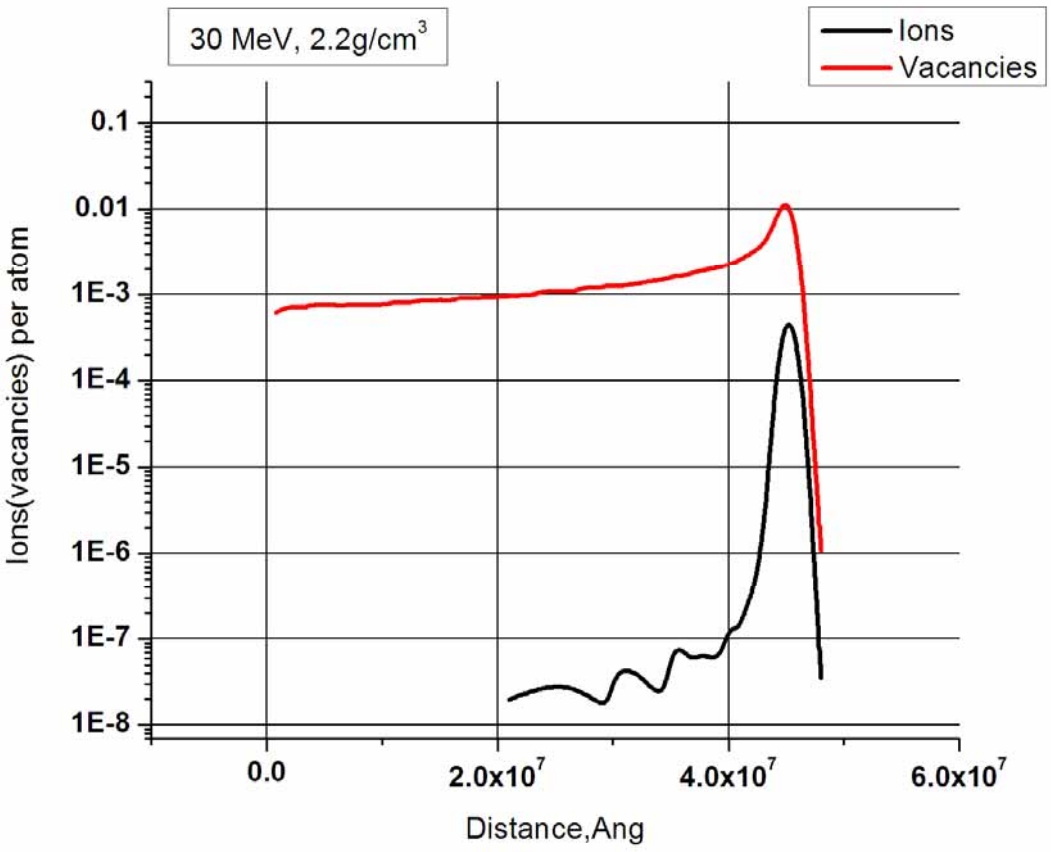

Fig. 30. Calculation results of profile distribution for primary radiation defects (vacancies, the red curve) and profile of stopped protons (black curve), depending on the penetration depth of protons in the graphite material with the density ρ_1 = 2.2 g/cm^3 under irradiation of protons with energy 30 MeV and the full dose of irradiation Φ = 10^{18} protons/cm^2. The levels of radiation damage presented here for D_{max} = 1.28x10^{-2} dpa; D_{min} = 1.08x10^{-6} dpa and <D> = 1.63x10^{-3} dpa.

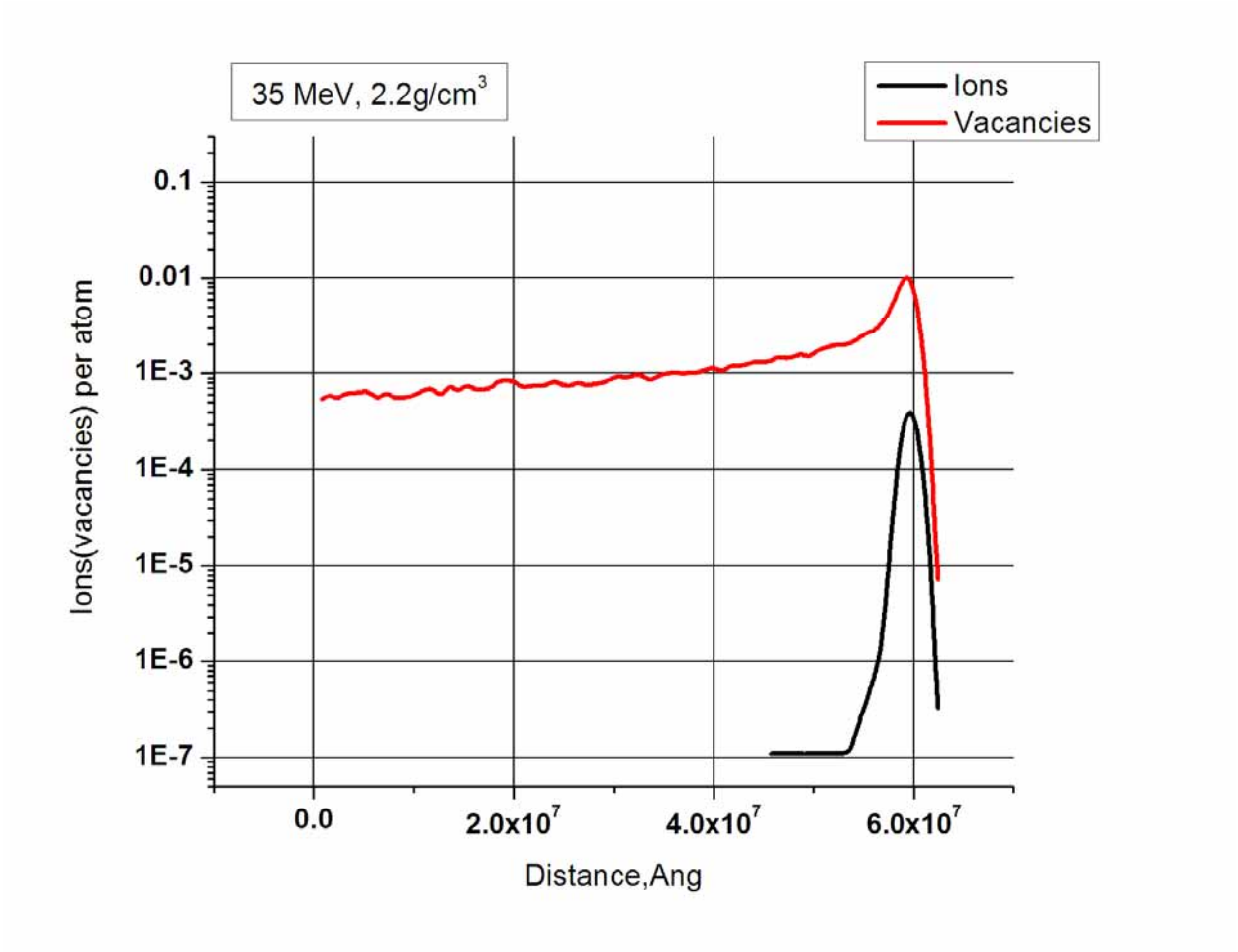

Fig. 31. Calculation results of profile distribution for primary radiation defects (vacancies, the red curve) and profile of stopped protons (black curve), depending on the penetration depth of protons in the graphite material with the density ρ_1 = 2.2 g/cm^3 under irradiation of protons with energy 35 MeV and the full dose of irradiation Φ = 10^{18} protons/cm^2. The levels of radiation damage presented here for D_{max} = 1.13x10^{-2} dpa; D_{min} = 7.3x10^{-7} dpa and <D> = 1.41x10^{-3} dpa.

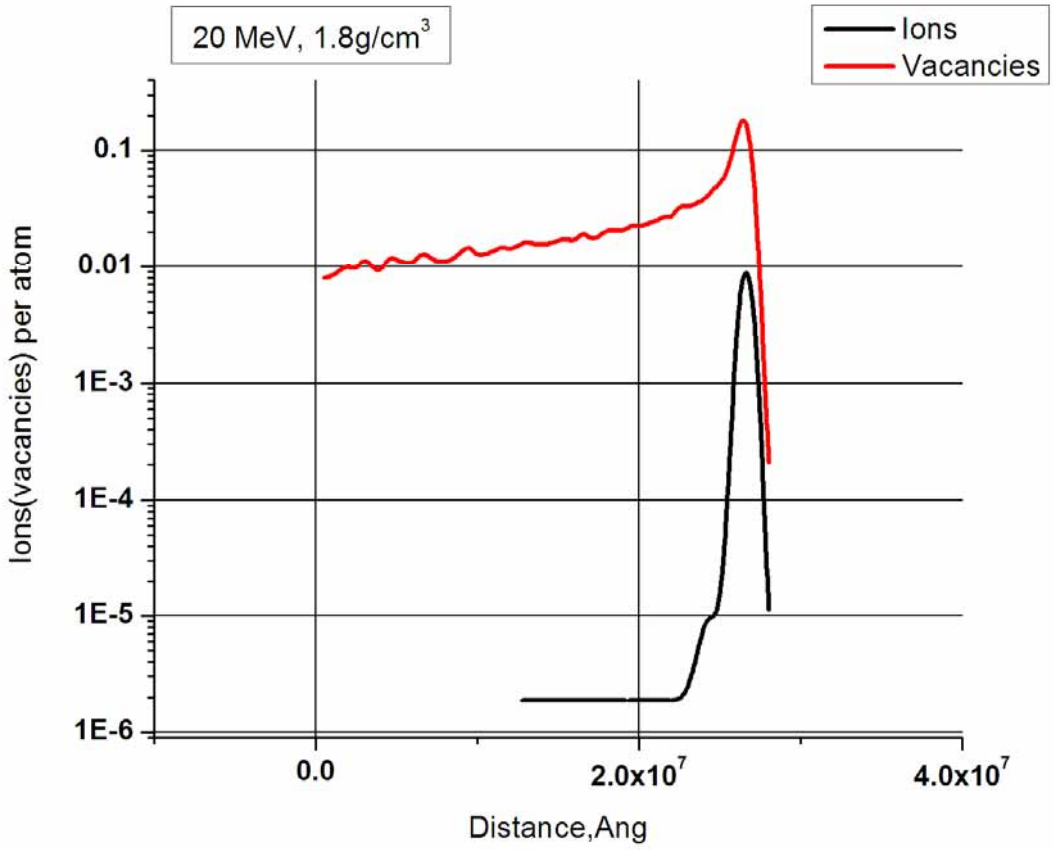

Fig. 32. Calculation results of profile distribution for primary radiation defects (vacancies, the red curve) and profile of stopped protons (black curve), depending on the penetration depth of protons in the graphite material with the density ρ_1 = 1.8 g/cm^3 under irradiation of protons with energy 20 MeV and the full dose of irradiation $\Phi = 10^{19}$ protons/cm^2. The levels of radiation damage presented here for D_{max} = 0.218 dpa; D_{min} = 3.99 x10^{-6} dpa and <D> = 2.58 x10^{-2} dpa.

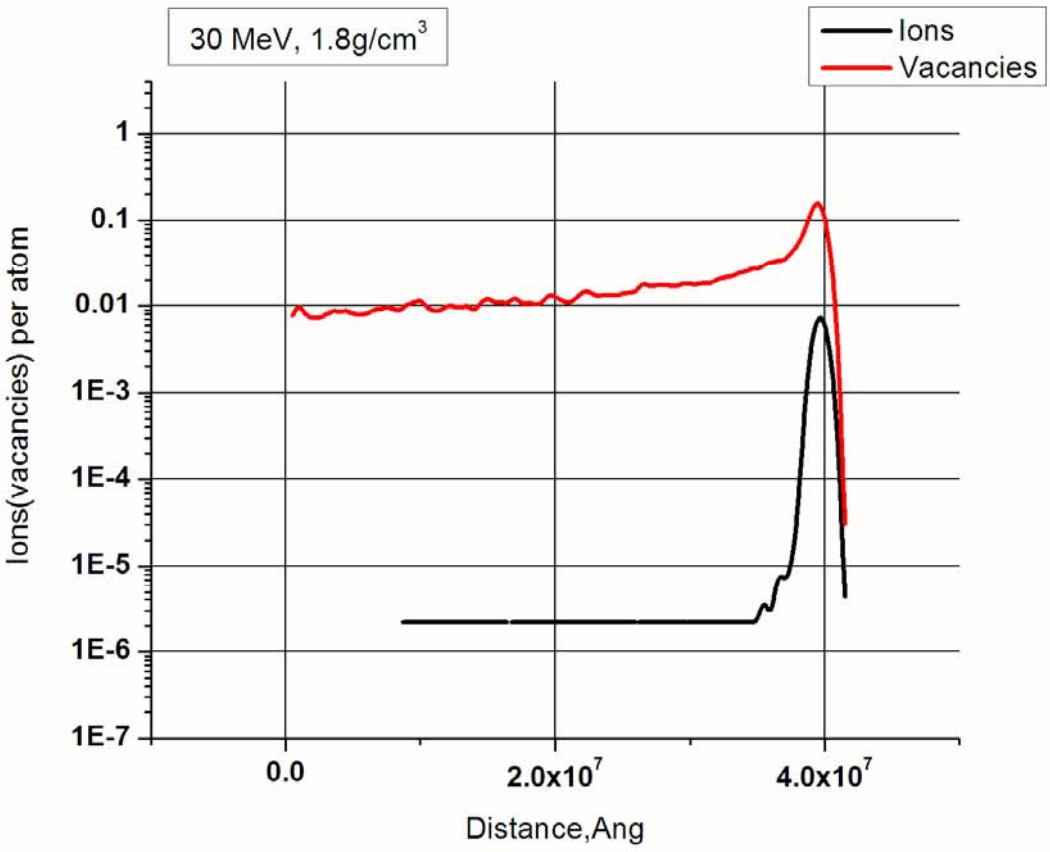

Fig. 33. Calculation results of profile distribution for primary radiation defects (vacancies, the red curve) and profile of stopped protons (black curve), depending on the penetration depth of protons in the graphite material with the density ρ_1 = 1.8 g/cm^3 under irradiation of protons with energy 25 MeV and the full dose of irradiation Φ = 10^{19} protons/cm^2. The levels of radiation damage presented here for D_{max} = 0.172 dpa; D_{min} = 3.08x10^{-5} dpa and <D> = 2.01x10^{-2} dpa.

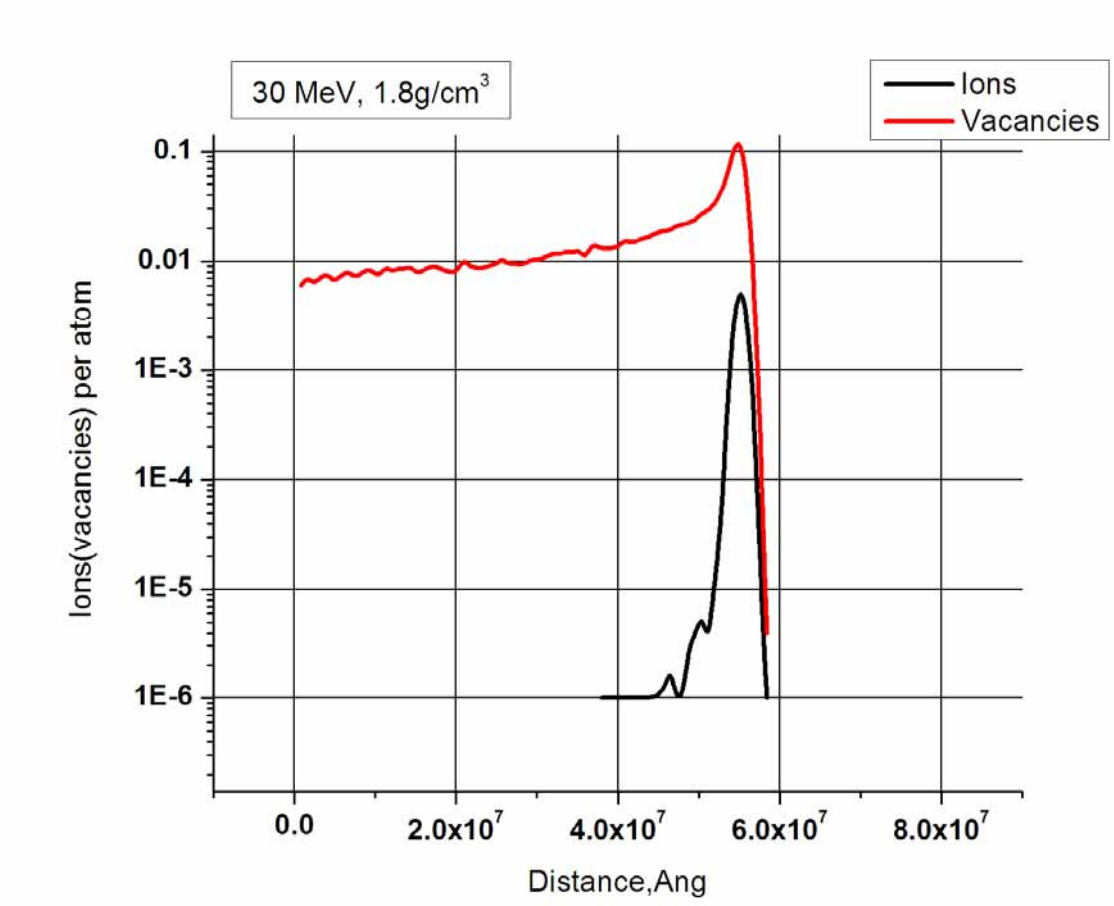

Fig. 34. Calculation results of profile distribution for primary radiation defects (vacancies, the red curve) and profile of stopped protons (black curve), depending on the penetration depth of protons in the graphite material with the density ρ_1 = 1.8 g/cm^3 under irradiation of protons with energy 30 MeV and the full dose of irradiation $\Phi = 10^{19}$ protons/cm^2. The levels of radiation damage presented here for D_{max} = 0.123 dpa; $D_{min} = 3.99 \times 10^{-6}$ dpa and $\langle D \rangle = 1.63 \times 10^{-2}$ dpa.

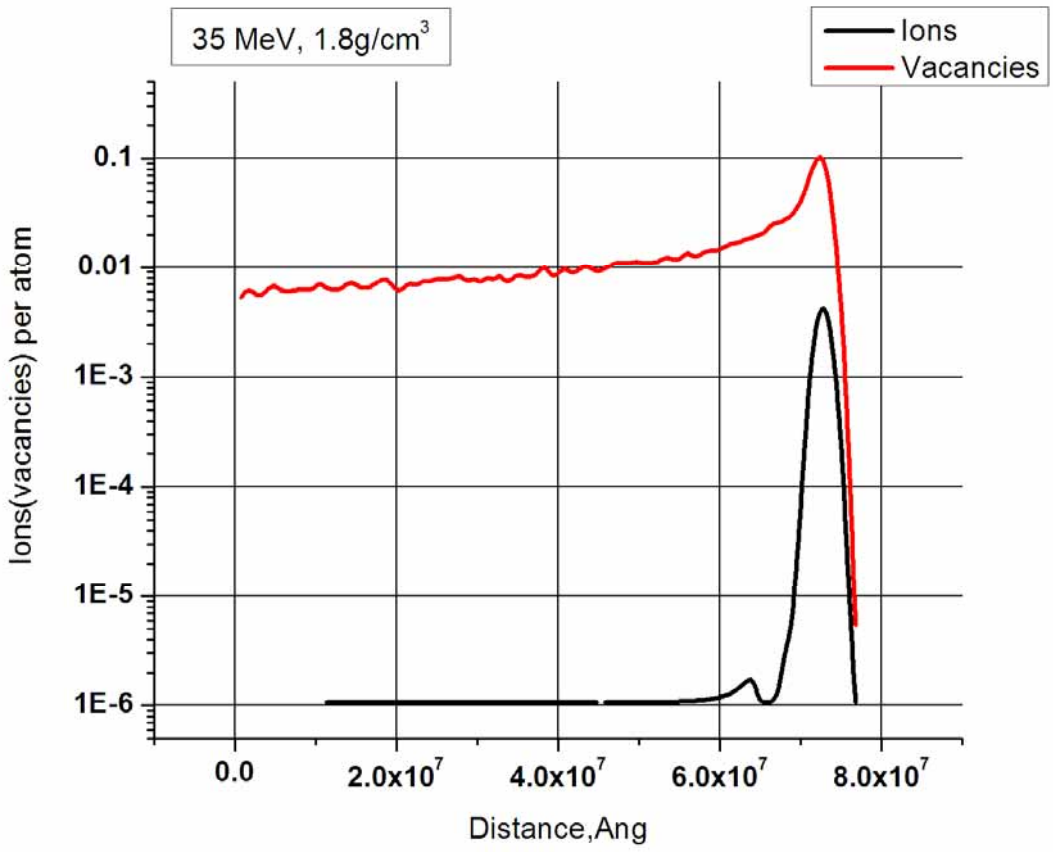

Fig. 35. Calculation results of profile distribution for primary radiation defects (vacancies, the red curve) and profile of stopped protons (black curve), depending on the penetration depth of protons in the graphite material with the density ρ_1 = 1.8 g/cm^3 under irradiation of protons with energy 35 MeV and the full dose of irradiation Φ = 10^{19} protons/cm^2. The levels of radiation damage presented here for D_{max} = 0.104 dpa; D_{min} = 5.37x10^{-6} dpa and <D> = 1.38x10^{-2} dpa.

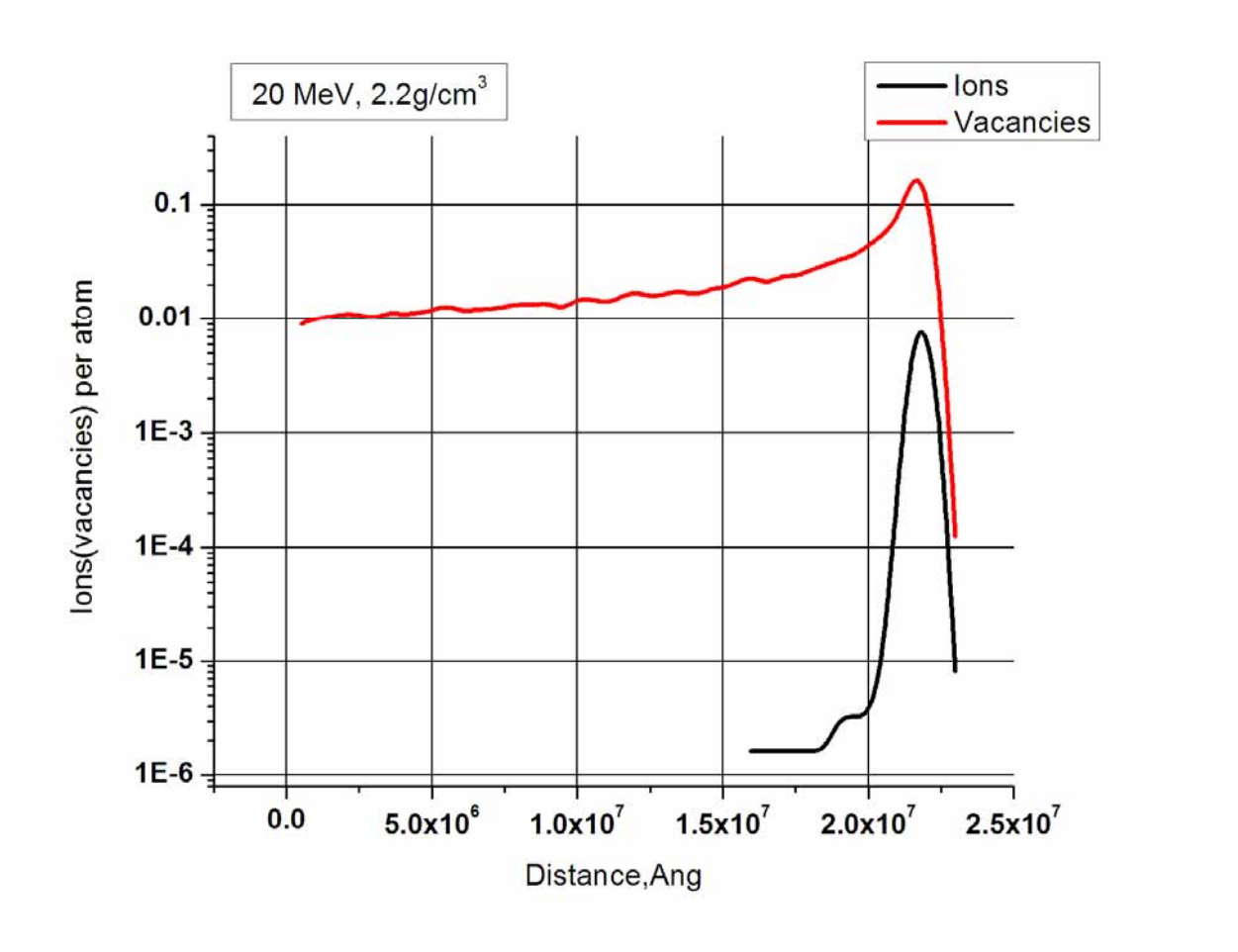

Fig. 36. Calculation results of profile distribution for primary radiation defects (vacancies, the red curve) and profile of stopped protons (black curve), depending on the penetration depth of protons in the graphite material with the density ρ_1 = 2.2 g/cm^3 under irradiation of protons with energy 20 MeV and the full dose of irradiation Φ = 10^{19} protons/cm^2. The levels of radiation damage presented here for D_{max} = 0.184 dpa; D_{min} = 1.25x10^{-4} dpa and <D> = 2.54x10^{-2} dpa.

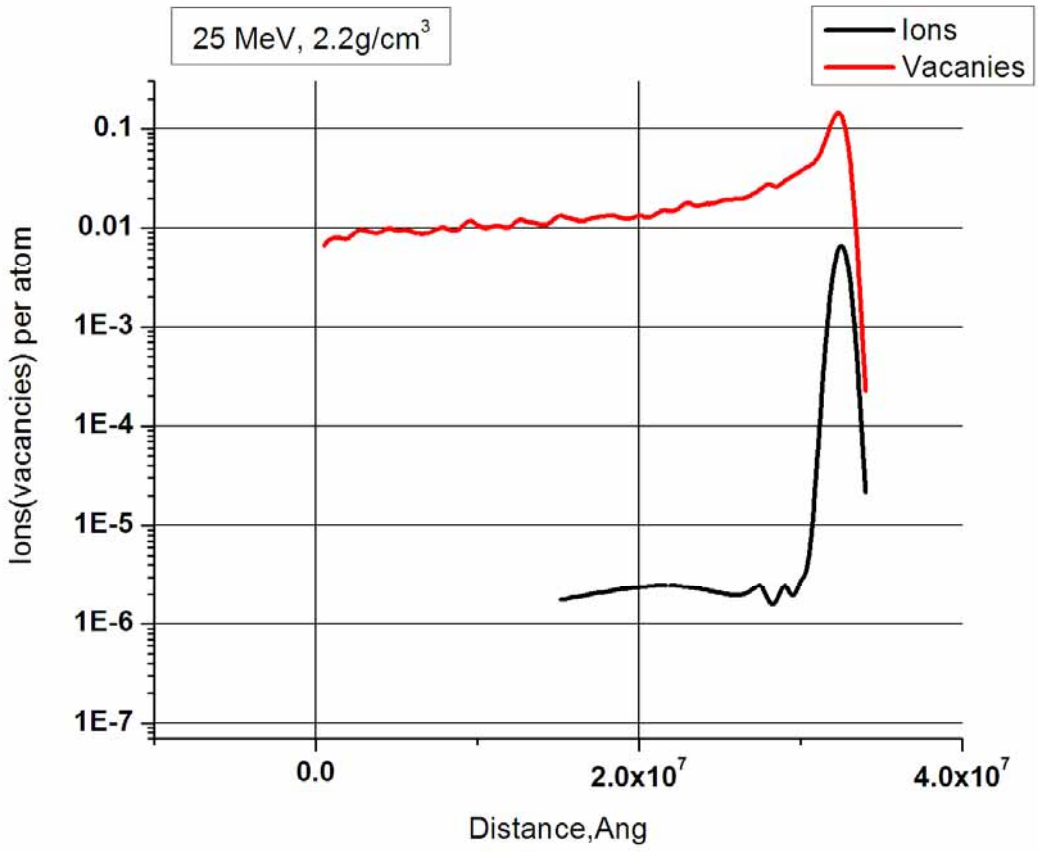

Fig. 37. Calculation results of profile distribution for primary radiation defects (vacancies, the red curve) and profile of stopped protons (black curve), depending on the penetration depth of protons in the graphite material with the density ρ_1 = 2.2 g/cm^3 under irradiation of protons with energy 25 MeV and the full dose of irradiation Φ = 10^{19} protons/cm^2. The levels of radiation damage presented here for D_{max} = 0.161 dpa; D_{min} = 2.26x10^{-4} dpa and <D> = 2.03x10^{-2} dpa.

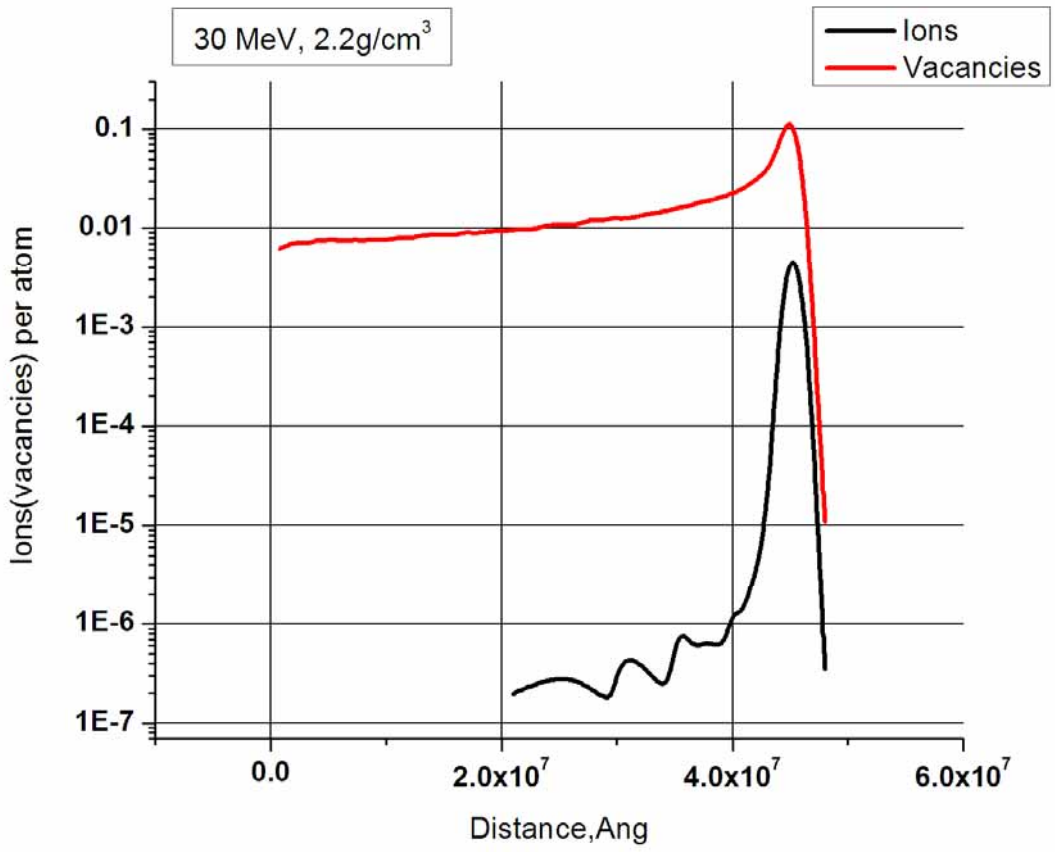

Fig. 38. Calculation results of profile distribution for primary radiation defects (vacancies, the red curve) and profile of stopped protons (black curve), depending on the penetration depth of protons in the graphite material with the density ρ_1 = 2.2 g/cm^3 under irradiation of protons with energy 30 MeV and the full dose of irradiation Φ = 10^{19} protons/cm^2. The levels of radiation damage presented here for D_{max} = 0.128 dpa; D_{min} = 1.08x10^{-5} dpa and <D> = 1.63x10^{-2} dpa.

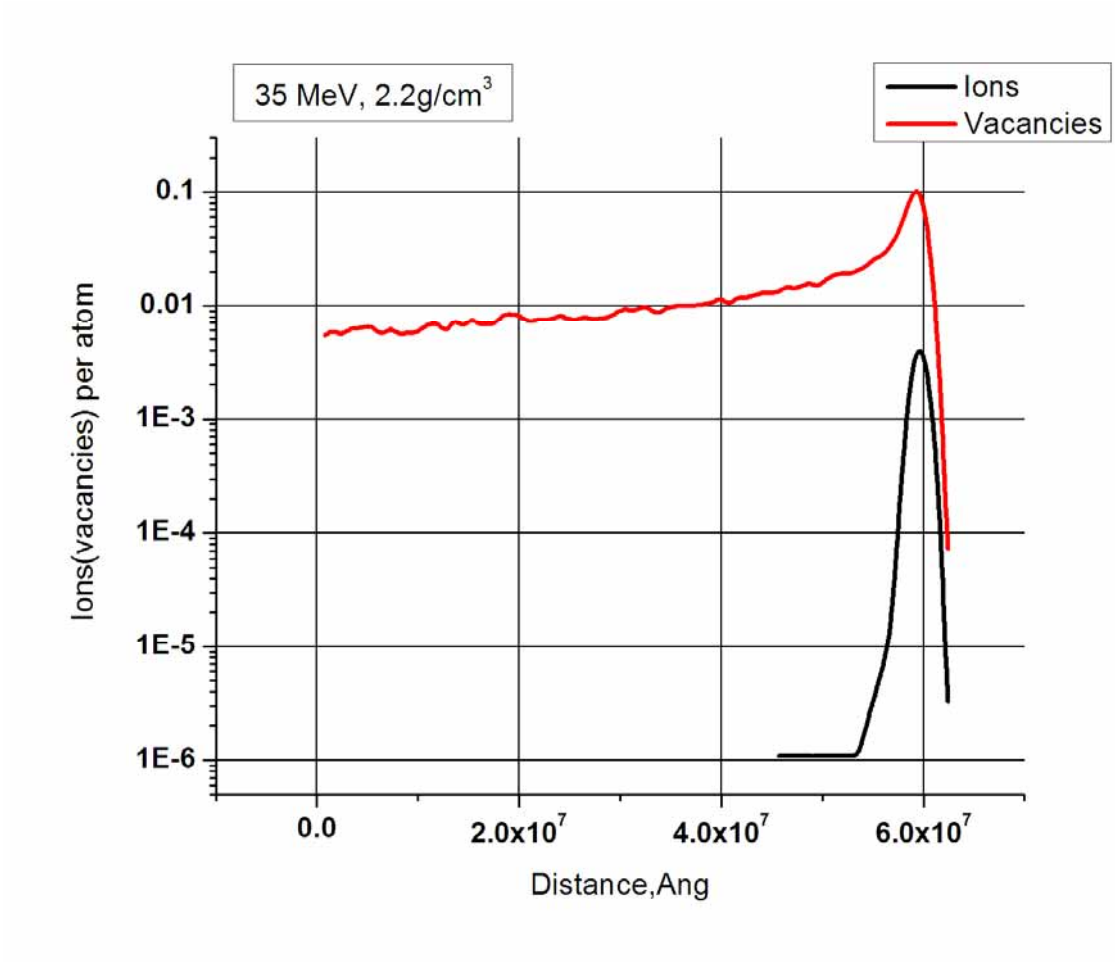

Fig.39. Calculation results of profile distribution for primary radiation defects (vacancies, the red curve) and profile of stopped protons (black curve), depending on the penetration depth of protons in the graphite material with the density ρ_1 = 2.2 g/cm^3 under irradiation of protons with energy 35 MeV and the full dose of irradiation Φ = 10^{19} protons/cm^2. The levels of radiation damage presented here for D_{max} = 0.113 dpa; D_{min} = 7.3x10^{-6} dpa and <D> = 1.41x10^{-2} dpa.

8. Experimental investigations of radioisotopic composition of AC-150 sample.

In order to study radiation resistance of irradiated graphite samples and analysis of changes in their physical-mechanical properties the knowledge of impurity element composition and changes in the composition during irradiation process is needed. To perform this procedure a method of semiconductor gamma spectrometry is used for the radionuclide analysis of the sample composite material based on AC-150 graphite, irradiated at the RRC-KI cyclotron. Exposition and processing of gamma spectra, identification and radionuclide analysis is performed using a gamma spectrometer on the basis of detector of high-purity germanium (HPGe).

Spectrometric system for shielded measurements using a passive protection against external radiation created on the basis high-purity germanium (HPGe) IGC-12 (Princeton Gamma Tech, USA). Active volume of the detector is 66 cm^3, the effectiveness is 12.5% compared to a standard 3x3-inch NaI (Tl) detector, and resolution for the line of Co-60 with energy 1332.5 keV is not worse than 2.0 keV. Detector unit (with preamplifier) and a working chamber for 10x15 cm^2 samples are surrounded by 10 cm thick blocks of lead. From the output of preamplifier (ORTEC-572) the signal comes to multichannel amplitude analyzer (AMA-03F) which connected to a serial port of the PC.

In radionuclide analysis of samples of any geometric shapes (point, flat and bulk) the experimental method is used for determining the effectiveness of gamma-quanta registration irradiated from any point in the upper hemisphere close to the detector in the context of concept of "effective center detector" (ECD). Absolute value of the efficiency is calculated to determine the energy considering the following parameters: distance from the sample to detector, its size (diameter, height), material of the matrix of sample and container. In addition, spectrometer can be calibrated in 20 "standard" geometries.

Generalized formula for determination of the efficiency is calculated by 150 experimental points of absolute value of the efficiency for different energies and different distances. For their measurements were used 7 different sets of model spectrometric gamma sources. The average value of integral errors between measured and calculated values is 4.5%. The program implemented calculation of mass coefficients for gamma radiation decay for 20 most common material samples: solution, organic, soil, glass, hydrogen, nitrogen, oxygen, chlorine, carbon, sulfur, phosphorus, beryllium, aluminum, silicon, germanium, iron, copper, zirconium, gold, uranium, and for 13 container materials: plastic (polyethylene), teflon, glass, concrete, aluminum, silicon,

germanium, iron, copper, zirconium, cadmium, gold, lead. The device is certified. Certificate of Russian state standard on verification of gamma spectrometer (PPD IGC-12, analyzer AMA-03F, bundled software GRANIT) № 7691 is valid until 19.02.2008.

A sample of a composite material on the basis graphite under the title "AC-150" has been received for analysis in 11.10.2007. Sample size: rectangular prism 4x4x25 mm. A sample was irradiated by high-energy protons (E_p = 32 MeV, proton dose is $\Phi = 1.0 \cdot 10^{18}$ cm^{-2}) at the RRC-KI cyclotron. The area of irradiated material was about 15 mm.

The exposition of radiation γ-radiation has been performed during 10000 seconds (3 hours) at a distance of 90 mm from the front cryostat detector twice: in 11.10.2007 and 15.10.2007. The interval of time between expositions corresponds to 4 days. Comparison of the results of analysis for two spectra (activities detection of radionuclides) makes it possible to increase the reliability of identification lines for γ-radiation taking into account a half-life.

Investigated results are presented in Figure 40 and tables 8 and 9.

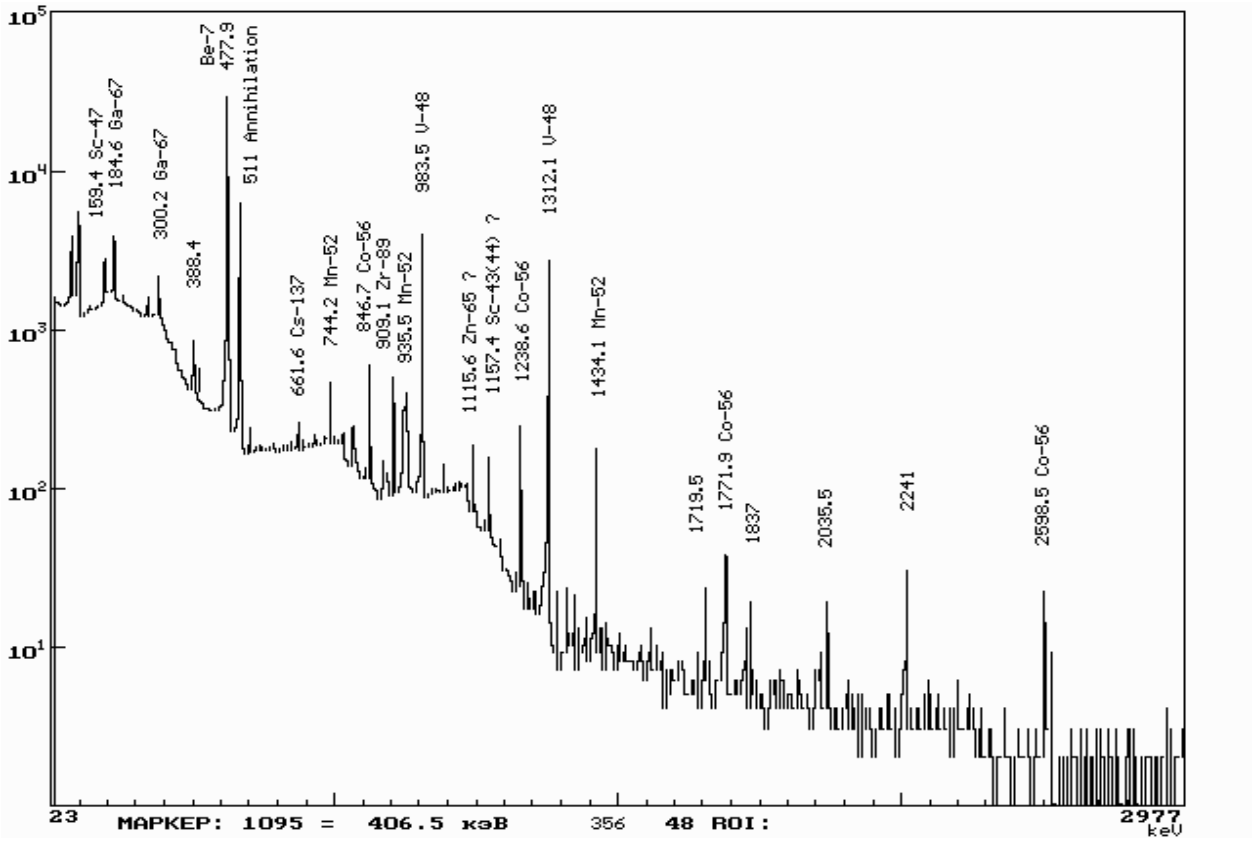

Fig. 40. Spectrum of γ-radiation of AC-150 sample. Exposition 11.10.2007.

Table 8. Radionuclide composition of the A-150 sample. Confident identification.

Isotope	$T_{1/2,}$ days	Lines spectrum/table	Activity, Bq 11.10.2007.	Activity, Bq 15.10.2007.	Error %	Comment
^{7}Be	53.10	1 / 1	79400	75900	10	Detected 1 line with a good statistics, “decay check” is satisfactory
^{48}V	15.97	2 / 2	2650	2230	10	Detected 2 lines with a good statistics, “decay check” is satisfactory
^{52}Mn	5.59	4 / 4	153	107	10	Detected 4 lines with a good statistic, “decay check” is satisfactory
^{56}Co	78.76	6 / 7	269	266	10	Detected 6 lines with a good statistics, “decay check” is satisfactory
^{67}Ga	3.26	6 / 6	1180	520	15	Detected 6 lines with a good enough statistics, “decay check” is satisfactory
^{89}Zr	3.27	1 / 1	24.9	12.4	10	Detected 1 line with a good statistics, “decay check” is satisfactory
^{96}Tc	4.28	4 / 4	51.4	22.7	25	Detected 4 lines with a weak statistics, “decay check” is satisfactory

Table 9. Radionuclide composition of the A-150 sample.

Isotope	$T_{1/2}$, days	Lines spectrum/table	Activity, Bq 11.10.2007.	Activity, Bq 15.10.2007.	Error %	Comment
^{46}Sc	83.85	2 / 2	21.0	14.2	25	Detected 2 lines with a weak statistics, “decay check” is acceptable
^{47}Sc	3.42	1 / 1	214	75.8	15	Detected 1 line with a sufficient statistics, “decay check” is satisfactory
^{51}Cr	27.70	1 / 1	257	180	25	Detected 1 line with a weak statistics, “decay check” is acceptable
^{57}Co	270.9	1 / 1	13.4	15.1	30	Detected 1 line with a weak statistics, “decay check” is acceptable
^{65}Zn	244.1	1 / 1	19.5	17.7	15	Detected 1 line with a sufficient statistics, “decay check” is acceptable

The main results can be summed up as follows:

1) In the spectrum of γ-radiation of samples lines of radiation radionuclides with half-life from units to hundreds of days is identified. Presumably, they are all products of activated impurity isotopes in the material of graphite composite under proton beam irradiation.

2) the most intense line E=9keV with high probability associated with the decay of the isotope ^{7}Be (E=5keV, $T_{1/2}$=279.5 days).

3) Isotopes ^{48}V, ^{52}Mn, ^{56}Co, ^{67}Ga, ^{89}Zr, ^{96}Tc are identified with high probability that confirms the existence of several lines in the spectrum and changes in isotope activity during 4 days in between the two expositions of the spectrum (“decay check").

4) Isotopes ^{46}Sc, ^{47}Sc, ^{51}Cr, ^{57}Co, ^{65}Zn are identified with less probability. In general, this is due to the weak intensity (statistics) of lines and the existence of the only one line.

5) For a more accurate identification similar studies should be carried out preferably in 30-50 days.

9. General analysis of changes in graphite collimator materials under irradiation by proton beam at RRC-KI cyclotron facility.

The analysis of changes the physical properties of irradiated graphite collimator materials includes the study of dose dependency (from 10^{17} protons/cm^2 to 3.10^{19} protons/cm^2) for the following values: coefficient of thermal conductivity, resistivity, the coefficients of thermal expansion, changes in the density and crystal lattice parameters, the analysis of changes in mechanical properties: analysis of changes of elasticity modules, sthrenght to tensile, stress to rupture. Studies of changes in these properties of irradiated materials were carried out for the various orientations of threads (fibers) of AC-150 graphite composite materials at different radiation doses of protons

As noted above, the samples were installed at a special substrate in the water cooling environment, which were connected with thermocouples to control the temperature of irradiation. This construction of the target unit allows of guaranteed low irradiation temperature (20-50 ° C).

In these experiments in the window for irradiation 3 samples were installed with a different orientation to texture (R, T, A - along the axis of samples) and, moreover, with different planes orientation of samples in relation to the proton beam the planes R, T and A were also selected.

Flat samples in the form of parallelepipeds with section 4x4 mm and 25 mm in length were used for research. See table.

The study of the radiation resistance of graphite was performed under irradiation of samples by protons with energy 32 MeV (cyclotron) at RRC-KI cyclotron at room temperature for three irradiation doses. The first dose was chosen fairly low - about $\Phi_1 = 10^{17}$ protons/cm^2. The second dose was $\Phi_2 = 10^{18}$ protons/cm^2 and the third dose order $\Phi_3 = 10^{19}$ protons/cm^2, followed by conversion the displacements per atom (dpa)

10. Results of analysis of physical-mechanical properties changes in graphite samples after first irradiation with proton dose up to 10^{17} protons/cm^2.

As noted above, the samples were installed at a special substrate in the water cooling environment, which were connected with thermocouples to control the temperature of irradiation. This construction of the target unit allows of guaranteed low irradiation temperature (20-50 ° C).

In these experiments in the window for irradiation 3 samples were installed with a different orientation to texture (R, T, A - along the axis of samples) and, moreover, with different planes orientation of samples in relation to the proton beam the planes R, T and A were also selected.

Flat samples in the form of parallelepipeds with section 4x4 mm and 25 mm in length were used for research. See table.

Таблица. 10. Changes in physical-mechanical properties of AC-150 composite after irradiation.

Sample №.	E_{init}/E_{irr} GPa	ΔE/E, %	ρ_{init}/ρ_{irr}, 10^{-6} Ohm*m	Δ ρ/ ρ , %	$\lambda_{init}/\lambda_{irr}$ W/mK	Δλ/λ, %	$\sigma_{init}/\sigma_{irr}$ MPa	Δσ/σ, %
First irradiation (0.0002 dpa)								
4R(TA-1)	3,5/4,0	14	28,8/29,65	3	50/48	6	6,0/	7
4T(AR-1)	8,1/8,86	9	5,65/8	42	215/150	30	5,8/	5
4A(RT-1)	9,2/9,6	4	6,2/9,4	52	215/130	39	6,1/	2
Second irradiation (0.002 dpa)								
4R(TA-2)	4,8/7,0	46	29,9/62,5	109	51/25	51	6,0/	21
4T(AR-2)	9,3/10,4	12	5,7/17	198	215/80	62	5,8/	6
4A(RT-2)	8,8/9,5	8	5,75/12	109	215/105	51	6,1/	4
Third irradiation (0.02 dpa)								
4R(TA-3)	3.7/5.5	48.8	27.6/108	290	51/15	70	6,1/	22
4T(AR-3)	8.3/9.1	9.6	5.56/26,8	370	215/55	74	5,7/	5
4A(RT-3)	9.4/10.2	8.5	5.5/26,5	381	215/56	72	6,0/	4

Note:
1. Changes of the coefficient of thermal conductivity were estimated by the correlation curve.
2. Changes of tensile were estimated by the changes in the ratio of elasticity modulus.

10.1. Analysis of modulus of elasticity (E) change of irradiated samples.

As a result of the first irradiation the samples were irradiated to doses of 10^{17} particles/cm^2 (about 0.0002 dpa) - samples with numbers 4R(TA-1), 4T(AR-1) and 4A(RT-1). In doing so, the value of elasticity module E for these samples changed as follows:

-- For sample 4R(TA-1) module of elasticity increased by 14%

-- For sample 4T(AR-1) - 9.4%

-- For sample 4A(RT-1) - 4%

10.2. Analysis of strength change of irradiated samples.

Measurements of tensile for AC-150 graphite after irradiation are not directly carried out, because the samples were very small and, moreover, it is destroying the method of investigation. But numerous experiments with nuclear graphite and composite carbon materials that we have in Russia and abroad showed that between changes of strength and elasticity module there is a direct link. In general the expression is presented by power dependence, where the degree is in the range from ½ to 1. In most cases the strength of graphite under irradiation equals to the square root of the change in elasticity module:

$$\sigma_{irr} / \sigma_{init} = \sqrt{E_{irr} / E_{init}}$$

As part of this relationship the changes of tensile for AC-150 graphite were estimated. See the table from which it follows that its strength under irradiation doses up to 0.01 dpa increases by about 5%.

10. 3. Analysis of resistivity change of irradiated samples.

For sample 4R(TA-1) the resistivity increased by 2.9%, for sample 4T(AR-1) by 43%, for sample 4A(RT-1) by 51.6%.

10.4. Analysis of thermal conductivity change of irradiated samples.

Thermal conductivity after irradiation was not directly measured as for its measurement a heating of the sample was needed and because irradiaton was performed at room temperature, then in the process of measuring radiation due to defect annealing the coefficient of thermal conductivity will change). Therefore, in this situation it is better to evaluate its value by change resistivity using the correlation between them. It should be noted that the same dependencies observed for all carbon materials including nuclear graphite and its composites in both the initial and irradiated state, although the nature of curves may be somewhat different. Using these results thermal conductivities for all three sample cuttings can be determined sufficiently reliable.

So, for direction R (sample № 4R(TA-1)) the value of resistivity after the first irradiation increased from $28.8*10^{-6}$ to $29.65*10^{-6}$ Ohm*m and the value of the coefficient of thermal conductivity should decrease from 51 W/m • K to 48 W/m • K respectively.

For sample with tangential cutting (№ 4T(AR-1)) the value of resistivity after the first irradiation increased from $8.1*10^{-6}$ to $8.86*10^{-6}$ Ohm*m and the value of the coefficient of thermal conductivity should decrease from 215 W/m • K (average value for all measurements of samples with tangential and axial cuttings) to 150 W/m • K respectively.

For sample with axial cutting (№ 4A(RT-1)) the value of resistivity after the first irradiation increased from $9.2*10^{-6}$ to $9.6*10^{-6}$ Ohm*m and the value of the coefficient of thermal conductivity should decrease from 215 W/m • K (average value for all measurements of samples with tangential and axial cuttings) to 130 W/m • K respectively.

10.5. Profilometry measurements of irradiated samples.

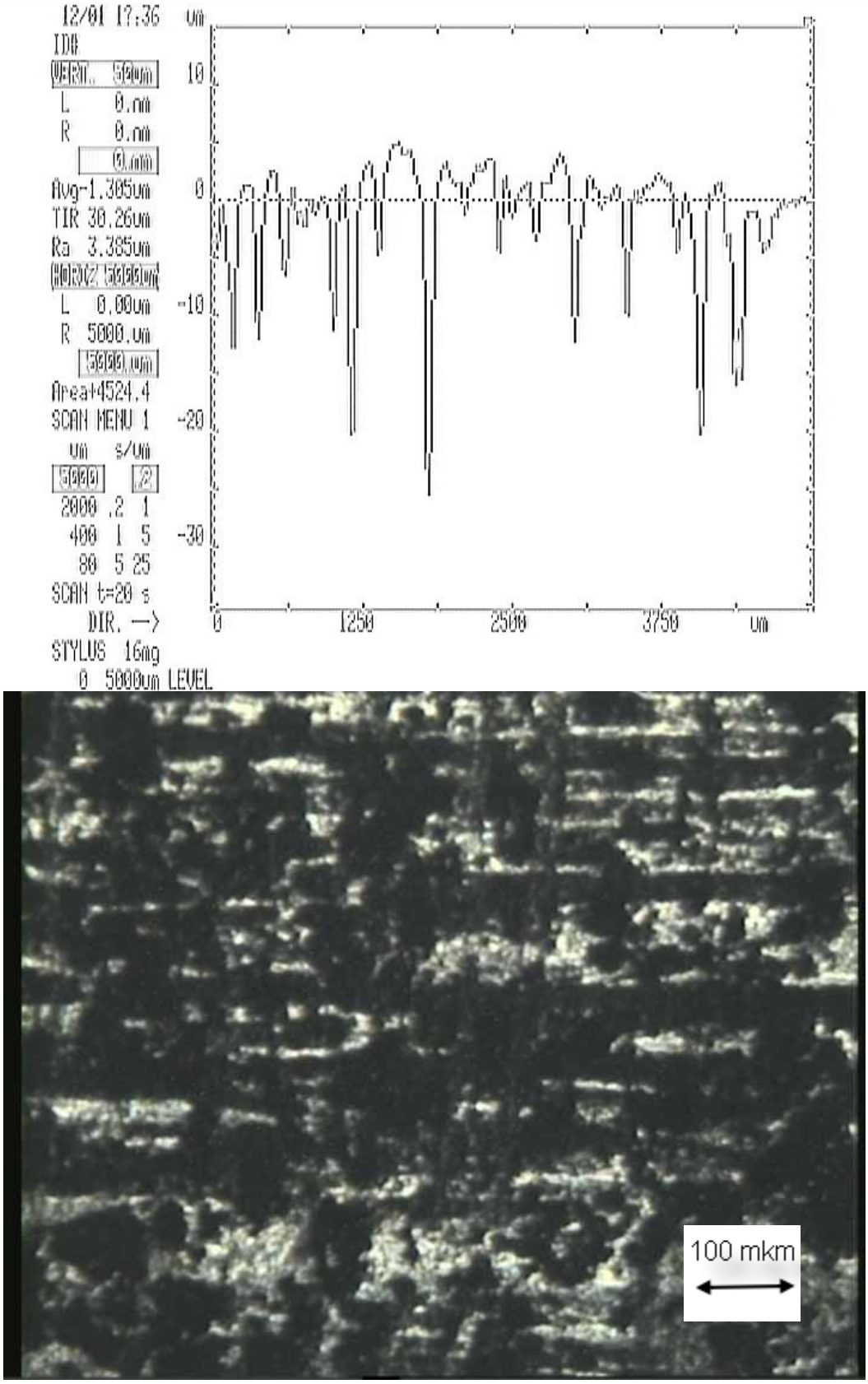

Fig.41. Result of profilometry measurements and microstructure of the irradiated 4R(TA-1) sample to dose of 10^{17}protons/cm^2.

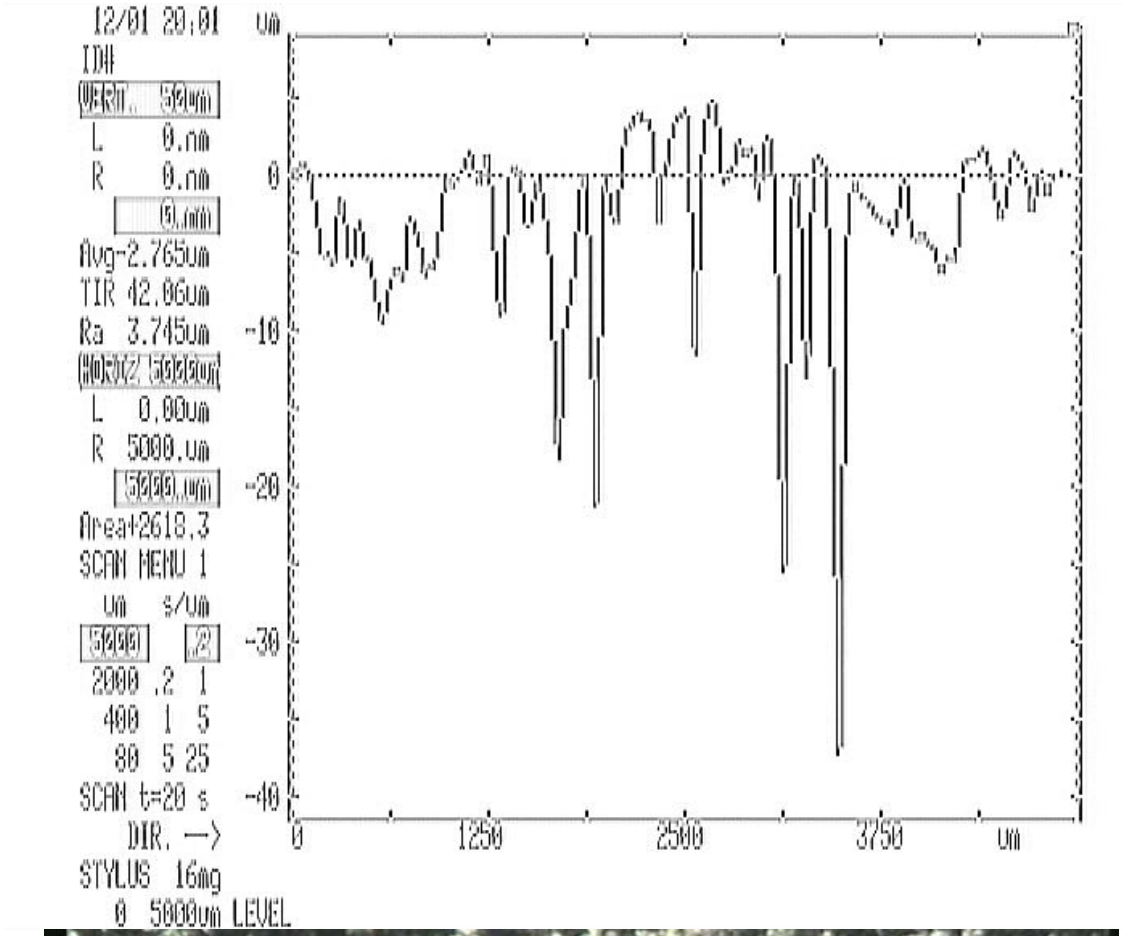

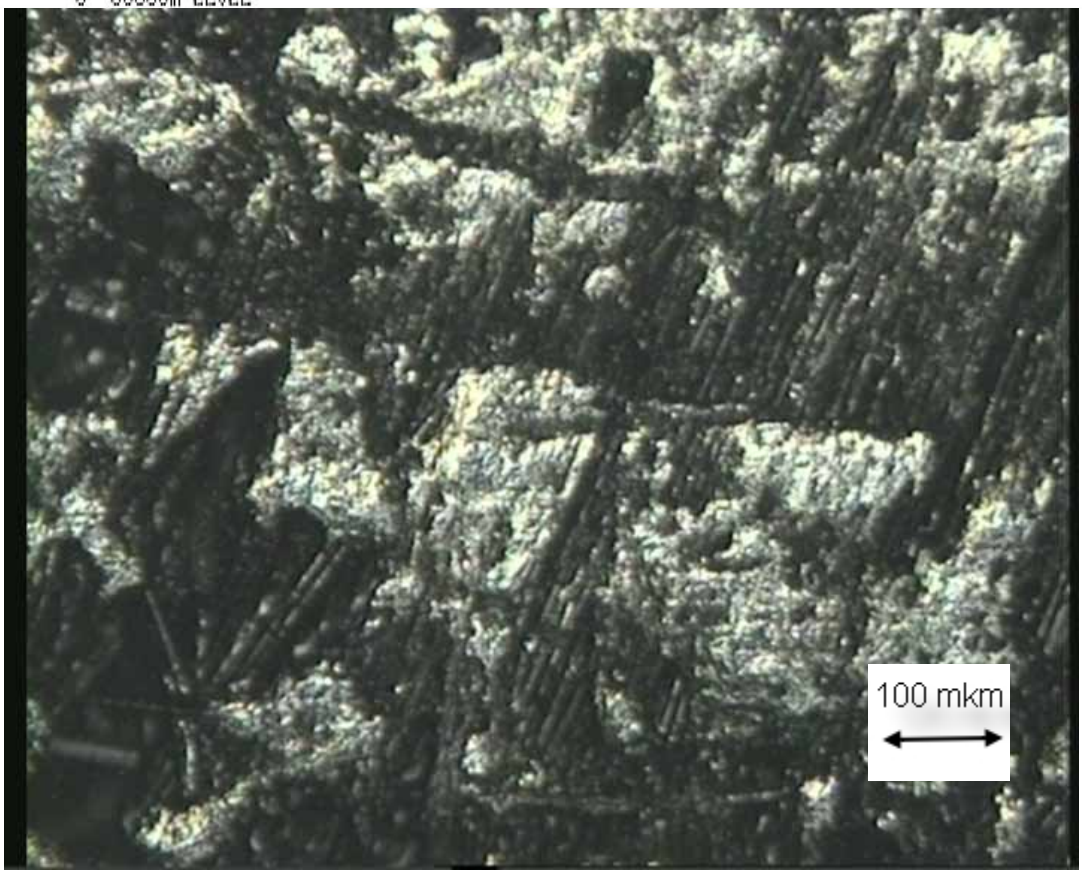

Fig.42. Result of profilometry measurements and microstructure of the irradiated 4A(RT-1) sample to dose of 10^{17}protons/cm^2.

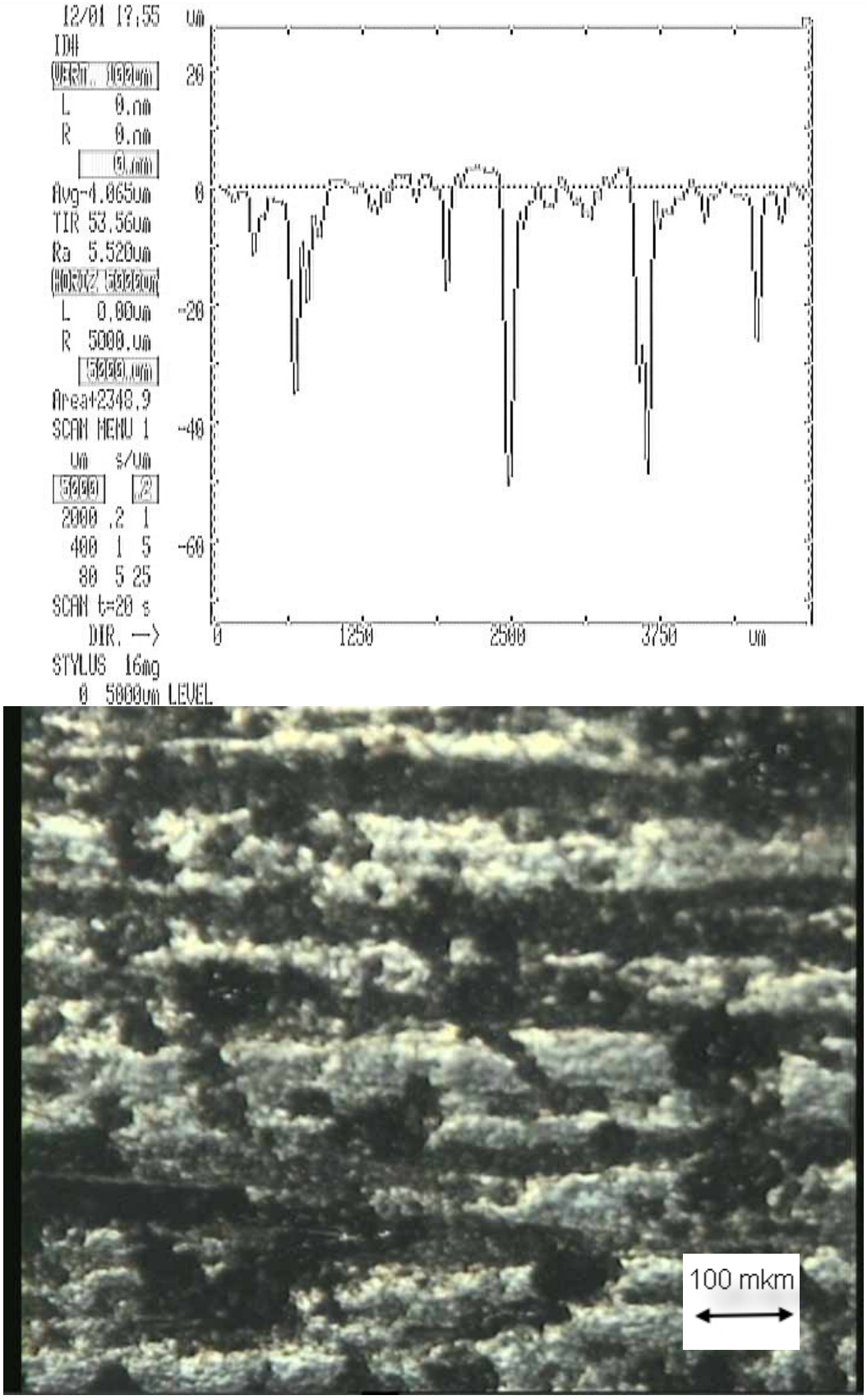

Fig.43. Result of profilometry measurements and microstructure of the irradiated 4T(AR-1) sample to dose of 10^{17}protons/cm^2.

11. Results of analysis of physical-mechanical properties changes in graphite samples after second irradiation with proton dose up to 10^{18} protons/cm^2.

11.1. Analysis of strength change of irradiated samples.

As a result of the first irradiation with 30 MeV protons the samples were irradiated to doses of 10^{18} protons/cm^2 (about <D> = 1.63x10^{-3} dpa) - samples with numbers 4R(TA-1), 4T(AR-1) and 4A(RT-1). In doing so, the values of elasticity modules E for these samples are changed as follows:

-- For sample 4R(TA-1) module of elasticity increased by 100%

-- For sample 4T(AR-1) – 11.8%

-- For sample 4A(RT-1) – 3.4%

The strength of graphite in the radial direction increased most significantly (to 20%), in the tangential and axial directions about 5%

Electrical Resistivity

The electrical resistivity for sample 4R(TA-2) is increased by 109%, for sample 4T(AR-2) by 198%, for sample 4A(RT-1) by 108%.

Thermal conductivity

Making the above comparison of chages in resistivity thermal conductivity coefficient can be estimated after second irradiation.

So, for direction R (sample № 4R(TA-2)) the value of resistivity after the first irradiation increased from 29.9*10^{-6} to 62.5*10^{-6} Ohm*m and the value of the coefficient of thermal conductivity should decrease from 51 W/m • K to 25 W/m • K respectively.

For sample with tangential cutting (№ 4T(AR-2)) the value of resistivity after the first irradiation increased from 5.7*10^{-6} to 17*10^{-6} Ohm*m and the value of the coefficient of thermal conductivity should decrease from 215 W/m • K (average value for all measurements of samples with tangential and axial cuttings) to 80 W/m • K respectively.

For sample with axial cutting (№ 4A(RT-2)) the value of resistivity after the first irradiation increased from 5.75*10^{-6} to 12*10^{-6} Ohm*m and the value of the coefficient of

thermal conductivity should decrease from 215 W/m • K (average value for all measurements of samples with tangential and axial cuttings) to 105 W/m • K respectively.

11.2. Radiation forming and weight loss of composite graphite materials of LHC collimator under proton irradiation.

Measuring the size of the samples in two mutually perpendicular directions after the second irradiation showed that they have changed quite significantly (swelling of samples is about 5%) with approximately equal numbers for all directions of cutting. It shold be noted that the measurements were conducted with the help of a micrometer and accuracy of measurement is not very high, but grouping of the measurement results showed that it is indeed a fact. In terms of volume swelling that value correspond to 1.5%. Along with the size measurements re-weighting of the samples was performed. According to the results obtained weight of samples decreased by approximately 0.5%.

11.3. Profilometry and microstructure analysis of irradiated samples with dose 10^{18} protons/cm^2.

Measurement of the profile of samples carried out with the use of "ALFA-STEP" device with a magnification up to 100 times using automatic recording of profilogram surface during scanning process. The accuracy (error) of measurement is chosen such (± 0,5 microns) to compensate graphite sample surface roughness caused by its porosity. Unfortunately, this is an unavoidable porosity that lies in the very structure of the reactor graphite (the volumetric value is 25-30% and the distribution of pore size is in the range of 1-300 microns).

Result of profilometry is shown in the following figures for the three samples of graphite from billet № 4.

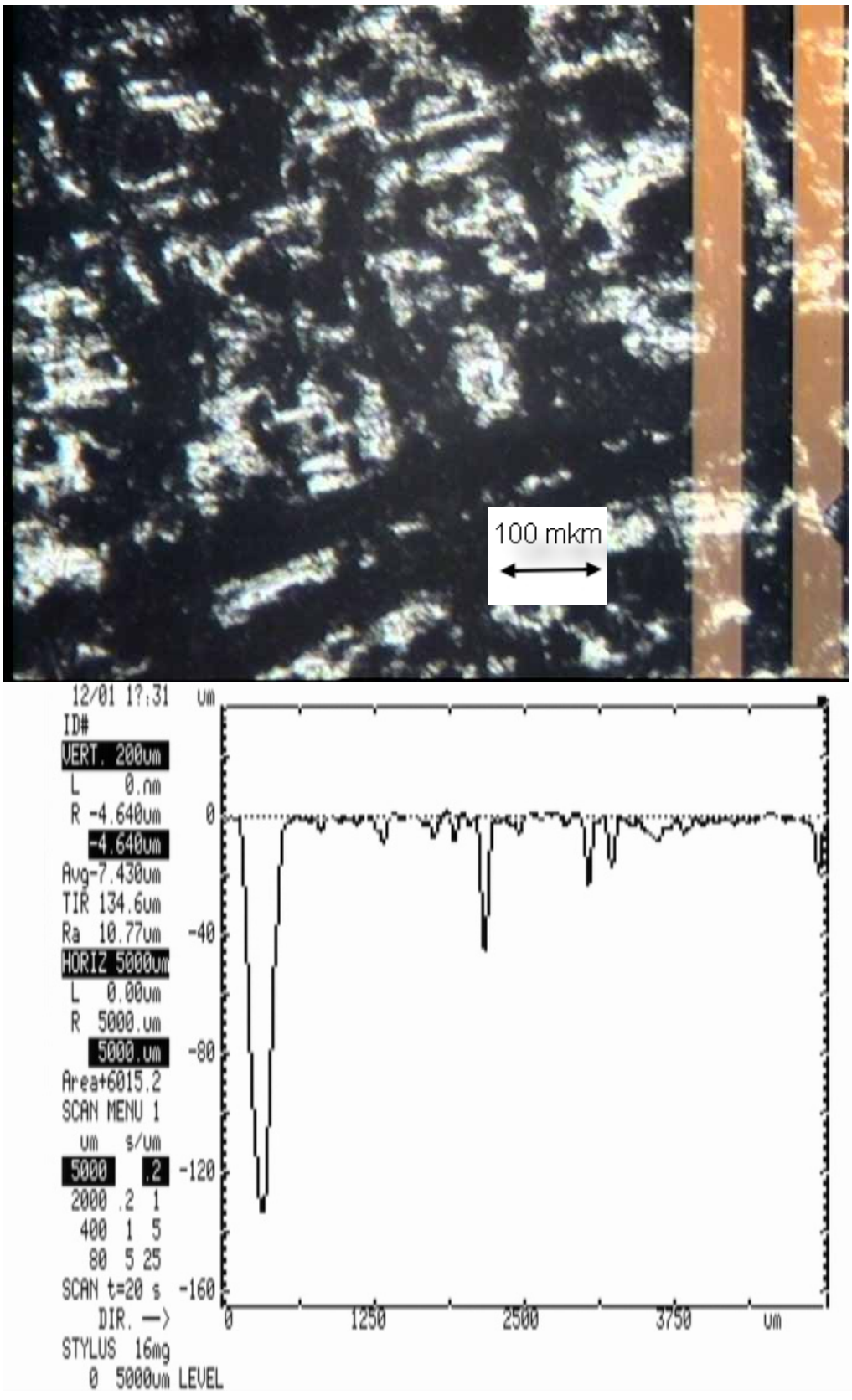

Fig.44. Result of profilometry measurements and microstructure of the irradiated 4R (TA-2) sample to dose of 10^{18}protons/cm^2.

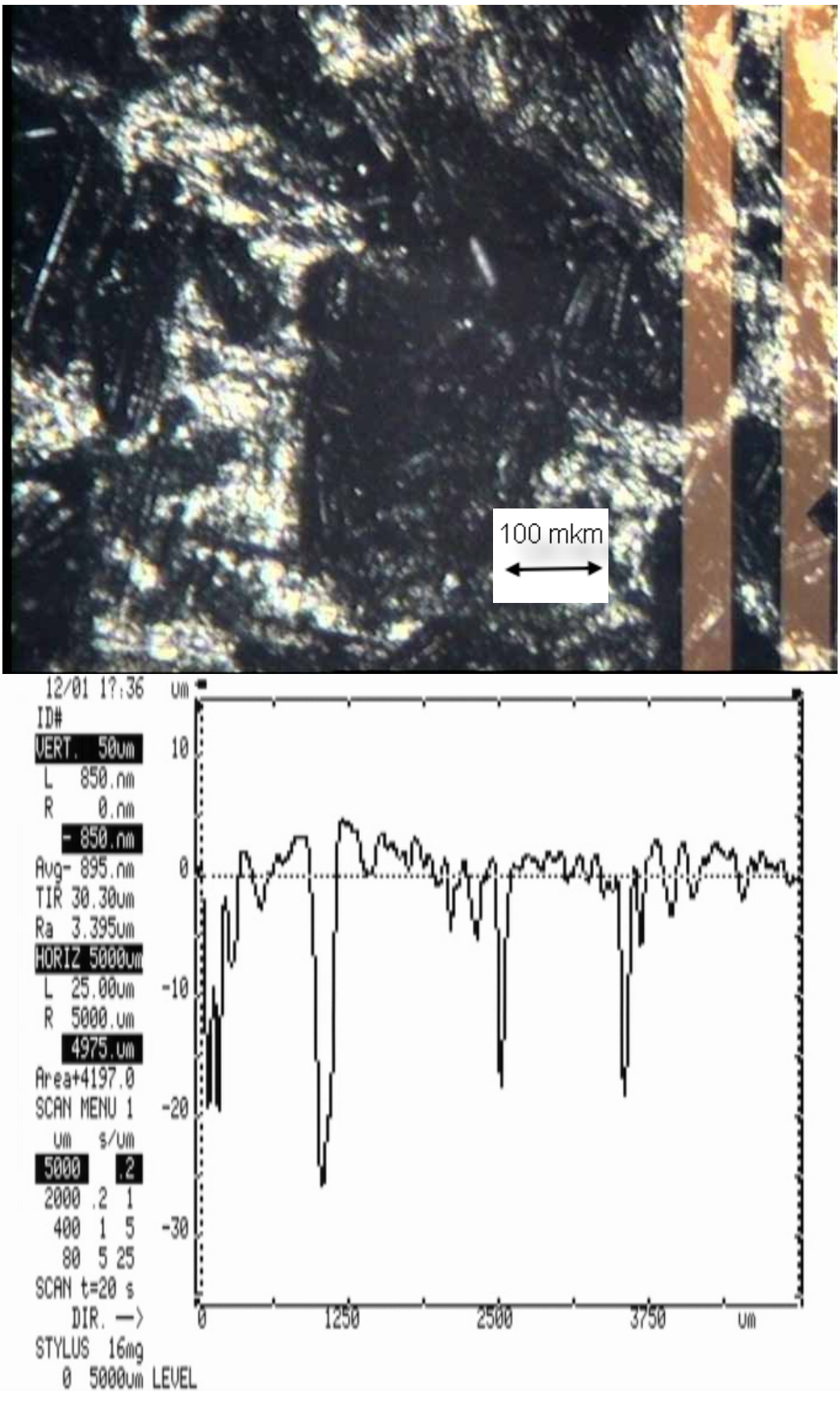

Fig.45. Result of profilometry measurements and microstructure of the irradiated 4A(RT-2) sample to dose of 10^{18}protons/cm^2.

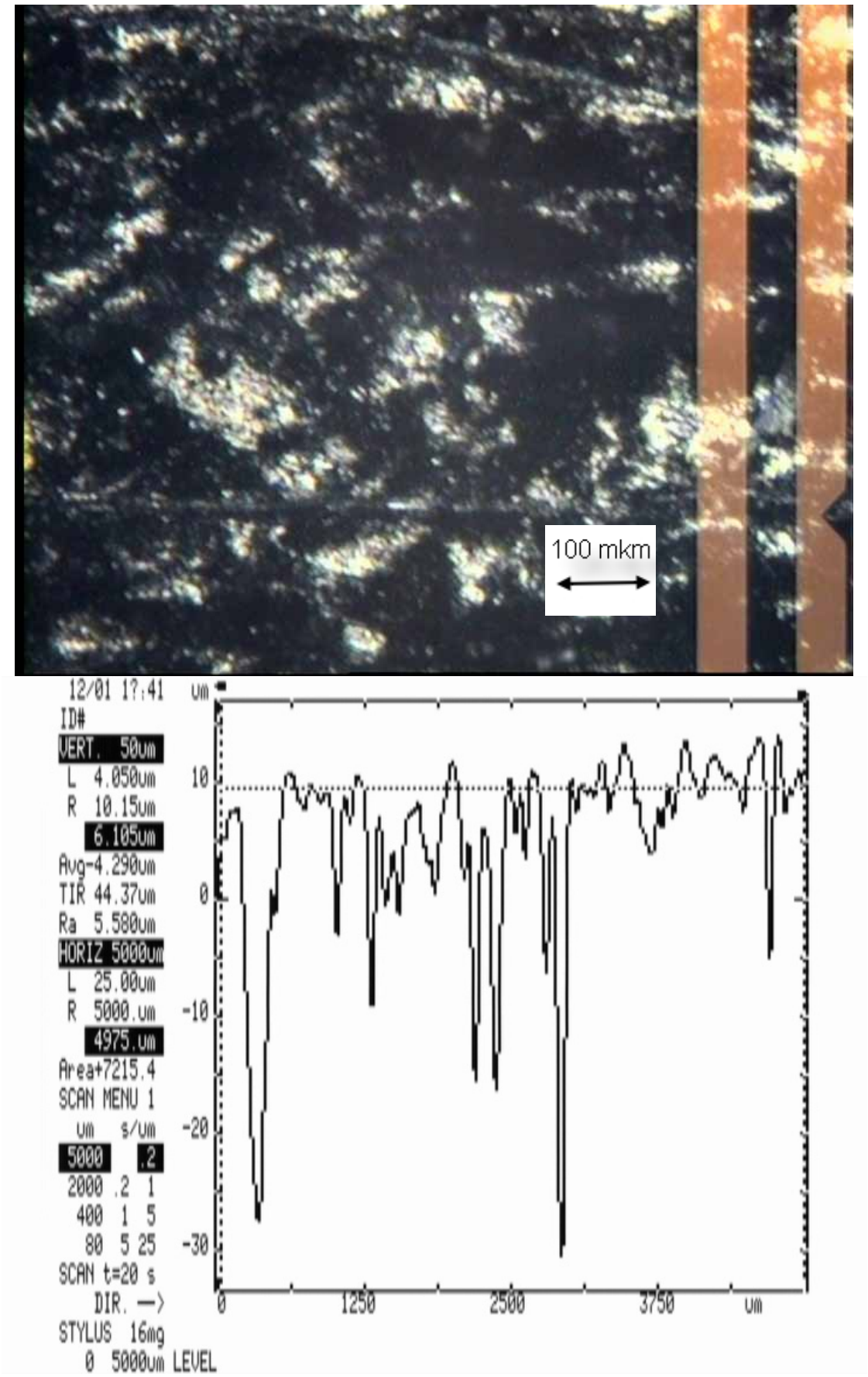

Fig.46. Result of profilometry measurements and microstructure of the irradiated 4T(AR-2) sample to dose of 10^{18}protons/cm^2.

Optical photographs of the surface samples of graphite with a magnification of 100 times showed that a substantial change in the nature of the surface of samples compared with unirradiated condition has not happened, although there is also observed a texture of samples for various cuttings.

12. Results of analysis of physical-mechanical properties changes in graphite samples after third irradiation with proton dose up to 10^{19} protons/cm^2.

It should be said that this is a very large dose and in terms of fluence of neutrons in the reactor irradiation it corresponds to approximately $2 \cdot 10^{21}$ n/cm^2 and for standard reactor graphite GR-280 it is close to the critical fluence of neutrons, in which the graphite loses its function as a structural material.

Results of the study of physical-mechanical properties of graphite samples revealed that their changes are approximately the same, but the extent of these changes is significantly higher. Elasticity modulus as well as resistivity is increasing while thermal conductivity is decreasing. Weight loss of the samples rersists and according to the results of exposure we can state that this process occurs at a constant speed with increasing doses and although it's relatively small, after the third exposure it reaches a value of 5-7%. This is presumably can be related to surface erosion graphite samples under the influence of the proton beam.

As to radiation forming of graphite, the size of the samples after the third irradiation increased by (0.5-0.7)% with the volume change of 1.65%. These values are roughly the same (slightly more) as those after the second irradiation, but perhaps this is also linked to the erosion of surface samples and in the absence of the erosion these changes could be large.

Table 11. Changes of size of the samples after irradiation.

Sample №.	B_{init}/B_{irr}, mm	ΔB/B, %	H_{init}/H_{irr}, mm	ΔH/H, %	ΔV/V, %	P_{init}/P_{irr}, g	ΔP/P, %
First irradiation (0,0002 dpa)							
4R(TA-1)	4,06/4,06	0	3.96/3,96	0	0	0,622/0,622	0
4T(AR-1)	4,04/4,04	0	4.02/4,02	0	0	0,674/0,674	0
4A(RT-1)	4,07/4,07	0	4.12/4,12	0	0	0,671/0,671	0
Second irradiation (0.002 dpa)							
4R(TA-2)	3,97/3,99	0,5	4.14/4,16	0,48	1,48	0,668/0,663	0,7
4T(AR-2)	3,89/3,91	0,5	4.02/4,04	0,5	1,5	0,658/0,653	0,8
4A(RT-2)	4,07/4,085	0,4	3.98/4,00	0,5	1,4	0,678/0,673	0,7
Third irradiation (0.02 dpa)							
4R(TA-3)	4,01/4,025	0,4	3.9/3,92	0,5	1,4	0,635/0,593	7
4T(AR-3)	4,02/4,045	0,6	4.12/4,14	0,5	1,6	0,666/0,614	8,4
4A(RT-3)	4,09/4,12	0,7	4.09/4,11	0,5	1,7	0,700/0,659	6,2

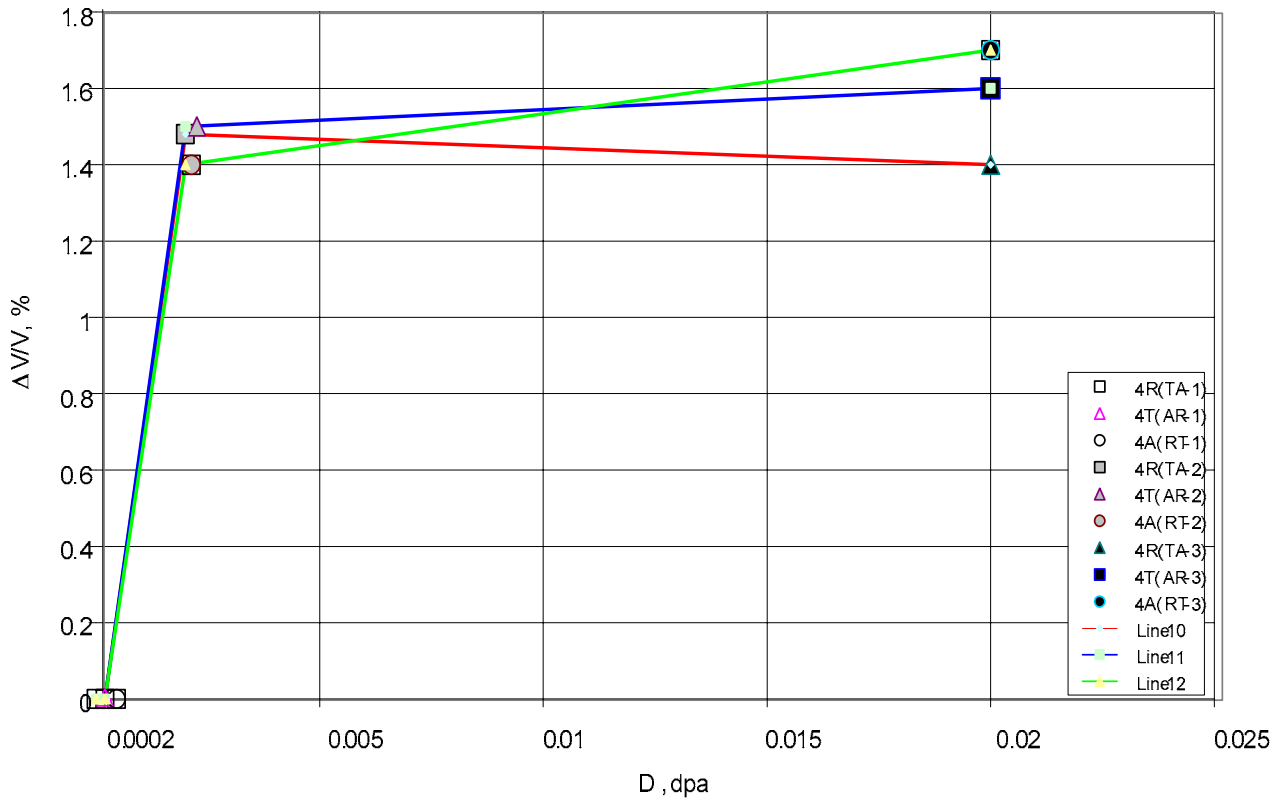

Fig.47. The relative change in volume of samples for AC-150 material depending on the doses.

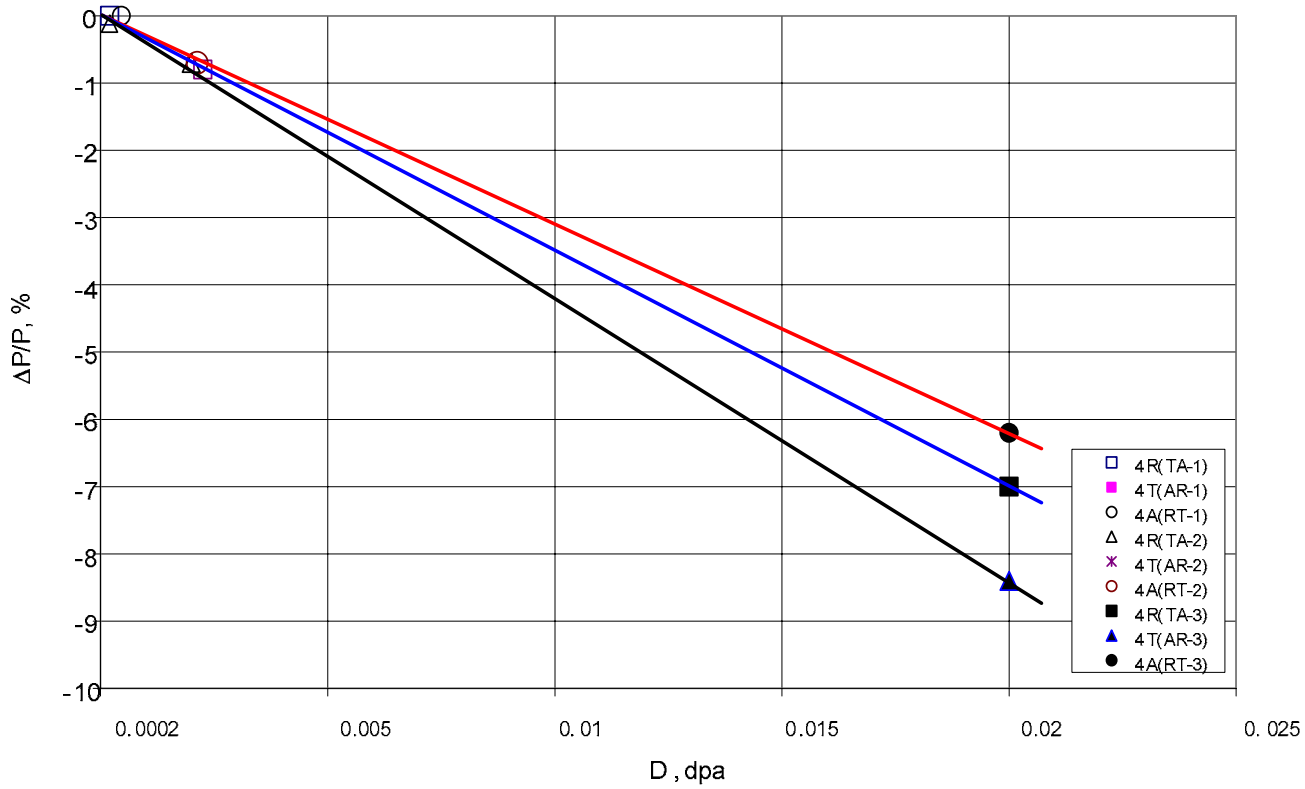

Fig.48. The relative change in density of samples for AC-150 material depending on the doses.

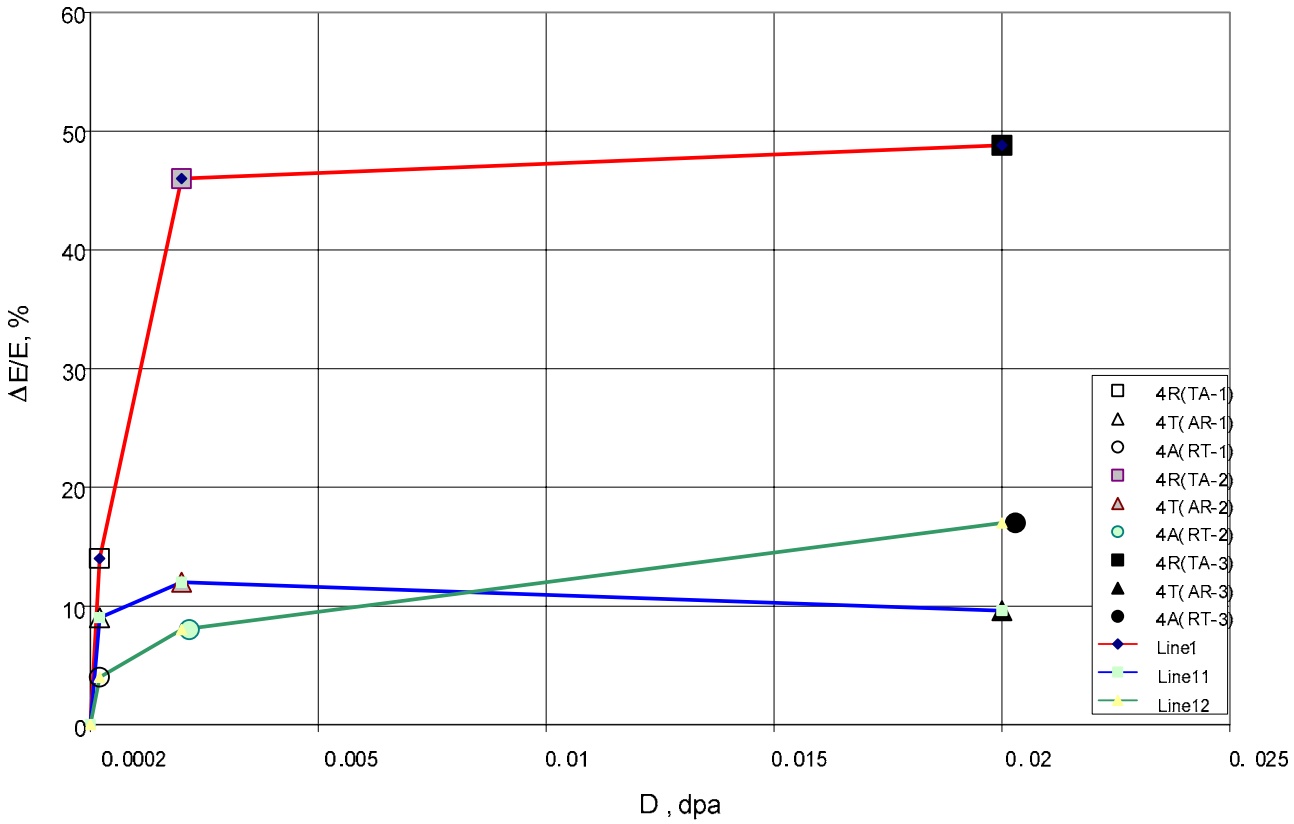

Fig.49. The relative change in elasticity modulus of samples for AC-150 material depending on the doses.

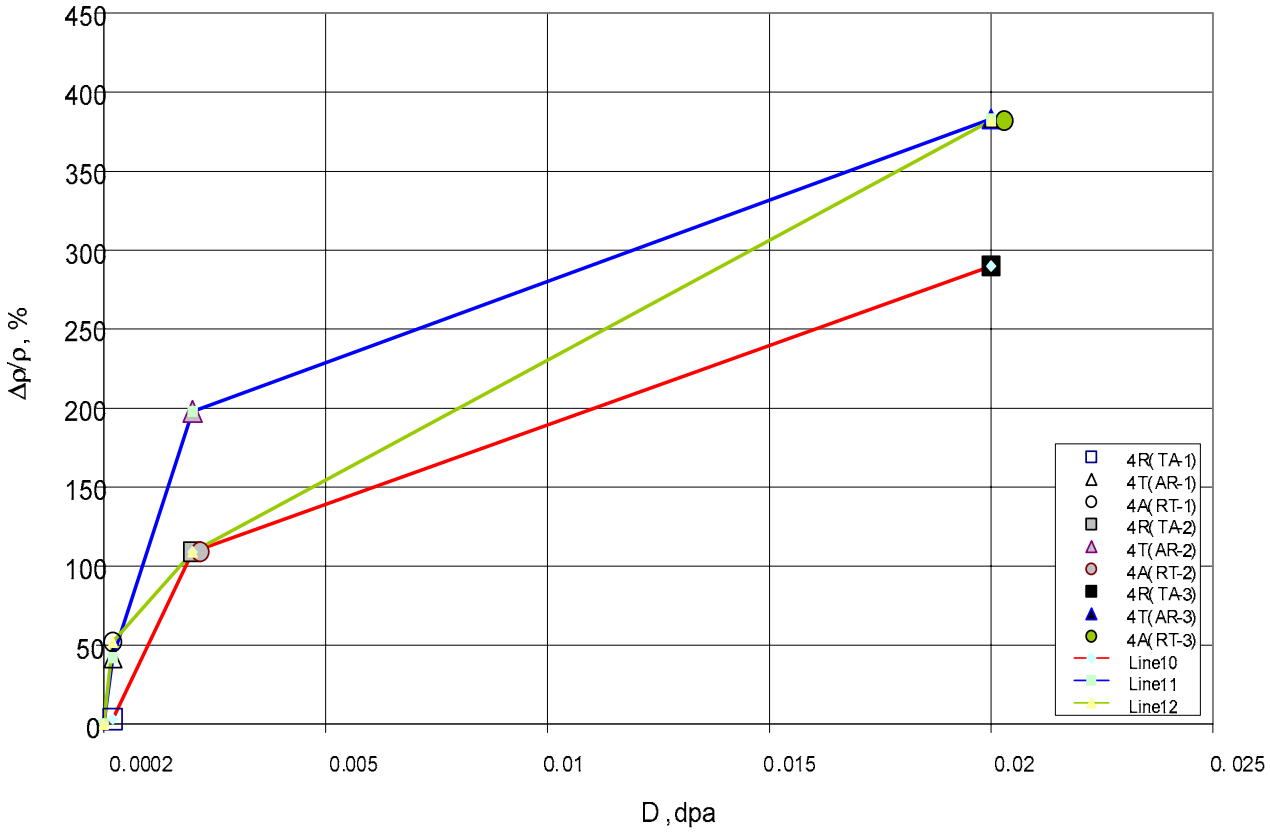

Fig. 50. The relative change in resistivity of samples for AC-150 material depending on the doses.

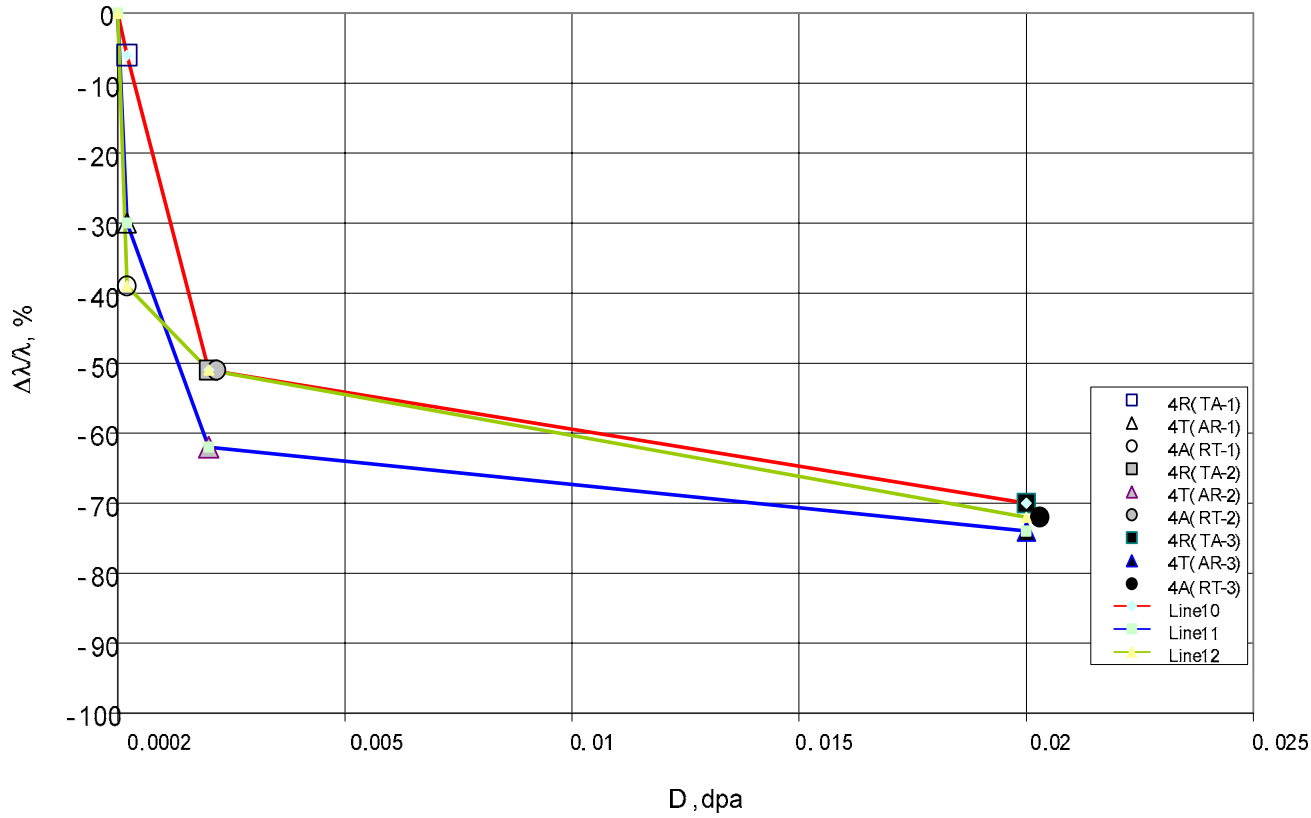

Fig.51. The relative change in thermal conductivity of samples for AC-150 material depending on the doses.

Profilometry of irradiated samples with dose 10^{19} protons/cm^2

Results of profilometry are presented in the figures 52-54 for the three samples of graphite billet № 4. Analysis of the results shows that the nature of surface of the samples is substantially similar to the first and second irradiation.

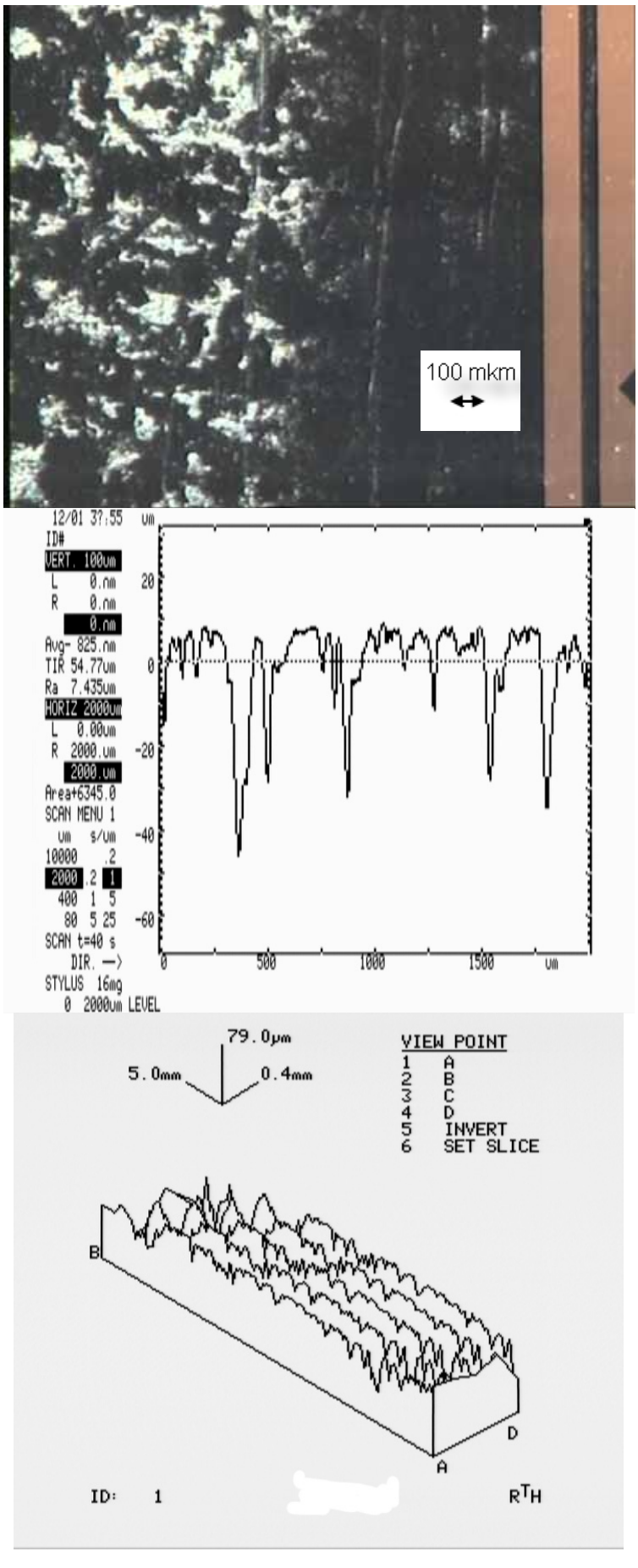

Fig. 52. Profile of the surface and microphotography of 4R (TA-3) sample.

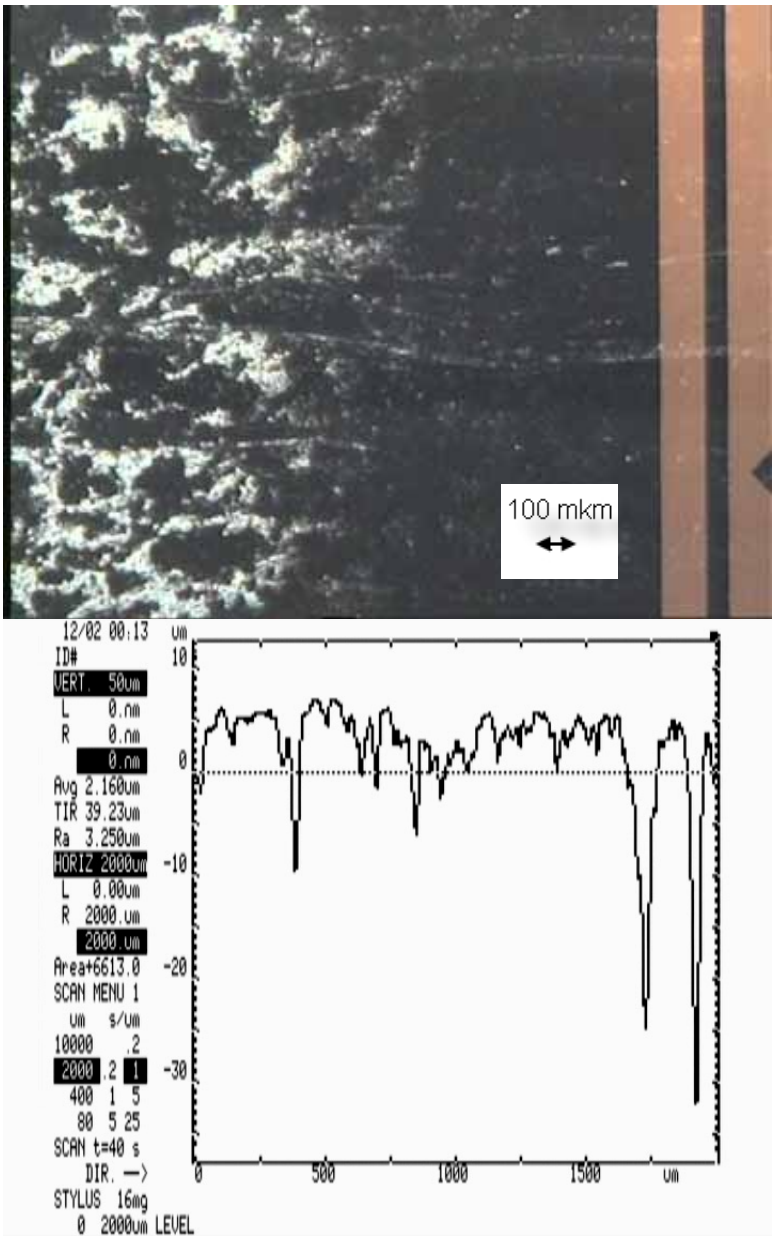

Fig. 53 Profile of the surface and microphotography of 4T(AR-3) sample.

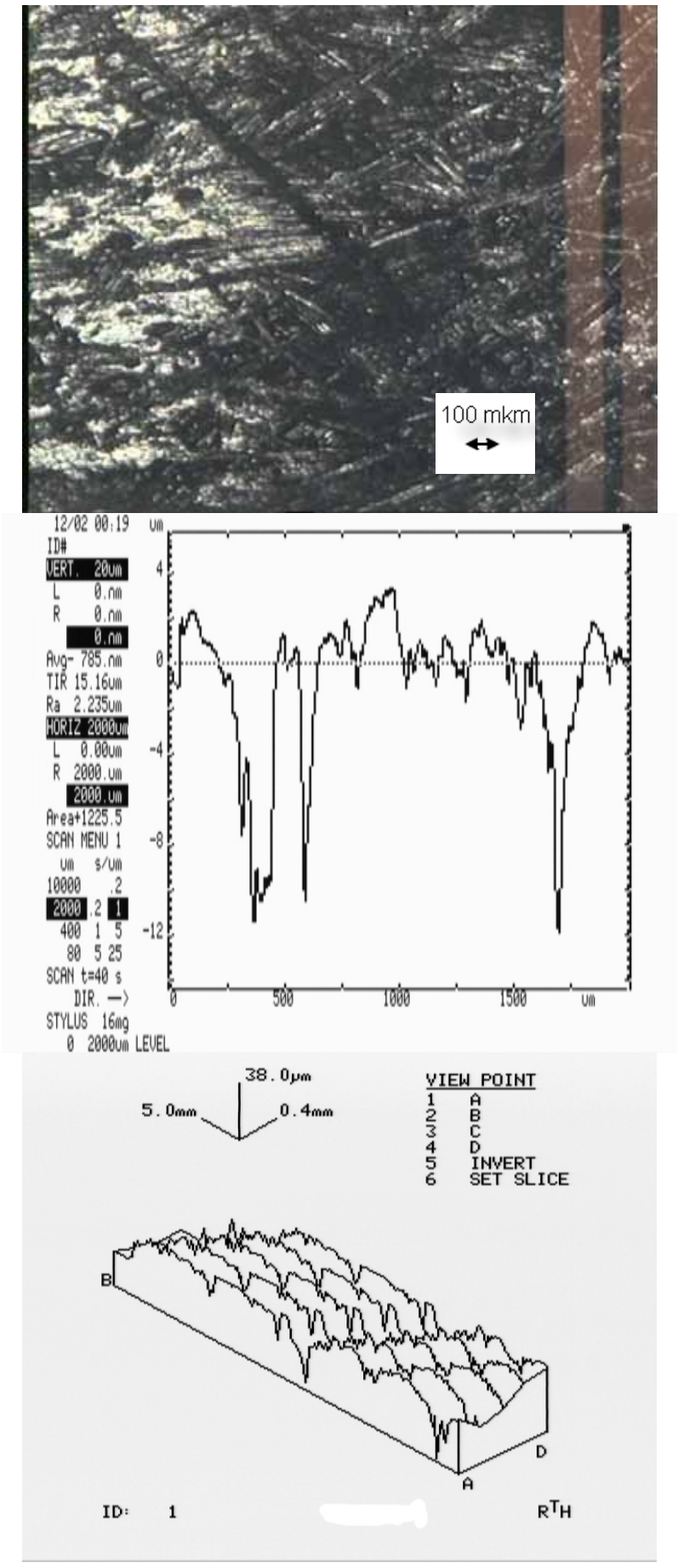

Fig. 54. Profile of the surface and microphotography of 4A(RT-3) sample.

13. Measurements of mechanical prorerties of irradiated LHC collimator materials including deflection curve and deformation up to rupture.

Research results for changes in mechanical properties of irradiated LHC collimator materials with protons of energy up to 30 MeV in the range of radiation doses from 10^{17} to 10^{19} protons/cm^2 are shown in Fig.55-57. These figures show the changing of deflection curves and deformation to rupture of various LHC collimator materials.

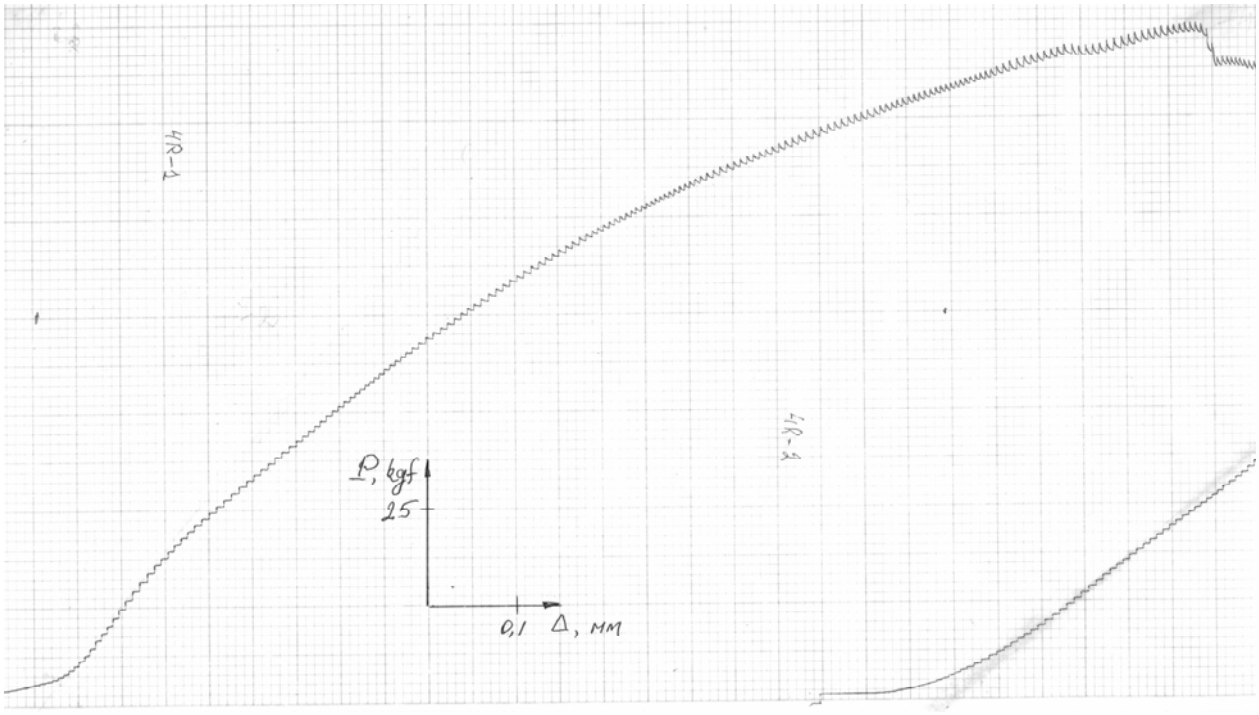

Fig.55. Changes in the deflection curve for 4R-1 sample irradiated with protons to dose of 10^{17} protons/cm^2.

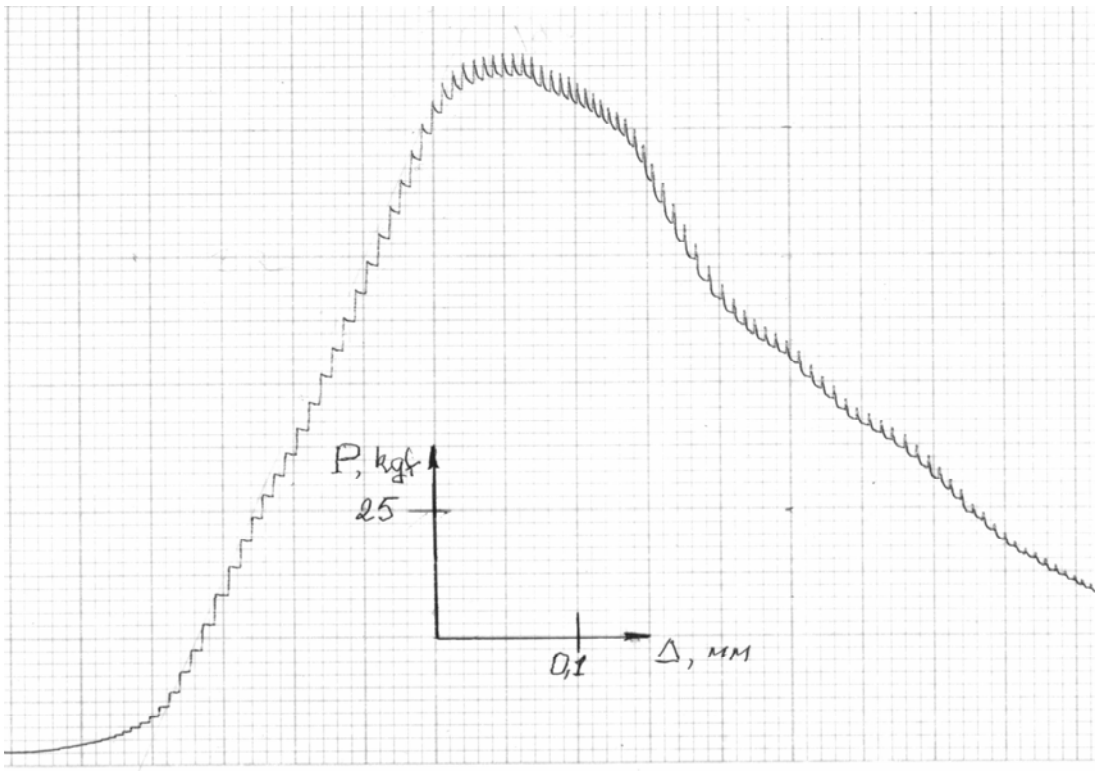

Fig.56. Changes in the deflection curve for 4A-2 sample irradiated with protons to dose of 10^{18} protons/cm^2.

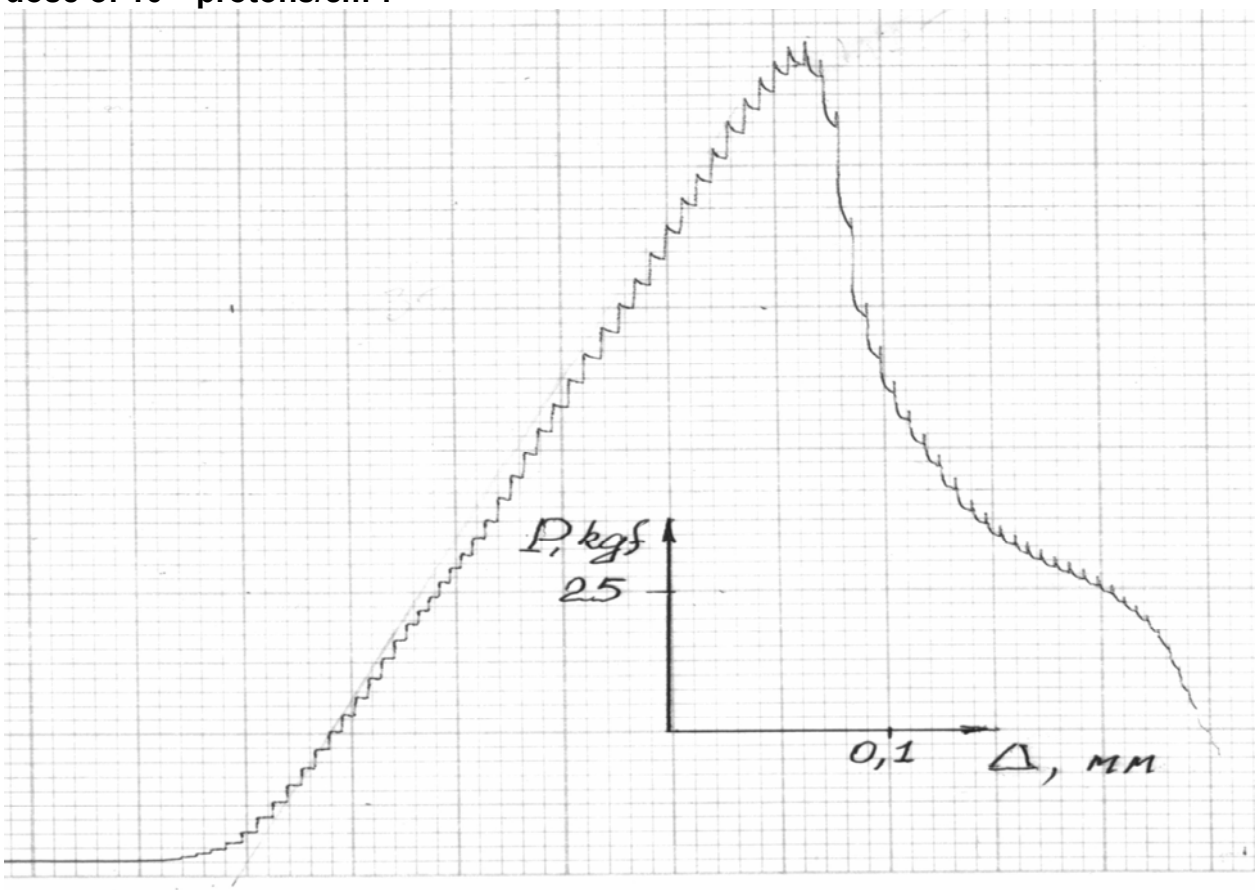

Fig.57. Changes in the deflection curve for 4T-3 sample irradiated with protons to dose of 10^{19} protons/cm^2.

14. The results of analysis of physical-mechanical properties changes in graphite samples after forth irradiation by proton beam with the energy 30 MeV up to proton dose $3*10^{19}$ protons/cm^2 (about 0.06dpa).

For the fourth series of irradiation two samples of AC-150 composite graphite and one sample of the same size of a standard block of domestic graphite reactor GR-280 were selected for comparison with the nature of neutron radiation damage and ion irradiation. Samples were selected from pre-prepared samples from billet № 10, table 12.

Table12. The results of investigations of initial physical-mechanical properties of graphite samples. Billet № 10

Sample №.	d, g/cm^3	E, GPa	ρ, 10^{-6} Ohm*m	α, 10^{-6}, 1/K
10R(TA-1)	1.66	3.2	27.8	10.3
10R(TA-2)	1.66	2.96	30	
10R(TA-3)	1.66	3.2	29.1	
Average value	1.66	3.12	28.9	
Standart deviation	0	0.13	1.1	
10T(AR-1)	1.65	9.3	5.6	0.25
10T(AR-2)	1.64	9.1	5.1	
10T(AR-3)	1.56	9.3	5.7	
Average value	1.62	9.2	5.4	
Standart deviation	0.04	0.11	0.3	

10A(RT-1)	**1.54**	**8.4**	**5.5**	**-0.6**
10A(RT-2)	**1.64**	**8.4**	**5.7**	
10A(RT-3)	**1.63**	**9.16**	**5.6**	
Average value	**1.60**	**8.65**	**5.6**	
Standart deviation	**0.06**	**0.4**	**0.1**	

Note: values of coefficient of thermal expansion given for the interval 100-200 ºC.

Samples № 10A (RT-1) and № 10R (TA-1) were selected. Initial properties of these samples are given in Table 12.
Geometric dimensions and weight of the samples are given in Table 13.

Table 13. Determining the physical-mechanical properties of the samples. Billet №10

Sample №	**L, mm**	**B, mm**	**H, mm**	**Weight, P, g.**
10R(TA-1)	**24.72 (Radial direction of cutting)**	**4,17 (Tangential direction of cutting)**	**4.05 (Axial direction of cutting)**	**0,688**
10A(RT-1)	**24.6 (Axial direction of cutting)**	**4.06(Radial direction of cutting)**	**4.14 (Tangential direction of cutting)**	**0,634**
GR-280	**25,15 (Perpendicular direction of cutting)**	**4.10 (Perpendicular direction of cutting)**	**4,07 (Parallel direction of cutting)**	**0,705**

14.1. Irradiation procedure on RRC KI cyclotron.

Irradiation was performed in the flow of water. Irradiation temperature of graphite according to thermocouple readings did not exceed 100 ^{o}C for the whole irradiation period of time (about month) for all samples.

Samples we placed on graphite holder and on the top (near edges) we covered with copper foil. Thus only the central area of the samples was irradiated (approximately 15mm*15 mm) while edges of the samples remained in the unirradiated condition.

Samples were placed on the holder in a way that the beam of protons faced the different planes in regard to the textures of graphite.
Thus a 10R(TA-1) sample was installed in such a way that the proton beam was directed to the face T, a 10A(RT-1) sample of was installed in such a way that the proton beam was directed to the face R. A sample of GR-280 graphite was located so that the flow of protons was sent to the face with a parallel direction of cutting relative to the axis of billet forming (this graphite is obtained by pushing through die).

14.2. Results of irradiation. Visual inspection of irradiated graphite samples.

After irradiation samples were held for about a week in order to diminish induced activity and then taken off the holder and directed to study the complex material RRC KI.
Visual inspection revealed that from all of three samples the only sample of 10A(RT-1) remained intact, though it is clearly seen a partial detachment of the upper layer of graphite from the side (face) R. Figure 61.

The other two samples after irradiation were broken after irradiation around the middle of samples.

In addition traces of a very noticeable erosion of graphite in irradiated zones were visible for all samples. (black soot surface)

Thus it was possible to carry out measurements of the properties of samples only one sample (10A(RT-1)).

14.3. Measuring the properties of graphite after irradiation.

14.3.1. Measuring the linear dimensions of samples and weight loss.

Measuring the size of samples in cross-sectional plane showed that samples decreased by about 10%, Table 14. A sample of reactor graphite was destroyed so that it was impossible to measure its size with sufficient accuracy.

Table 14. Changes of size of the samples after irradiation

Sample №	L, mm	B, mm	H, mm	Weight, P, g.
10R(TA-1)	24.72 (Radial direction of cutting)	4,15(Tangential direction of cutting)	4.00 (Axial direction of cutting)	0,537
10A(RT-1)	24.6 (Axial direction of cutting)	4.04(Radial direction of cutting)	4.10(Tangential direction of cutting)	0,430

14.3.2. Profilometry and photographs of irradiated samples.

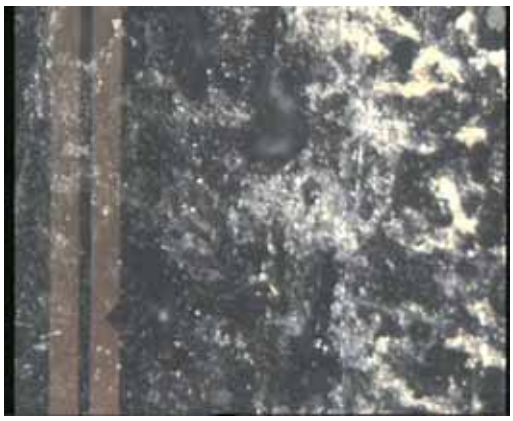

Figure 58. 10R(TA-1)A sample, the distance between markers is 20 μm

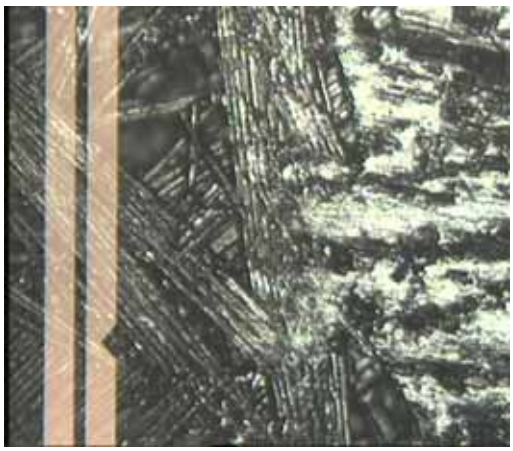

Figure 59. 10A(RT-1)R sample, the distance between markers is 20 μm

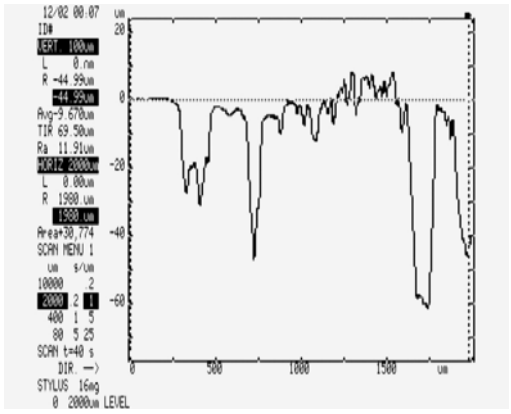

Figure 60. 10A(RT-1)T sample, the distance between markers is 20 μm

Profilometry results showed that the surface of samples subjected to strong erosion and obtaining reliable results for shrinkage (swelling) of graphite is also difficult. Depth of pores (micro cracks) reaches 60 microns.

The photos of the 10A(RT-1) sample surface (from the side of face R) is clearly visible structure of the threads (fibers) which are also severely fractured and the matrix material (filling) almost not visible (large cavities).

Photos of the same sample from side of face T (Figure 60) showed that the layered structure persists but layers can’t be also recognized quite clear.

Photos of various surfaces of samples are given in Appendix 1.

14.3.3. The measurements of physical-mechanical properties of graphite.

During research process the following measurements were made: weight loss of the samples, resistivity, elasticity module (dynamic) and the coefficient of thermal expansion. The results are presented in Table 15.

Table 15. Changes of physical-mechanical properties of AC-150 composite after proton irradiation.

Sample №.	E_{irr}/E_{init} GPa	ΔE/E, %	ρ_{irr}/ρ_{init}, 10^{-6} Ohm*m	Δ ρ/ρ, %	$\alpha_{irr}/\alpha_{init}$ 10^{-6}, 1/K	Δα/α, %	d_{irr}/d_{init} g/cm^3	Δd/d, %	P_{irr}/P_{init} g	ΔP/P %
Fourth irradiation (0,06 dpa)										
10R(TA-1)			**514/27,8**	**1750**	**8,6/10,3**	**170**	**0,73/1,66**	**-56**	**0,537/0.688**	**-21,9**
10A(RT-1)	**1,6/8,4**	**-81**	**85,9/5,5**	**1460**	**3,3/-0,6**	**-16,5**	**1,1/1,54**	**-28,6**	**0,430/0,634**	**-32,2**

Note:

1. Values of coefficient of thermal expansion given for the interval 100-200 °C.

2. Changes of tensile were estimated by the changes in the ratio of elasticity modulus.

14.4. The results of investigations at dose 3.10^{19}proton/cm^2.

The studies have been made for the physical - mechanical properties of AC-150 composite after proton irradiation to doses of approximately 0.06 dpa and they shown that there is the sharp degradation of all the properties of graphite with these radiation doses (and at low temperature - about 100 ^{o}C). This is reflected as a loss of weight, reduced density, reduced module of elasticity and a sharp increase in the resistivity of the samples.

Thus the density of graphite samples cut along the axial direction of texture (10A(RT-1)) is reduced almost by half to a value of 0.73 g/cm^3, and for samples cut along the R axis (radial direction) it decreased by 28% to a value of 1.1 g/cm^3.

Modulus of elasticity of graphite dramatically reduced for samples cut in the radial direction 10R(TA-1). Its value decreased by 80% to 1.6 GPa. Direct tensile strength measurements of graphite failed but concerning the fact that the samples have already been fractured in the process of irradiation the strength of graphite also decreased sharply.

Measuring the value of resistivity for both cutting directions showed that it increased very strongly up to 15-17 times which also reflects the very strong changes of graphite structure and that is clearly visible on the surface microphotography of the samples.

With regard to measuring a value of the coefficient of thermal expansion, then for R direction (across the fibers) it slightly decreased from 10.3 to $8.6 \cdot 10^{-6}$ K^{-1} and for direction A (along the fibers) significantly increased from 0.6 to $3.3 \cdot 10^{-6}$ K^{-1}.

Conclusion

In conclusion it should be noted that such a rapid degradation of the properties of graphite occurs also due to the irradiation in water cooling environment as this lead to the washing out of the matrix. We have already carried out the experiments on the research of antifriction graphite (AG-1500) in water cooling environment under neutron irradiation in the reactor. The results also confirmed that under irradiation in water degradation of the properties of graphite is significantly faster than under irradiation in air or in a vacuum.

Figure 61. A general view of irradiated graphite samples. Upper - A10(RT-1), middle - GR-280, lower - 10R(TA-1).

Figure 62. Photos of the 10R(TA-1) sample surface from the side of face A after proton irradiation.

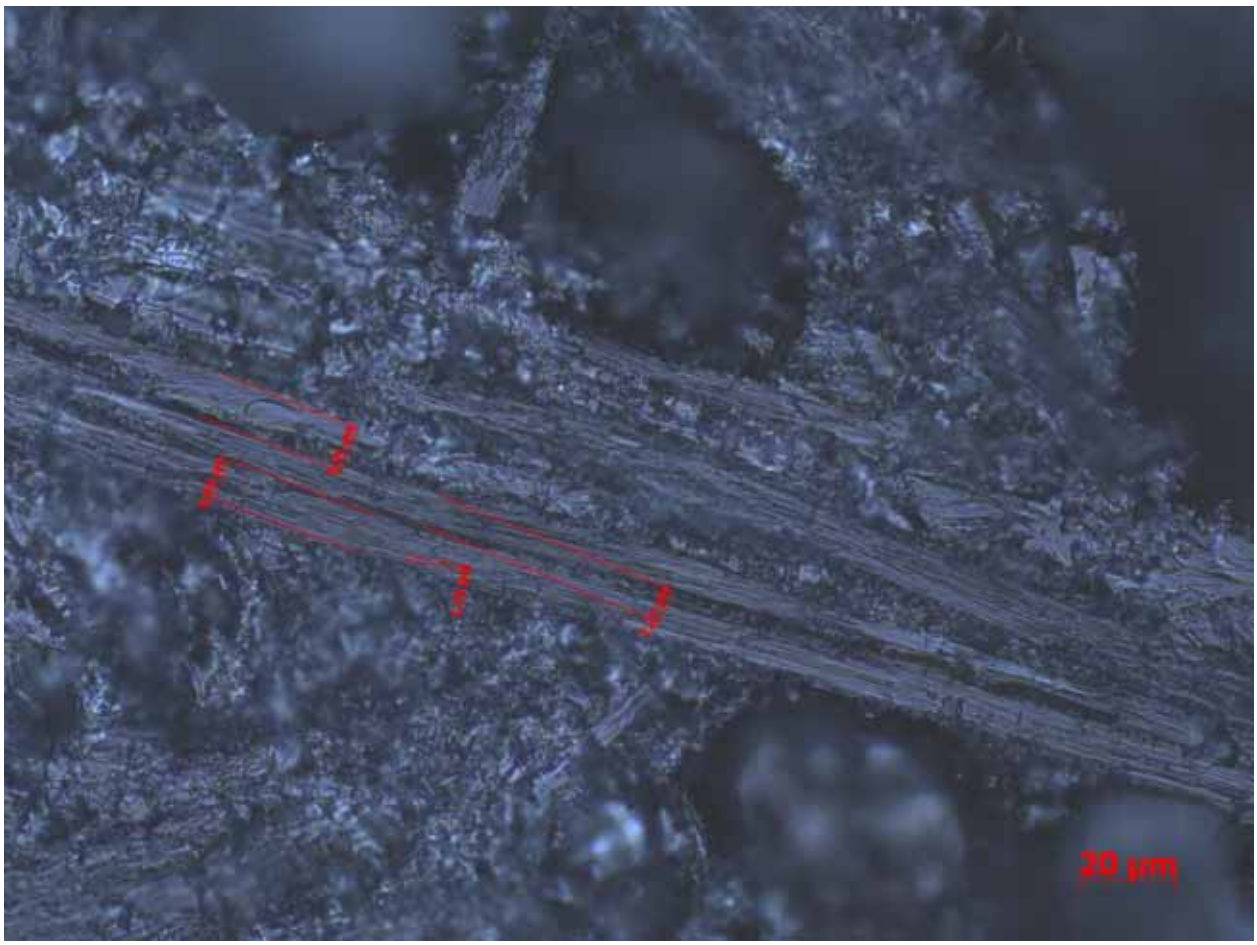

Figure 63. Photos of the 10R(TA-1) sample surface from the side of face T after proton irradiation.

Figure 64. Photos of the 10A(RT-1) sample surface from the side of face R after proton irradiatio

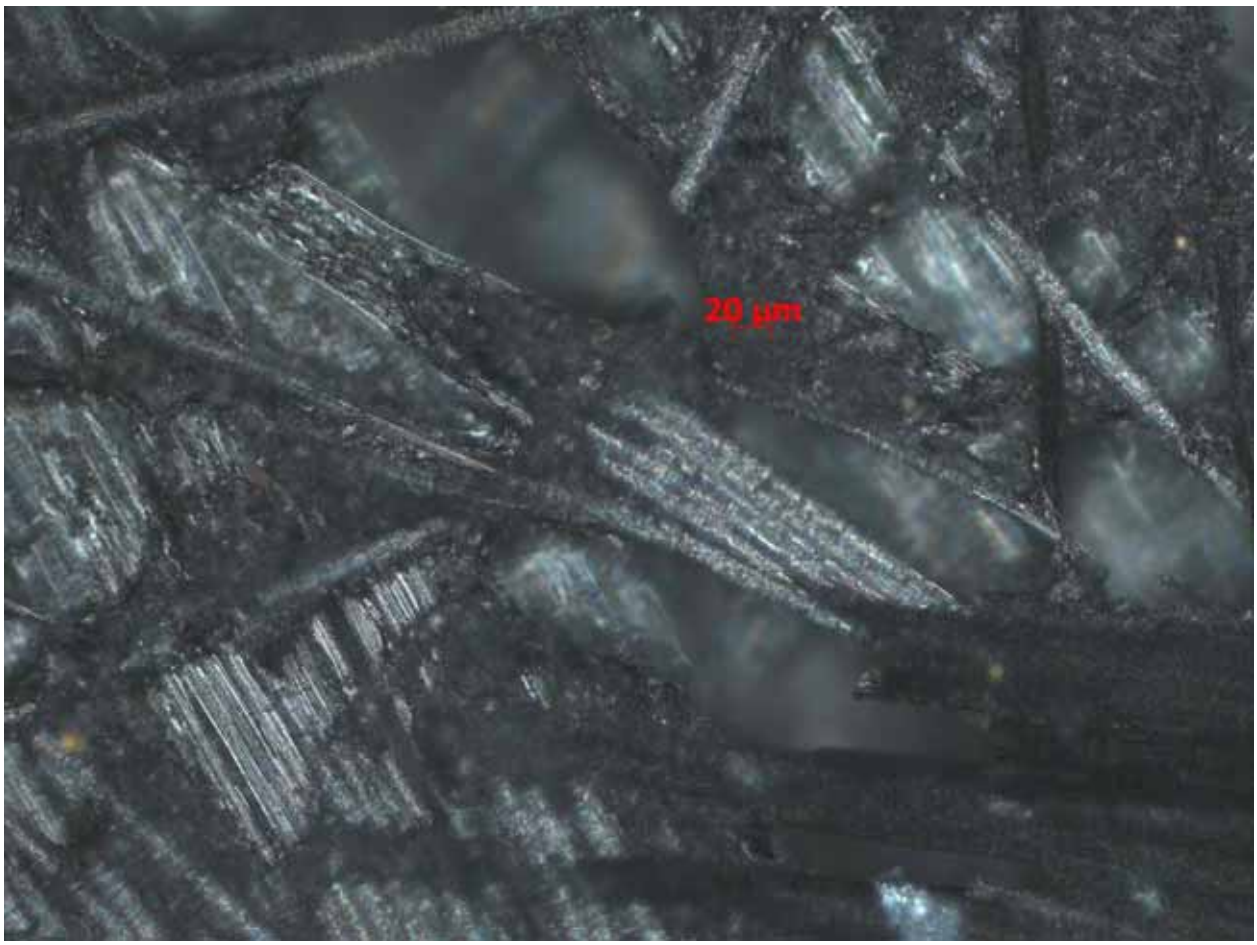

Figure 65. Photos of the 10A(RT-1) sample surface from the side of face R after proton irradiation. Filming in polarized light.

Figure 66. Photos of the 10A(RT-1) sample surface from the side of face T after proton irradiation. The left half of the photo is irradiated surface, right is unirradiated.

15. Conclusion.

Obtained experimental results of changes in physical - mechanical properties of graphite samples of material AC-150 in different directions with their different doses of radiation with the energy of protons up to 30 MeV in the range of radiation doses from 10^{17} protons/cm^2 until dose 3.10^{19} protons/cm^2 demonstrate that the nature of physical-mechanical properties of AC-150 graphite corresponds to the general laws for carbon materials characteristics under irradiation, in particular, the standard block graphite GR-280, that was used for graphite stack for all RBMK-1000 reactors, those are increased strength, increased resistivity, decreased thermal conductivity. However, the properties of graphite for various cuttings may vary significantly in different ways and the most significant changes occur for the samples with radial cutting. Finally the more strong degradation of physical-mechanical properties of graphite collimator materials in the dependence on irradiation dose has been observed along the graphite fiber in graphite collimator composite materials for LHC.

Thus, there is a sharp increase in the volume of samples (up to 1.5%), increase in elasticity module (50%), an increase of resistivity (up to 350%), reduction the coefficient of thermal conductivity (by 70-80%). The changes of resistivity and thermal conductivity correspond of the changing nature of these properties under neutron irradiation - a dramatic change in the initial stage of irradiation, followed by the stage of saturation. All these changes can be seen in bulk specimens, that also confirms the reliability of the results.

Estimation of the overall radiation resistance of AC-150 graphite is quite difficult because of its very high anisotropy, but one can, for example, use "quality indicator" of graphite - (criterion of Kingery - M^{TS}.) It is normally used to estimate the graphite material in terms of its durability ($M^{TS} = \sigma\lambda/E\alpha$). This combination of properties provides a minimum level of thermal stress in graphite constructions.

From this point of view M^{TS} value for AC-150 graphite is about 5000 for A and T directions (mostly because of the very low value of the coefficient of thermal expansion in these directions) and 70 for the radial direction. For comparison the GR-280 graphite has a value in the parallel direction of sample cutting equal to 120 and 75 for the perpendicular.

Thus one can conclude that composite graphite AC-150 has a very high thermal durability and substantially surpasses on this indicator GR-280 graphite.

16. Appendix 1: Methods of the measurements of thermal and physical-mechanical properties of carbon based materials in RRC "Kurchatov institute".

All techniques are certificated with ASTM-standards (1982 Annual Book of ASTM Standards, PART 17. Standards Relating to Refractories; Glass; Ceramic Whitewares; Porcelain Enamel; Manufactured Carbon and Graphite Products)

16.1. Methods of the measurement of thermal properties.

Thermal conductivity
Thermal conductivity coefficient may be measured by two methods

16.1.1. Kohlrausch method.

Thermal conductivity coefficient (λ) is measured using technique of steady state regime when sample is heating by steady current.
This technique permeet us to measure thermal conductivity coefficient and specific electrical resistance simultaneously.
Range of measurement -50-750 ^{o}C.
The sample sizes: diameter 3-10 mm, length – 25-70 mm.
This technique is certificated with ASTM-standards.

16.1.2. Pulse method (Parker technique).

This technique permits us to measure thermal conductivity coefficient (α) using laser flash.
Range of measurement -20- 1000 ^{o}C.
The sample sizes: diameter 5-12 mm, thickness – 2-5 mm.
To receive the value of the thermal conductivity coefficient (λ) this value should be multiply by the value of specific heat.

This technique is certificated with ASTM-standard.

16.1.3. Measurements of the value of specific heat is measured using scanning calorimeter DSC-404-PEGASUS manufactured by NETZCH (Germany).

Range of measurement -20- 1650 ^{o}C.
The sample sizes: diameter 3-12 mm, length – up to 25 mm.
This technique is certificated with ASTM-standard.

16.1.4. Thermal expansion coefficient measurements.

For measurement of this parameter the dilatometer DIL-402-CD manufactured by NETZCH (Germany) is used.

Range of measurement -20- 1200 ^{o}C.
This technique is certificated with ASTM-standard.

16.1.5. Density measurements (d).

For measurement of this parameter hydrostatic weight devise (SURTORIUS) is used (NETZSH, Germany)

16.2. Physical-mechanical property measurements.

16.2.1. Measurements of mechanical strength.

For measurement of strength properties and elastic modulus (static) universal strength machine INSTRON- 1253 (UK) is used.

16.2.2. Measurements of Elastic modulus (dynamic).

For measurement of this parameter the resonance technique is used. This technique is certificated with ASTM-standards.

16.3. Measurements of radiation induced expansion coefficient.

The measurement of specimen profile (radiation induced expansion) carry out with the ALBHA-STEP device (TENCOR-INSTRUMENTATION, USA).

Figure 67. Hot cells of RRC KI Institute of reactor materials and technologies

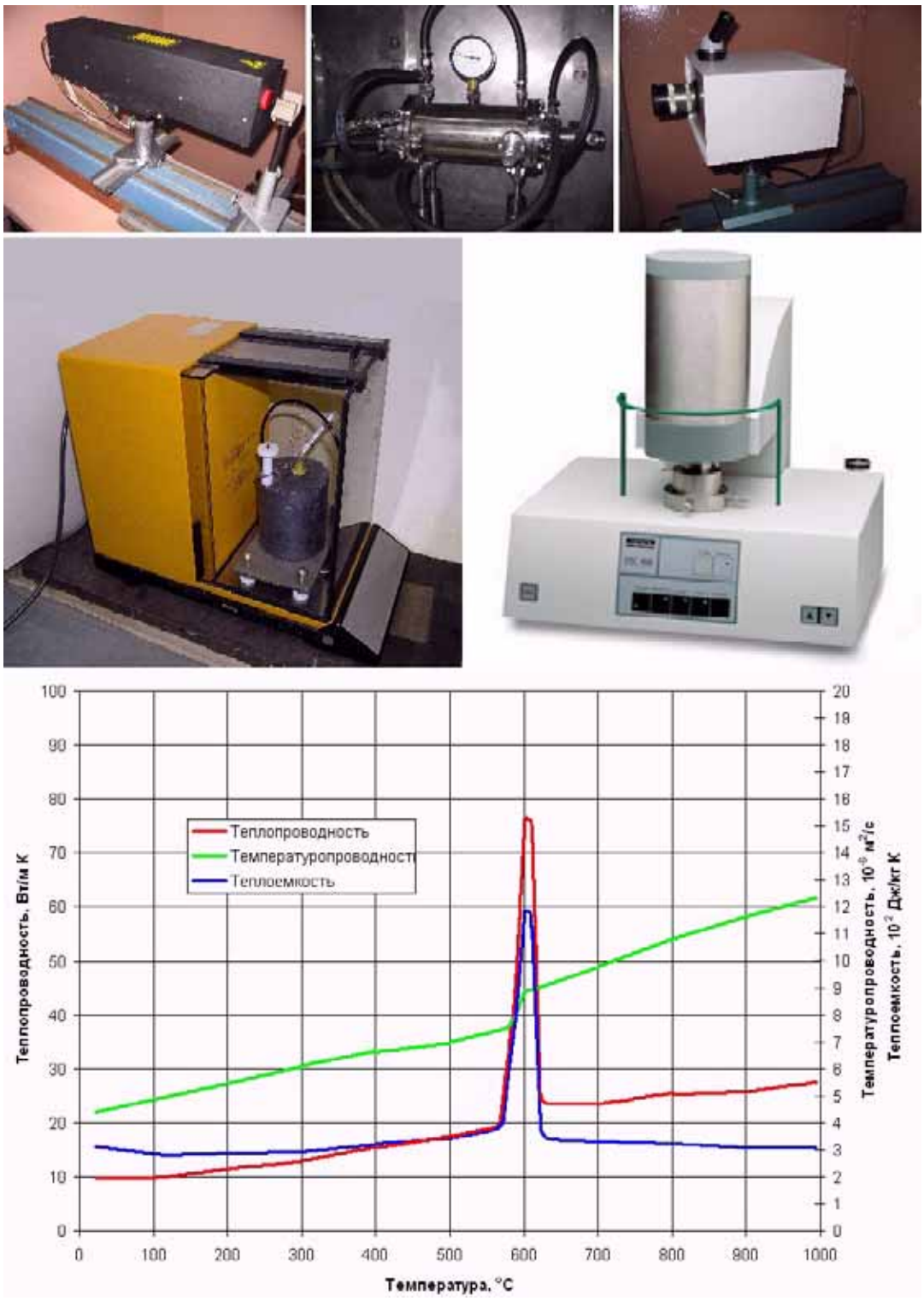

Figure 68. Thermal properties measurements installation.

Figure 69. Calorimeter NETZSH (DSC-404-PEGASUS)

Figure 70. Dilatometer NETZSH – (DIL-402-CD)

Figure 71. Universal strength machine INSTRON- 1253 (UK)